A Microfluidic System for Pathogen Detection Based on DNA Hybridization

by

Xuan Weng

A thesis
presented to the University of Waterloo
in fulfillment of the
thesis requirement for the degree of
Doctor of Philosophy
in
Mechanical Engineering

Waterloo, Ontario, Canada, 2014

AUTHOR'S DECLARATION

I hereby declare that I am the sole author of this thesis. This is a true copy of the thesis, including any required final revisions, as accepted by my examiners.

I understand that my thesis may be made electronically available to the public.

Abstract

With the great development of the microfluidics, the applications of microfluidic devices in conducting biomedical research have been drawn substantial interests from scientists and researchers all over the world. These microfluidic lab-on-a-chip systems create clinically useful technologies and have a number of competitive advantages over the conventional biomedical instruments due to the reduced reagents/samples consumption, decreased analysis times and operational costs. In addition, the microfluidic lab-on-a-chip systems facilitate the development of the portable devices and have the ability of automatically performing the multiple assay processes.

At the present, increasing attention has been paid to the preventive detection of foodborne pathogens as the foodborne illness becomes a serious concern to the public health throughout the world. Early detection and notification of foodborne pathogenic bacteria is therefore of considerable significance in food safety control. DNA-based hybridization technique, as a rapid diagnosis tool for detecting foodborne pathogens, has presented distinctive advantages over the conventional microbiological culture-based methods for pathogen detection such as high sensitivity, specificity and rapidity, especially in the detection of the bacteria samples of low concentrations.

In this thesis, a microfluidic platform combining DNA hybridization assay technique to detect foodborne pathogens is investigated. As the hybridization assay involves sequential loading and washing processes, magnetic beads are used as the matrix to immobilize the hybridization product; meanwhile microvalves are designed in the microfluidic chip to manage the sequential flow loading. In the first two designs, gravity force is used to drive the flow in the microchannels. A pair of electrokinetically-controlled oil droplet valves and electrothermally actuated phase change microvalves are used in these two microfluidic system, respectively. LabVIEW program was coded to implement the automatic operations of the assay. In the further improved microfluidic system, electrokinetics is applied to drive the flow, and a programmable High Voltage Sequencer is used to achieve the flow transportation automatically in an assay analysis cycle. Since no microvalves are required, this electrokinetics-based assay simplifies the preparation process of the microfluidic chip.

Light absorption detection is used to analyze the quantified concentrations of the samples. This optical detection is verified firstly by a microscope. Later, a low-cost, miniaturized optical module is developed, which consists of a photo-detector and LED. The optical detection module is controlled by self-made circuit and coded LabVIEW program.

To examine the performance of the microfluidic system, *Salmonella* and *Listeria monocytogenes* are used as a sample pathogen models. Based on the obtained results, the presented system successfully achieve the significantly reduction in reagent / sample consumption (up to 40 folds) compared with using the commercial test kit following the same protocol in conventional labs. In addition, the quantitative detection can be obtained in approximately 20 min, and the detection limit is as low as 10^3~10^4 CFU/mL. The microfluidic DNA hybridization assay chip demonstrated in this thesis presents an excellent potential in the development of a portable device for point-of-testing applications.

Acknowledgements

First and foremost I would like to express my deepest gratitude to my supervisor Professor Dongqing Li for his encouragement, guidance, patience and continuous support throughout my graduate studies and research at University of Waterloo. His insight and enthusiasm for research has motivated me to continue a career in this field. I would also thank Dr. Shu Chen and Dr. Honghe Cao in Laboratory Services Division, University of Guelph for providing the reagents and bacterial samples.

The support I have received from my colleagues and friends over the last four years has been invaluable. My special thanks go to Mr. Hai Jiang, Dr. Chan Hee Chon, Dr. Junsheng Wang, Dr. Yasaman Daghighi, Dr. Saeid Movahed, Ms. Fang Zhang, Ms. Chunyan Nan and Dr. Xudong Wu. I have learned a lot from these excellent people.

My sincere gratitude should also be extended to the members of in my committee: Dr. Hyock Ju Kwon, Dr. Patricia M. Nieva, Dr. C. Perry Chou and Dr. Keith Warriner for their precious time examining my thesis.

I owe a big thank you to my beloved husband Hai Jiang and my lovely little one Ivan. I am grateful to my sister, Mom and Dad.

I would like to thank the Mechanical and Mechatronics Engineering department of University of Waterloo for giving me the opportunity to study here.

Finally, the financial support of the Canada Research Chairs program and the Natural Sciences and Engineering Research Council (NSERC) of Canada through a research grant to Professor Dongqing Li is also appreciated.

To Ivan and Hai
for endless love beyond the years

Table of Contents

List of Figures

List of Tables

Nomenclature

C_i	Concentration of the *i*-th sample
D_i	Diffusion coefficient of the *i*-th sample
F	Volume force
I	Unit diagonal matrix
N	Flux vector
n	Normal vector to the boundary
P_0	Constant pressure
P	Pressure
t	Time
V	Velocity
ρ	Density of the fluid
η	Dynamic viscosity of the fluid

Acronyms

AFNOR	Association Fran çaise de Normalisation
AOAC	Association of official analytical chemists
RDHA	RNA-DNA hybridization assay
ECM	Electrochemical
ECODSV	Electrokinetically-controlled oil-droplet sequence valves
EDL	Electrical double layer
FRET	Fluorescence resonance energy transfer
EOF	Electro-osmotic flow
GRE	Giant electrorheological
MEMS	Microelectromechanical systems
PCR	Polymerase chain reaction
PDMS	Polydimethylsilicone
PEG	Poly-ethyleneglycol
PMMA	Poly (methyl methacrylate)
PNIPAAm	Poly N-isopropylacrylamide
RT	Room temperature
SPR	Surface plasma resonance
TFT	Thin film transistor
TMT	Thin membrane transducers
SWNTs	Single-walled carbon nanotubes

Chapter 1

Introduction

1.1 Background and motivation

In recent years, food safety has become one of the greatest concerns all over the world. Early detection of foodborne pathogenic bacteria is therefore a crucial task in microbiological analysis to control food safety. Many methods have been developed in order to detect foodborne pathogens. However, the biggest challenges remain detection speed and sensitivity. Traditionally, foodborne pathogens are identified by microbiological culture, followed by immunological methods to detect antigens, and/or biochemical reactions (Swaminathan and Feng, 1994). These detection methods are labor-intensive and time-consuming. DNA-based hybridization assay is an essential component in many of the current standard molecular biology techniques and becomes increasingly important in clinical diagnosis, for instance, for the detection of foodborne pathogenic bacteria (Cano et al., 1992; Flowers et al., 1987). Many of products based on DNA hybridization technology are available commercially and have been successfully validated by the AOAC and/or AFNOR (AFNOR 2010; AOAC 2009). For example, a popular commercial kit for *Salmonella* detection is the GeneQuence *Salmonella* Microwell assay (Neogen, Lansing, MI, USA). DNA-based hybridization assays provide highly sensitive and precise methods for the sequence-specific analysis of nucleic acid. However, besides the cost of a spotting instrument, analysis time is also a concern. Usually a conventional hybridization assay test needs hours to complete because it is a multi-step, labor-intensive process (Blackburn, 1993; Maciorowski et al., 2006; Swaminathan and Feng, 1994). Automation of DNA hybridization test generally requires a complex and cumbersome robotic technique for fluid handling, which is not only extremely expensive but also prevents the assay from being a tool for point-of care detection.

The advantages of using the microfluidic methods have been demonstrated for on-chip PCR (Chen et al., 2007; Mitterer and Schmidt, 2006), DNA analysis (Ali et al., 2003; Erickson et al., 2004; Fan et al., 1999; Ferguson et al., 2009; Sun and Kwok, 2006), enzyme assay (Curey et al., 2001; Hadd et al., 1997; Xu and Ewing, 2005), and chemical synthesis (Dexter and Parker, 2009; Salimi-Moosavi et al., 1997). The microfluidic techniques also provide a highly promising way to miniaturize DNA hybridization assays (Berti et al., 2009; Cao et al., 2010; Chen et al., 2008a; Heule and Manz, 2004; Javanmard and Davis, 2011; Li et al., 2009a; Mai et al., 2007; Mulvaney et al., 2007). A vast number of studies on

DNA hybridization efficiency in microfluidic flow channels have proven that microfluidics-based technologies are capable of enhancing the hybridization efficiency dramatically due to the high surface-area-to-volume ratio and decreased diffusion distance provided by the microchannel, leading to the significant reduction of the hybridization reaction time (Heule and Manz, 2004; Mai et al., 2007; Wang and Li, 2011). In addition to high hybridization efficiency, microfluidic DNA hybridization assay has another significant feature of low sample consumption, which generally benefits from its micro-scale size. Microfluidic biochips and microarrays can be employed in DNA hybridization assays as promising tools for the development of miniaturized, low-cost, rapid and portable DNA diagnostic devices.

1.2 Hypothesis

Handheld and rapid diagnostic devices for pathogen detection help reduce hospitalization and timely isolation in case of infectious pathogens. Microfluidics-based platforms for DNA hybridization assays facilitate the development of such rapid, cost-effective, sensitive and portable diagnosis device.

1.3 Research objectives

According to the hypothesis, the major objective of this thesis is to develop a microfluidic system towards portable device for pathogen detection using DNA hybridization assays. Compared to the conventional method and current microfluidic DNA hybridization assay, this microfluidic system will significantly reduce the assay time and the cost while have a comparable or even lower detection limit. What is more important, this microfluidic system lights a pathway for the portable pathogen diagnosis device development. The detailed objectives of this system are listed below:

- rapid detection
- automated procedure
- low sample/reagent consumption
- no external pumps, valves and tubing
- no expensive optical instruments
- high sensitivity & low detection limit

1.4 Outline of thesis

The complete thesis comprises the following major sections:

Chapter 1 serves as an introduction to this thesis, including an overview of the DNA-based hybridization assays technology and the applications of microfluidics in foodborne pathogens detection. The motivation, objectives and the scope of the thesis are also given in this chapter.

Chapter 2 reviews the recent advances on the merging of microfluidics to DNA hybridization assays, as well as their advantages and disadvantages. Specifically microvalve fabrication methods in microfluidic systems are discussed and compared. A brief review of foodborne pathogen detection and DNA hybridization technology is demonstrated.

Chapter 3 demonstrates a microfluidic RNA-DNA hybridization assay chip with electrokinetically controlled oil droplet valves. The on-chip sequential operations of reagent delivery and washing processes in the hybridization assay are performed by gravity-based pressure-driven flow controlled by a pair of electrokinetically-controlled oil-droplet sequence valves (ECODSV). Numerical method is used to simulate the fluidic processes of reagents in the complex microchannel network and an optimized hybridization assay microfluidic chip is developed. The application of this on-chip assay to detect *Salmonella* is demonstrated.

Chapter 4 presents an RNA-DNA hybridization assay microfluidic chip integrated with electrothermally actuated phase change microvalves. Paraffin wax is used as the phase change material in the valves and thin film heaters are used to electrothermally actuate microvalves. Gravity-based pressure driven flow and phase-change microvalves are used to realize the sequential loading and washing processes. Light absorption is measured by a photo-detector to determine the concentrations of the samples. The automatic control of the complete assay is implemented by self-coded LabVIEW program. To examine the performance of this chip, *Salmonella* and *Listeria monocytogenes* are used as the model samples.

Chapter 5 describes an electrokinetically-controlled RNA-DNA hybridization assay microfluidic chip. Numerical simulation is conducted to investigate the flow field of the microchip. The automatic sequential reagent dispensing and washing processes are realized by a programmable High Voltage Sequencer. A miniaturized optical detection module is used to obtain quantified results. The light source and the photo-detector of the optical detection module are controlled by self-coded LabVIEW program. *Salmonella* and *Listeria monocytogenes* bacteria of different concentrations are tested on the microfluidic RNA-DNA hybridization assay chip.

Chapter 6 compares the features and performance of the three proposed microfluidic systems, summarizes the major findings and contribution of this thesis. Recommendations for future projects are briefly outlined.

Chapter 2

Literature Review

2.1 Foodborne pathogen detection

Foodborne pathogens are responsible for million cases of foodborne diseases over the world every year, costing billions of dollars in medical care and lost productivity (Thorns, 2000; CDC, 2007). Early detection of foodborne pathogenic bacteria, such as *Salmonella*, *Campylobacter*, *Escherichia coli* O157:H7, *Listeria monocytogenes* is therefore an important task in microbiological analysis to enhance food safety. In recent years, many methods have been developed in order to detect foodborne pathogens; however, the biggest challenges remain detection speed and sensitivity. There are some requirements for pathogen sensors (Heo and Hua, 2009). First, they should present high sensitivity and high specificity as well as a low detection limit. Second, they are capable of rapid analysis. Third, portability and ease-of-use are important for on-site monitoring. Fourth, automation is another significant factor.

Traditionally, foodborne pathogens are identified by microbiological culture (AOAC, 1984; Maciorowski, 2006), followed by immunological methods to detect antigens, and/or biochemical reactions. These detection methods are labor-intensive and time-consuming, it often takes several days to complete the processes (Blackburn, 1993; Maciorowski et al., 2006). In addition, most of conventional methods require bulky and expensive instrumentation and cannot be used on-site (Heo and Hua, 2009). For this reason a substantial number of alternative rapid screening methods have been developed to produce results more quickly for food and environmental samples. Many of these are available commercially and have been successfully validated by the AOAC and/or AFNOR (AOAC, 2009; AFNOR, 2010). The AOAC database of performance tested methods contains hundreds of products for the rapid detection of foodborne pathogens. These products utilize several different technologies, including novel culture techniques, immune-magnetic separation (Lynch et al., 2004; Kumar et al., 2005; Taban et al., 2009), EIA- and ELISA-based assays incorporating fluorescent or colorimetric detection (Eyigör et al., 2007; Wyatt et al., 1995), simple lateral flow assays incorporating immune-chromatographic technology (Quintavalla et al., 1996; Muldoon et al., 2007; Urata et al., 2009), and molecular techniques (Naravaneni and Jamil, 2005) such as DNA hybridization (Ali et al., 2003; Erickson et al., 2004; Fan et al., 1999; Ferguson et al., 2009; Sun and Kwok, 2006) and PCR-based assays (Chen et al., 1997; Rodriguez-Lazaro et al., 2003; Malorny et al., 2004; McGuinness et

al., 2009; Löfström et al., 2008). These molecular techniques provide rapid genetic tests for the detection and identification of pathogens in clinical diagnostics. For example, PCR is a very promising approach for sensing bacterial pathogens and presents distinct advantages of selectivity, specificity, sensitivity and rapidity over traditional detection methods for foodborne pathogens (Hernández et al., 2009). However, more efforts are required to further improve its performances. For example, false-positive and false-negative PCR results may occur and hence appropriate controls are essentially included in the PCR system (Malorny et al., 2003; Velusamy et al., 2010). In addition, real-time PCR, the most commonly used technology for quantification of specific DNA fragments, still involves expensive and complicated detection protocols based on fluorescent tagging, requiring skilled workers to carry out the tests (Basuray et al., 2009; Velusamy et al., 2010). DNA-based hybridization assay has become another essential component in many of the current standard molecular biology techniques, especially in clinical diagnosis, for instance, for the detection of foodborne pathogenic bacteria (Cano et al., 1992; Flowers et al., 1987; Spiess et al., 2007; Cleven et al., 2006). DNA-based hybridization assays provide highly sensitive and precise methods for the sequence-specific analysis of nucleic acid. However, besides the cost of a spotting instrument, analysis time is also a concern. Usually a conventional hybridization assay test needs hours to complete because it is a multi-step, labor-intensive process (Blackburn, 1993; Maciorowski et al., 2006; Swaminathan and Feng, 1994). Automation of DNA hybridization test generally requires a complex and cumbersome robotic technique for fluid handling, which is not only very expensive but also prevents the assay from being a tool for point-of care detection.

Generally, food samples contain very low concentrations of pathogens, thus almost all test protocols hence include an enrichment step. So far, detection improvements have been undergoing in two directions: one is the approach that decreases the time required for pre-enrichment and/or post-enrichment to recover pathogens prior to the actual detection; the other is to decrease the assay or detection time by applying concentration and/or detection techniques to replace culture on selective agars and further confirmatory tests. Most of them claim to produce a result in approximately 48 hours or less, depending on the enrichment protocol. However, while the enrichment step is similar among most of these products, the actual detection time vary from hours to less than an hour. In addition, many commercial kits require costly manual handling during analysis or require expensive instruments for detection (AccuProbe®, 2011; GENE-TRAK®, 2008).

Among the foodborne pathogens, *Salmonella species and Listeria monocytogenes are* genetally found to be the two leading cause of foodborne illnesses in humans (Velusamy et al., 2010). Nowadays, human salmonellosis is a major public health problem worldwide (Pui et al., 2011). Salmonella infections are obtained from eating contaminated food, such as poultry, meats and eggs or water. Listeriosis is a severe infection caused by *Listeria monocytogenes* which is commonly found in water, sewage, unpasteurized dairy products, raw fruits and vegetables (Scallan et al., 2011). An estimates of foodborne illness caused by 31 major pathogens in United States from 2000–2008 shows that among the leading causes of hospitalization, *Salmonella* and *Listeria monocytogenes* are responsible for 35% and 19%, respectively (Scallan et al., 2011).

2.2 DNA hybridization technology

DNA hybridization is one of the molecular biology techniques for comparing and analyzing DNA and RNA molecules of identical or related sequences.

DNA hybridization technology is basically introduced in 1962 when Hall et al. showed that T2-specific RNA could be hybridized with heat-denatured T2 DNA and the hybrid isolated by cesium chloride density gradient centrifugation (Hall and Spiegelman, 1961). Later, Bolton et al. developed the solid-phase hybridization method via the immobilized DNA in gels of cellulose acetate or agar retaining the ability to form specific hybrids with complementary RNA (Bolton and Mccarthy, 1962). During 1960s to 1970s, Britten et al. and Nygaard et al. contributed a lot for the further development of the nucleic acid hybridization technique (Britten and Kohne, 1968; Nygaard and Hall, 1963). With the flourish development in molecular biology during early 1980s, DNA hybridization technique had an enormously improvement. Charles Sibley and Jon Ahlquist pioneered DNA-DNA hybridization technique by using DNA kinetics to investigate evolutionary relationships (Sibley and Ahlquist, 1984). To date, the hybridization efficiency and reliability have achieved significant enhancement due to the development of solid phase chemical synthesis technique and the advent of the automatic DNA synthesizer, which facilitates the preparation of the oligonucleotide probes. Therefore, this technique has become a powerful method applied in many diagnostic assays to analyze target DNA or RNA molecules.

A standard DNA hybridization assay utilizes a labeled nucleic acid probe to identify the related target molecules. During a hybridization process, DNA molecules, RNA molecules or one of each are heated above a certain temperature, which is called the melting temperature, to form single strands. Then the

cooled complementary single strands of probe and the single strands of target can combine to form a double-stranded molecules through base pairing ((Russom 2005; Chen 2010; http://ghr.nlm.nih.gov/glossary=dnahybridization). The amount of sequence complementarity indicates that how closely the two nucleic acids relate to each other. Most current nucleic acid detection methods involve using the labels coupled to specific probes. These labels can be fluorescent, chemiluminescent, or other functionalized modified molecules which can release optical signals to indicate the hybridization event (Ramsay, 1998; Kwakye and Baeumner, 2003). Liposomes (Esch et al., 2001), magnetic beads (Berti et al., 2009; Wen et al., 2007; Zhang et al., 2008; Edelstein et al., 2000) and gold particles (Taton et al., 2000; Park et al., 2002; Cao et al., 2002) have also been used as labels.

The speed of the DNA hybridization mainly determined by the starting concentration of the specific DNA sequences and the reaction time. High concentration of DNA sequences may reduce the time for the single-stranded DNA molecule to find its complementary strand forming double helices. The speed of hybridization is also related to the temperature and the concentration of monovalent cations. (Strachan T, Read AP, 1999)

2.3 Microfluidics

Generally, microfluidics refers to the manipulation of fluids in channels with cross-sectional dimensions on the order of tens or hundreds of microns. As a multidisciplinary field, microfluidics has the potential to be applied in many applications, ranging from biological analysis, chemical synthesis to optics and information technology, in which distinctive advantages of which have been presented such as the ability to handle minute samples, increase the detection accuracy and sensitivity, reduce the time for analysis and low cost.

Many microfluidic handling systems are under development for chemical diagnosis and analysis, such as flow cytometry, cell manipulation, cell separation, cell patterning, DNA and protein analysis and so on (Joo et al., 2010; Roman et al., 2007; Penchovsky, 2013). A microfluidic system usually consists of the following generic components: reagent and sample introduction method, flow driving, combining and mixing method on the chip and various other components such as detectors (Whitesides, 2006). At the present time, Lab-on-Chip applications are the area that has drawn highest attraction for research in microfluidics (Whitesides, 2006; Haeberle and Zengerle, 2007). The advantages of using the microfluidic methods have been demonstrated for on-chip polymerase chain reaction (PCR) DNA analysis, immunoassays (Cheng et al., 2001; Yang et al., 2001), enzyme assay and chemical synthesis.

Previously studies have shown that microfluidic chips allowed for rapid detection, high sensitivity, low consumption of samples/reagents, low cost, and portability (Sia and Kricka, 2008, Yi et al., 2006).

Microchips for microfluidic applications were initially fabricated from glass or silicon. The fabrication process was expensive and time-consuming (Tabeling, 2005). The introduction of polymeric-based materials to the microfluidics area attracted a large interest due to the simplicity and low cost of manufacturing the chips (Becker and Gärtner, 2008). PDMS (polydimethylsilicone) is one of the polymeric materials that draw the attention of researchers because of its favorable properties, such as optically transparent, ease of manufacturing and low cost, which suits different microfluidic applications.

One of the long term goals in the field of microfluidics is to create integrated, portable clinical diagnostic devices with high accuracy and short analysis time for home and bedside use, thereby eliminating time/labor consuming laboratory analysis procedures.

2.4 Microfluidics-based DNA hybridization assay

Although DNA hybridization assays offer distinctive advantages, such as superior sensitivity and specificity, today's DNA sensing based on DNA hybridization assay has many challenging issues, such as large reagent consumption, labor-intensive and time-consuming procedures as well as the involvement of bulky or expensive equipment (Blackburn, 1993; Maciorowski et al., 2006; Swaminathan and Feng, 1994). All of these are not favorable for the development of miniaturized, low-cost or disposable, and rapid diagnostic devices. With the rapid growth of the microfluidic technology, microarrays and microfluidic biochips have been extensively employed as promising tools for DNA analysis over the past decade (Penchovsky, 2013; Berti et al., 2009; Cao et al., 2010; Chen et al., 2008a; Heule and Manz, 2004; Javanmard and Davis, 2010; Mai et al., 2007; Mulvaney et al., 2007; Jin et al., 2009; Kwakye and Baeumner, 2003; Li and He, 2009; Senapati et al., 2009; Ben-Yoav et al., 2012; Chen et al., 2011). The advantages of applying microfluidics platform in DNA hybridization have been demonstrated in many representative works (Fan et al., 1999; Erickson et al., 2004; Ali et al., 2003; Sun and Kwok, 2006; Ferguson et al., 2009; Henry and O'Sullivan, 2012). It has been demonstrated that the ability to perform DNA analysis with micrometre resolution facilitates the realization of a functional hybridization assay (Lange et al., 2004). In addition to the low sample consumption and fast reaction rates brought by applying microfluidics technique, multi-sample processing can also be realized automatically in integrated microfluidic devices. Meanwhile, the production of the polymer-

based (PDMS) microfluidic chips may make these devices disposable and hence prevent any cross-contamination (Lien and Lee, 2010). All these facilitate the development of low cost, fast, sensitive and miniaturized diagnostic tools for DNA hybridization.

Microfluidic DNA hybridization assay has another significant feature, that is, it enhances the hybridization efficiency. Numerous studies on DNA hybridization kinetics in a microfluidic flow channel has proven that microfluidics-based technologies are capable of increasing the kinetic reaction rate, hence reduce the hybridization reaction time significantly. Kim et al. (2006a) presented that within the same period of time, DNA hybridization reaction in a microfluidic channel could generate higher signal intensities than a passive hybridization (typically takes several hours), especially for the sample of lower concentrations. Chung et al. (2003) obtained the similar results that on-chip DNA hybridization methods could not only increase the hybridization signals, but also decrease the nonspecific target-probe binding. Betanzos-Cabrera et al. (2008) presented that applying different shapes or physical characteristics of the microfluidic channels could help to enhance the binding efficiency of the oligonucleotides and hence shortened the reaction time. The hybridization reaction rate was found to be inversely proportional to dimensions of the microfluidic channels. In addition, the sensitivity and the reaction rate of the DNA hybridization could be enhanced by introducing micro-components (micromixers/micropumps) into the microfluidic system to generate continuous flow in the microchannel (Heule and Manz, 2004; Wang and Li, 2011).

Although the basic principle of microfluidics-based DNA hybridization assays is the same, the formats in which the hybridization can be operated are various. Generally, the formats of the current microfluidics-based DNA hybridization can be divided into several main types. The first one is based on directed liquid flow (Chung et al., 2003; Yuen et al., 2003; Yamashita et al., 2004; Sawada et al., 2007). The second type is the surface-based DNA hybridization, in which probe oligomers are immobilized onto the microchannel walls via chemical or physical immobilization techniques (Shamansky et al. 2001; Chen et al. 2002; Liu et al. 2004; Lingerfelt et al. 2007). The third type consists of those using probe-functionalized microbeads or other materials such as hydrogels (Seong et al. 2002; Olsen et al. 2002; Zangmeister and Tarlov 2004; Zangmeister and Tarlov 2003; Senapati S et al., 2009; Yang et al., 2009; Berti et al., 2009; Vojtíšek et al., 2010). In the following sections, we will review the working principles and their applications of these microfluidic DNA hybridization assays as well as their advantages and disadvantages.

2.4.1 Directed liquid flow-based microfluidic DNA hybridization assays

Microfluidic technology offers powerful tools to control the transport of micro/nanoliter liquid precisely within a microchannel network according to the defined strategies, such as sequential liquid/solution loading or mixing. By using the microfluidic technology, the complete DNA hybridization assay, including sampling, hybridization reaction, incubation, washing, can be conducted directly on a microfluidic platform in a liquid flow format (i.e., the probe-target reaction (hybridization) occurs in the flowing liquid). Kim et al. (2007) and Chen et al. (2008a) developed a rapid DNA assay in a microfluidic chip of alligator teeth-shaped microchannel network, as shown in Figure 2-1. Online fluorescence resonance energy transfer (FRET) detection technique was applied, and the changes of the FRET signal indicated the sequence-specific hybridization event between the target DNA (3′-GACTA ATCTC TCTCT TACAG GCACT ACAGA CTCGA CGTCC-5′) and the fluorescently labelled nucleic acid probes (5′-CTGAT TAGAG AGAGAA-TAMRA-3′ and 5′-TET-ATGTC TGAGC TGCAGG-3′). Two fluorescently labelled nucleic acid probes were mixed well and then all reagents and target DNA sample were introduced into the microchannel by pressure-driven flow. The structure of the alligator teeth in the microchannel was designed to enhance the mixing efficiency of all reagents passing through it. Confocal laser-induced microscopy was used for the fluorescence signal detection of final hybridization complex. The detection limit of the target DNA estimated by their system was 1.0×10^{-6} to 1.0×10^{-7} M. This analytical technique provided a promising diagnostic tool for real-time analysis of DNA targets in the solution phase.

Sawada et al. (2007) integrated a signal-processing circuit in a microfluidic DNA sensor for electrochemical detection. The microfluidic channel provided the reactor for DNA hybridization based on the laminar flow principle. The microchannel consists of one main flow channel (1 mm width, 10 μm depth, 100 nL capacity) and two inlet branches for dispensing probe DNA solution with the electrochemically active intercalator and the complementary target DNA solution. Three gold electrodes embedded in the main fluidic channel, working electrode (WE), reference electrode (RE) and Counter electrode (CE), were used to detect the hybridization reaction. In this method, the probe DNA solution and the target DNA solution were simultaneously dispensed from the two inlets, hence parallel laminar flows were generated in the main channel. Since the hybridization occurred only at the boundary of the laminar flows, they placed Au electrodes at the center of the microchannel for detecting the hybridization signal, while placed the additional electrodes on the sides of the microchannel for providing the reference signal. The advantages of this method are the integration of the electrochemical

sensor, microreactor and operational amplifiers, which permits successively cyclicvoltammograms measurement using only two simple electric power sources.

The advantage of directed flow-based microfluidic DNA hybridization assays is the easy introduction of the sample and the probes. However, as seen from the aforementioned studies, a relative long distance of microchannel or complicated microstructure in the microchannel was required in order to obtain acceptable hybridization efficiency. Although higher hybridization reaction rate can be achieved in the flow through a microfluidic channel, the limitation of hybridization efficiency still depends on the diffusion time between the probes and target molecules. Since the DNA probe density strongly influences the efficiency and the kinetics of the target/probe hybridization, the liquid flow-based microfluidic DNA hybridization assays have limited hybridization efficiency due to the limited concentration of the probes in a small volume of the reagent.

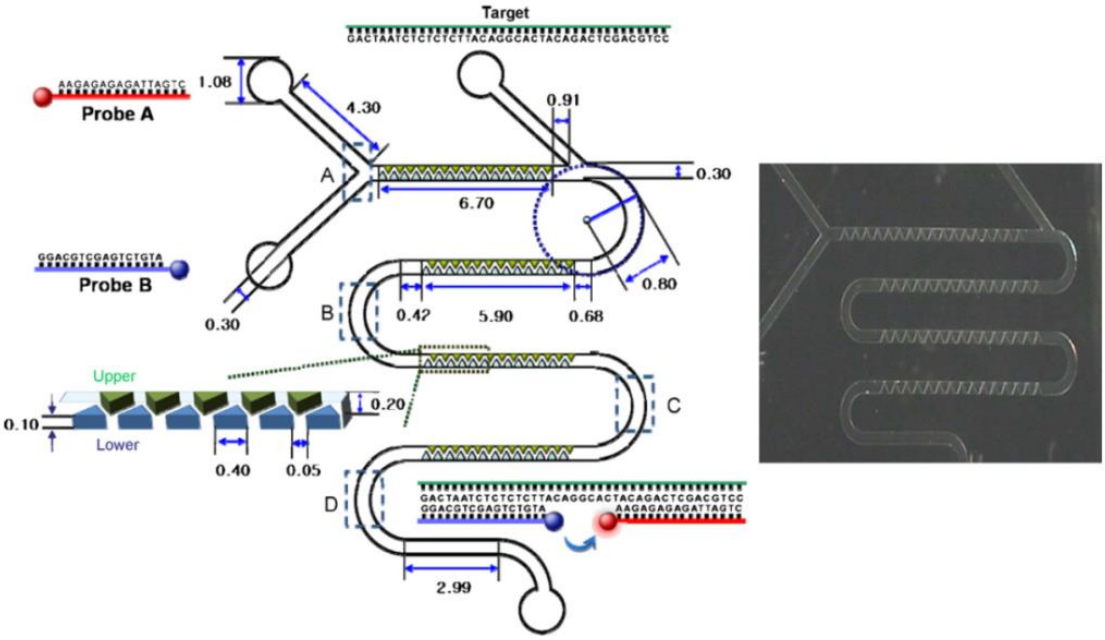

Figure 2-1 The chip layout and principle of an alligator teeth-shaped microfluidic DNA hybridization assay for the FRET detection. The dimensions of the microchannels were illustrated in the picture (unit: mm). The four rectangular areas were the fluorescence detection sites (Chen et al. 2008a)

2.4.2 Surface probe-based microfluidic DNA hybridization assays

Increasing the concentration of the probes in the microfluidic channel is one way to enhance the hybridization efficiency. The use of the solid support provides an efficient means for immobilizing the

capturing DNA/RNA probes and separating them from other reagents. These solid supports can be surfaces of the microfluidic structure. DNA probe molecules have been immobilized onto the walls of PDMS (and other polymeric) microchannels and subsequently applied in the application of DNA hybridization assays on microfluidic devices.

For example, Shamansky et al. (2001) attached photoactive biotin onto PDMS surfaces via a photopolymerization reaction, and then linked the fluorescently labelled or non-labelled avidin and biotinylated DNA probes to the biotin-immobilized surface for analyzing target DNA using a fluorescence-based hybridization assay. Wang et al. (2003) immobilized the DNA oligos onto a poly (methyl methacrylate) (PMMA) channel by using linkage chemistry to realize an imine bond between the surface aldehyde and the amine-terminated DNA. They demonstrated that the hybridization kinetics using their microchip was enhanced in comparison with the planar format. They successfully detected a point mutation in a K-ras oncogene at a level of 1 mutant DNA in

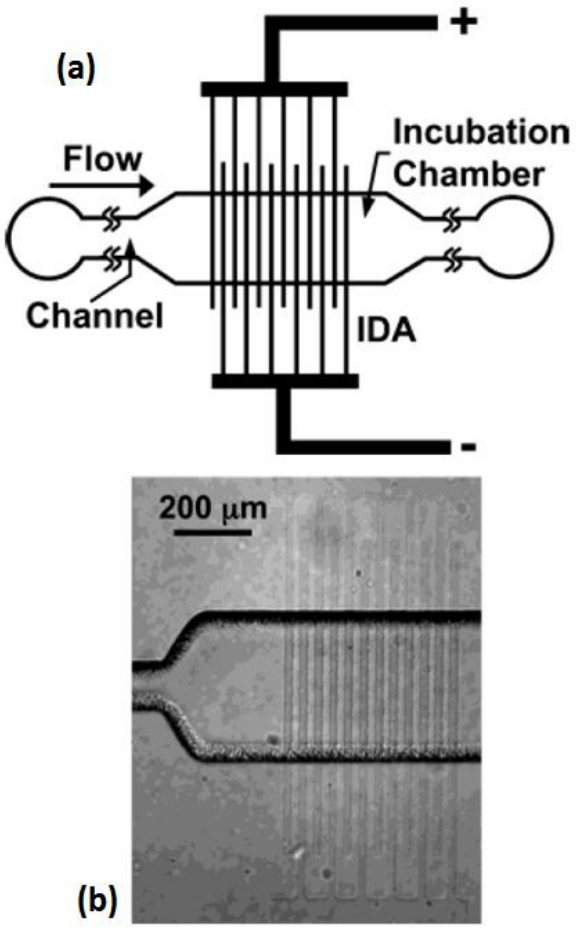

Figure 2-2 Schematic (a) and optical micrograph (b) of the PDMS micro-electrochemical device integrated with IDA for DNA hybridization (Liu et al. 2004)

10000 wild-type sequences by their chip. Chung et al. (2008) developed a microfluidic DNA chip by spotting probes DNA on the modified surfaces of a glass microfluidic channel in order to study the hybridization efficiency. They found that the hybridization efficiency could be improved by introducing the elevated hot-region temperatures and cold-region bulk flow velocities. Using these strategies, the hybridization signal was increased by 4.6-fold within 30 min by comparing with the conventional hybridization method. Huang et al. (2010) presented a multi-layer microfluidic chip for rapid DNA hybridization by using shuttle flow. Probes were immobilized on the gel pads which were patterned on the bottom glass substrate. Shuttle flow generated by integrated microvalves and micropumps on the upper two layers was used to deliver reagents and DNA target solution. Applying this system to detect four serotypes of dengue Virus genes (18mer), they achieved a detection limit of 100 pM in 90 s with a reduced sample consumption of 1 μL. Liu et al. (2004) directly coated DNA probes onto PDMS walls of a microfluidic device to conduct an enzyme-amplified electrochemical DNA assay. The DNA-immobilized PDMS surfaces were prepared by salinization of the surfaces with 3-mercaptopropyltrimethoxysilane firstly and then followed by the reaction between the 5'-acrylamide-modified DNA and the pendant thiol groups yielded on the surfaces after the salinization. An indium tin oxide interdigitated array (IDA) electrode array was used as the detector provides a steady-state current which indicated the concentration of hybridized DNA. As shown in Figure 2-2, the microfluidic system was composed of two flow channels (150 μm wide, 30 μm high) and an incubation chamber (400 μm wide, 30 μm high) with IDA sealed on the bottom PDMS surface. In their study, the detection limit of the DNA target was 1 nM in a volume of 20 nL, which corresponds to 20 attomoles of DNA.

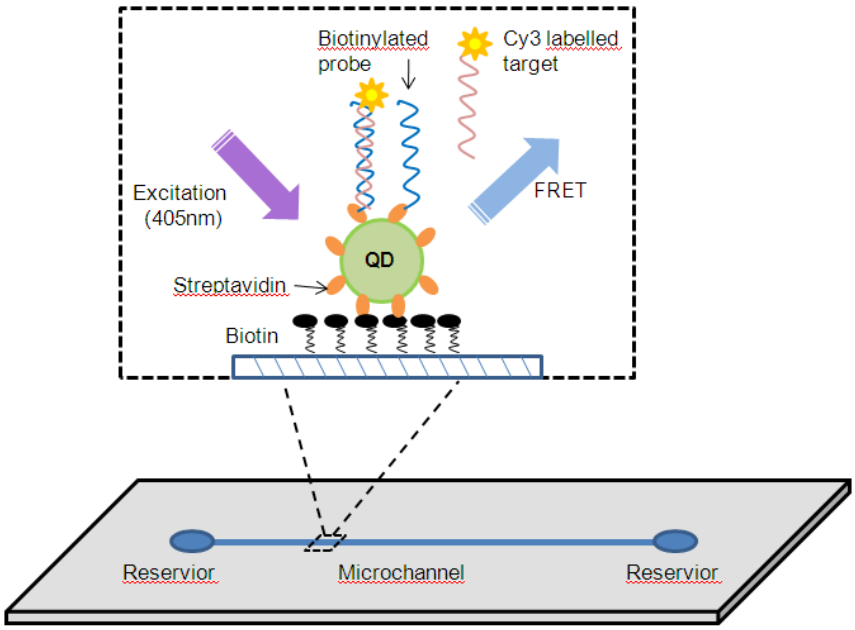

Figure 2-3 Schematic of the principle of the microfluidic hybridization assay using quantum dots and FRET (Tavares et al., 2010)

Tavares et al. (2010) developed a DNA hybridization assay microfluidic chip based on the fluorescence resonance energy transfer (FRET) and streptavidin coated CdSe/ZnS quantum dots (peak PL at 525 nm). The schematic of the microfluidic chip is shown in Figure 2-3. The streptavidin coated CdSe/ZnS quantum dots, oligonucleotide probes and target DNA were introduced sequentially to the microchannel by electrokinetic delivery. The streptavidin coated CdSe/ZnS quantum dots in this system had two functions. One is to act as a scaffold for immobilizing the oligonucleotide probes onto the microchannel surface by utilizing the high-affinity biotin-Streptavidin interaction; the other function is to be a donor in FRET, where Cy3 label associated with the target DNA was the acceptor. In their system, no detectable nonspecific adsorption of DNA was observed and showed its potential in multiplexed detection of DNA targets. The probes DNA can also be immobilized onto chemically modified gold surfaces for the hybridization detection by using surface plasma resonance (SPR) technique. SPR can provide extremely high sensitivity and low detection limit. However, it normally requires bulky and costly optical instruments, which are not favorable for miniaturization and integration (Lee et al., 2001; Sonntag et al. 2009). Malic et al. (2009) combined a digital electrowetting-on-dielectric microfluidic device to a surface plasma resonance biochip platform for DNA

hybridization. Thiolated DNA probes were covalently attached to gold surface via sulphur-gold linkages and active control of the immobilized probe density was achieved by using digital electrowetting-on-dielectric device. It was found that the DNA hybridization efficiency could be enhanced when DNA probes were immobilized under an applied potential rather than passive immobilization. In a DNA hybridization chip developed by Schüler et al. (2009a, 2009b), the micro electrodes were deposited on the surface of the DNA-chip with a gap between each other. After modifying the DNA-chips chemically with (3-glycidyloxypropyl)-trimethoxysilane, the single stranded (ss) capturing DNA probes modified with a C6-Aminolink on the 5' or 3' end were attached to modified surface in the gap between the electrodes. After the hybridization event of the target molecules, a streptavidin-horseradish-per oxidase- polymer was bound onto the hybridization complex in the gap between electrodes. In order to obtain the electrical signal, an enzyme-induced deposition of silver nanoparticles was introduced into the gap to bridge the gap between electrodes by a conductive silver layer. Thereby, the changing of the conductivity over the gap could be measured and hence the hybridization results could be analyzed. Figure 2-4 shows the structure of the DNA-chip and the steps of the assay. By their system, 60 minutes were required to reach the detection limit of 50 pM which is comparable to the conventional hybridization assay with the flow cell. They found that a significant reduction of the hybridization time could be realized by increasing the concentration of the target samples.

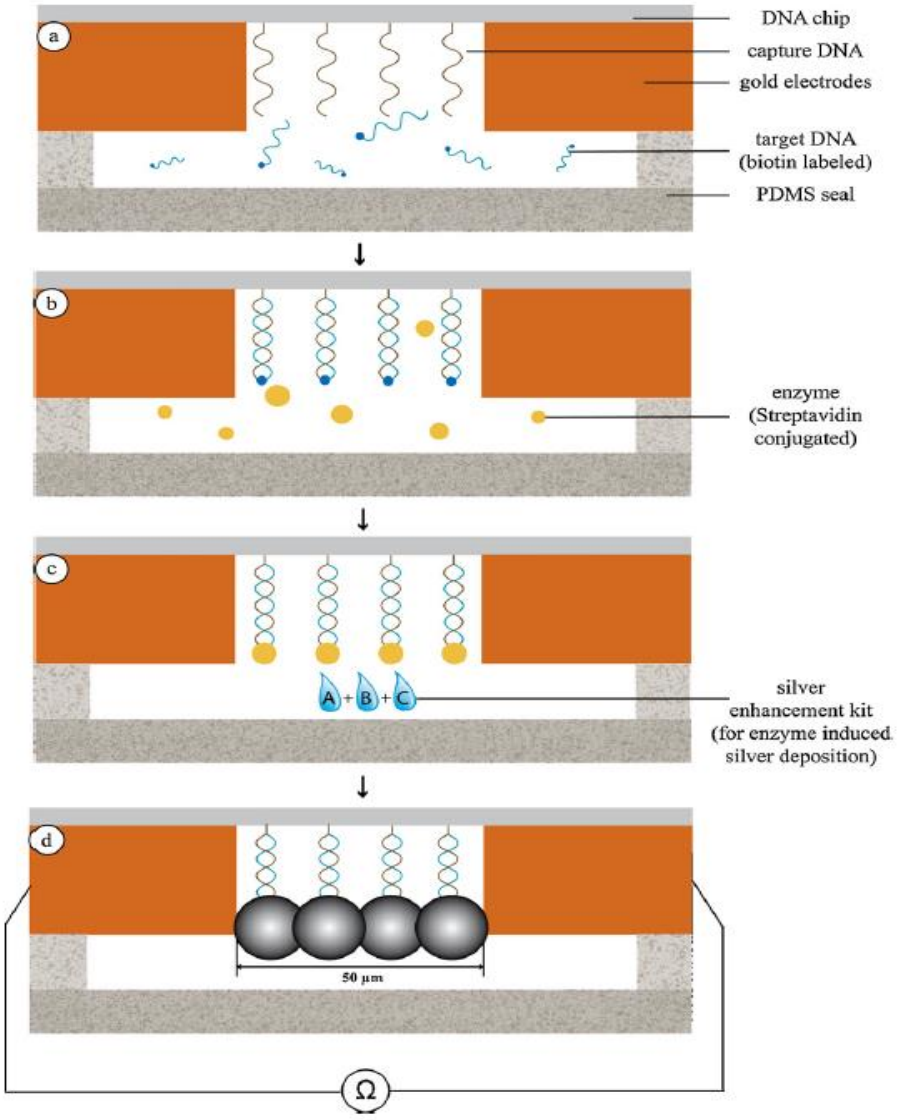

Figure 2-4 Schematic of the principle of an electrical DNA hybridization chip (a) capture ssDNA probes are immobilized on the surface of the gap between the electrodes; (b) biotin labelled target-DNA hybridizes to its specific probes; (c) streptavidin-horseradish peroxidase conjugate is bound to the biotin modification; (d) silver nanoparticles are deposited resulting from the enzymatic reaction. The read-out could be performed by either electrical measurement or optical transmission measurement via the properties of the deposited silver nanoparticles (Schüler et al., 2009b)

Table 2-1 gives a summary of some representative surface-based DNA hybridization chips. One limitation of the surface-based DNA hybridization chips is the immobilization of the probes on surfaces,

i.e., the oligonucleotides need to be fixed on a surface. The reliability and the complexity of this immobilization process affect the flexibility, the cost and the operation of the microfluidic DNA hybridization assays. Another limitation of the surface-based DNA hybridization assays is the relative long time for hybridization reaction, typically requires several hours or more because it generally depends solely on the diffusion of target DNA to the surface-bound probes (Jobs et al., 2002). However, Erickson et al. (2004) introduced an electrokinetically controlled DNA hybridization microfluidic chip based on surface DNA hybridization. They utilized electro-osmotic driven flow in their system to deliver samples/ reagents, which increased the reaction rate. By their system, the entire processes from sampling to obtain the hybridization detection result only required 5 min, meanwhile with a limit of detection at 50 pM. Furthermore, the bonding techniques used in making the microfluidic chips may have a significant influence on the surface probe-based microfluidic DNA hybridization. The chip bonding techniques (e.g., thermal, UV light, plasma treatment) may damage or denature the coated DNA molecules because of the high temperature or vapor effects and hence could decrease the efficiency of the assay (Brennan et al. 2009).

Table 2-1 Summary of representative surface-based microfluidic DNA hybridization chips

References	Attachment initiator	Sample volume	Detection limit	Sample type	Assay time and temperature	Chip materials	Flow method	Detection method
Schüler et al. (2009b)	_____	30 μL	50 pM	Biotin-labelled DNA	60 min, 95 ℃	Glass	_____	Electrical
Erickson et al. (2004)	Chemical	16 nL	50 pM	Cy3-labeled targets DNA	5 min, RT	PDMS	Electrokinetics	Fluorescence
Noerholm et al. (2004)	UV-light	~1mL	10 nM	Fluorescently labelled DNA	300 min, 80 ℃	Polymer	Syringe pump	Fluorescence
Benoit et al. (2001)	Chemical	50 μL	40 pM	Fluorescently labelled oligodeoxynucleotide (ODN) probe	180 min, RT	Glass	Pump	Fluorescence
Shamansky et al. (2001)	UV light	_____	50 μM	ROX-labelled DNA	60 min, RT	PDMS	_____	Fluorescence
Liu et al. (2004)	Chemical	20 nL	1 nM	Fluorescein-labelled DNA	230 min, RT	PDMS	Mechanical clamp	Electrochemical
Sonntag et al. (2009)	Light of 810 nm	90 μL	50 nM	Fluorescently labelled RNA	>90 min, 60 ℃	PDMS	Syringe pump & switching valve	SPR
Lee et al. (2001)	Near-infrared light	1 μL	~10 nM	Fluorescently Labelled DNA	>60min, RT	PDMS	Pressure Pumping system	SPR
Malic et al. (2009)	LED source of 800 nm	~1 μL	500 pM	Label-free DNA	15-20 min, RT	Glass	Electrokinetics	SPR
Huang et al. (2010)	UV-light	1 μL	100 pM	FITC labelled DNA	~30 min， RT	PDMS & Glass	Shuttle flow	Fluorescence

2.4.3 Bead-based microfluidic DNA hybridization assays

In order to address the drawbacks of the surface-based DNA hybridization assay aforementioned, bead-based technology are developed and the beads are used as modifiable surfaces. Various microbeads are commercially available and numerous target oligonucleotides can be attached onto the surface of the microbeads. Microbeads can be easily introduced into microfluidic systems. The customized probes attached on the microbeads can increase the flexibility of the hybridization assays in terms of detecting a desired target species and multiple targets simultaneously. In addition, using microbeads can significantly increase the total available reaction surface area, and hence result in higher assay sensitivity. Microbeads can be magnetic beads, metal nanoparticles (gold nanoparticles), liposomes or polymer beads. Among these materials, magnetic beads are widely used in most current microfluidic DNA hybridization assays.

Kim et al. (2006b) studied the hybridization efficiency when using probe-conjugated microbeads in a microfluidic DNA hybridization device. Target concentration, probe surface concentration and flow rate were the studied parameters to figure out the optimized conditions for enhancing the capture efficiency. They found that the microfluidic system could achieve a detection limit of ~10^{-10} M DNA, a selectivity factor of ~8×10^{3} and typical hybridization time of the order of minutes. Li and He (2009) employed a DNA hybridization assay based on magnetic beads with chemiluminescence (CL) and chemiluminescent imaging detection to detect sequence-specific DNA related to the avian influenza and obtained a detection limit at levels as low as 0.1 pM. Cheng et al. (2010) presented an open flow-based microfluidic DNA hybridization platform by employing dielectrophoresis (DEP). Probe functionalized silica nano-colloids were dielectrophoretically trapped in a cusp-shaped geometry. With the nanocolloid assembly, the fluorescently labelled target DNAs were trapped due to the hybridization and concentrated at the cusp for detection. This method offered pico-molar sensitivity, rapid hybridization in less than one minute at 100 pM concentration with no repeated washing, heating and other complicated hybridization buffers involved.

Kwakye and Baeumner (2003) developed microfluidic biosensor based on DNA hybridization, as shown in Figure 2-5. They employed two types of microbeads, super-paramagnetic beads and dye encapsulated liposomes, into their microfluidic system for immobilizing two different DNA probes complementary to the sequences of the target pathogen RNA to serve as the capture probe and detection probe, respectively. During the sensing process, a mixture of target RNA sample and probes reagents were drawn into the device via a syringe pump. After the probes hybridized to the target RNA, the liposome-target-bead complex was captured on a magnet housed at the capture zone. The concentration

of the target RNA was then quantified by the fluorescent intensity illuminated from the captured liposomes on the hybridization complex. In this method, all reagents need to be mixed prior to be introduced into the microfluidic device and hence cannot achieve the automatic sequential operation. In addition, the using of the syringe pump as the liquid driving mechanism prevents the miniaturization and the integration of the entire microfluidic system.

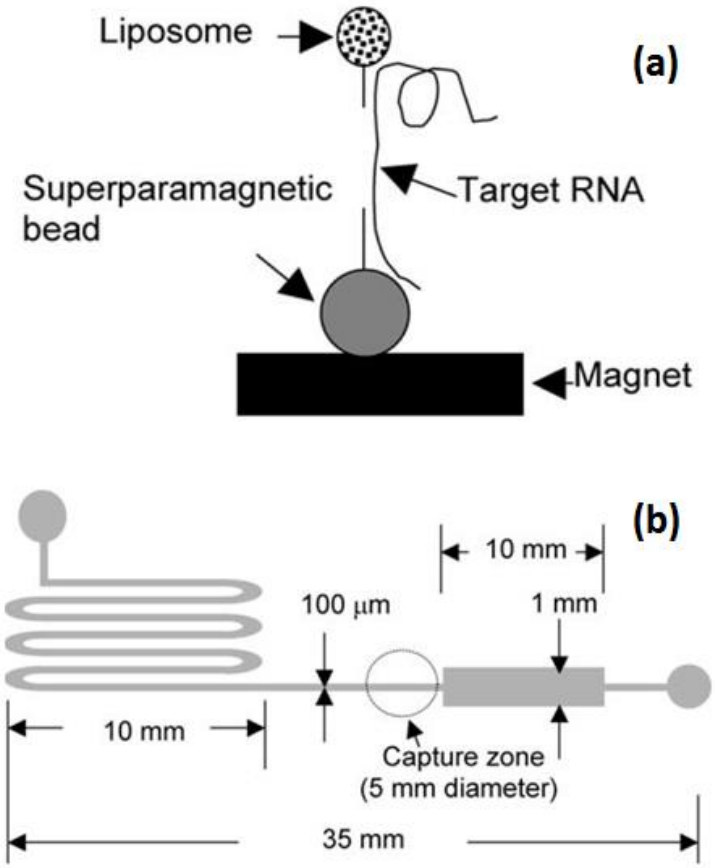

Figure 2-5 Principle and the schematic illustration of a microfluidic biosensor based on DNA hybridization. (a) Principle of the biosensor: when target RNAs is present, they hybridize to both the capture probes coated on a magnetic bead and the detector DNA probes coated on the liposome. The hybridized complex is subsequently captured by a permanent magnet; (b) Layout and dimensions of the microfluidic biosensor (Kwakye and Baeumner 2003)

Similarly, Zaytseva et al. (2005) demonstrated a beads-based microfluidic biosensor for pathogen detection based on DNA/RNA hybridization and liposome signal amplification. The total time required for an assay was approximately 15 min including the sample incubation time. Seong et al. (2002) presented a microbead-based microfluidic device combining weirs and hydrogel plugs (poly (ethylene glycol) diacrylates) for conducting DNA hybridization. The layout and dimensions of the microchannel

network are shown in Figure 2-6. The hydrogel plugs were used to separate the three chambers as well as facilitated the microbeads packing. Weirs were at the outlets of each microchamber. The using of hydrogel plugs and the weirs in their system overcame the difficulties in retaining the packed microbeads. Pump-driven flow was utilized to deliver different DNA probes-functionalized microbeads used for detecting specific DNA oligonucleotides in DNA mixtures into the three hybridization micro-chambers A, B and C via inlets I1-I3 and outlets O1-O3 subsequently. DNA mixture for detection was loaded from wells 3, 4 and the driving potential was applied via electrodes in wells 5 and 6. After hybridization, unhybridized target DNA was washed away by rinsing with buffer solution from wells I1-I3 and 1-3. The hybridization product was subsequently observed by a fluorescence microscopy. The hybridization reaction could be completed within 1 min in their system. By treating the final hybridization product with 0.1 N NaOH, the targets could be independently released and recovered from the microbeads. However, in their system, two flow-driven modes (pressure-driven flow and electrophoresis) were applied, which increase the complexity of operating the microfluidic system.

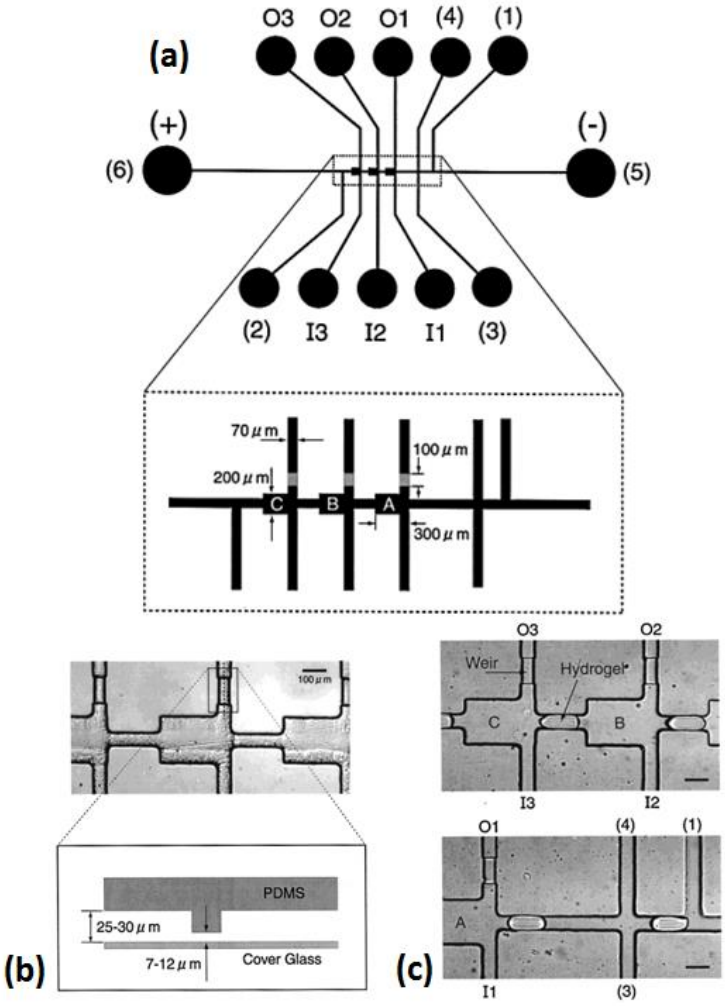

Figure 2-6 Schematic illustration and the optical image of the microchannel network of a microbead-based microfluidic device for the DNA hybridization. (a) The layout of the microchannel network. Paths I1-O1, I2-O2 and I3-O3 are used for flushing unpolymerized PEG-DA hydrogel liquid and dispensing biotinlated ssDNA probes. Well 3 is used for loading the target ssDNA solution. Electrodes are placed in wells 5and 6 to generate the driving potential. (b) The optical image of the microchannel network with the structure and dimensions of the weir. (c) The optical image of the microchannel network with hydrogel microstructures (Seong et al. 2002)

Senapati et al. (2009) developed a rapid, portable bead-based microfluidic platform for DNA hybridization. Carboxylated silica beads attached with a species-specific amino functionalized oligonucleotide primer (27-mer) were used to capture the fluorescently labelled target DNA. Their microfluidic chip carries a T-shaped microchannel. Microchambers for trapping the 10 μm functionalized beads were created by fabricating filters with pore dimension of 2~3 μm on both sides of the horizontal arm of the T-junction. In the hybridization process, the functionalized beads were packed in the micro-chamber firstly, followed by dispensing target DNA through the microchannel to the chamber. A laser scanning confocal microscope was used to observe and record the fluorescence images of the silica beads trapped within an 8×10^{8} μm^{3} small microfluidic chamber and then assessed the DNA hybridization. They claimed that their microfluidic method could enhance the hybridization dramatically due to the reduction of the diffusion time between the target DNA molecules and the surface of the probe-functionalized silica beads because the scale of the microchannel is extremely small. In addition, by introducing the beads, the sensitivity and the detection limit of the system were enhanced due to their larger surface area per unit volume.

By coupling streptavidin coated paramagnetic microbeads, Berti et al. (2009) proposed an electrochemical geno-sensor for hybridization detection on a commercial microfluidic platform produced by DiagnoSwiss S.A. Sandwich hybridization strategy was applied in their study. A PCR product serving as the target DNA sample was recognized by a capture probe and a biotinylated signalling probe. The modified-beads with biotinylated capture probe were introduced in a disposable cartridge bearing eight parallel microchannels etched in a polyimide substrate and incubated with target hybridization solution (diluted PCR products in 0.15μM of biotinylated signaling probe and phosphate buffer). After hybridization, the modified beads were trapped by magnets at the top of each microchannel, followed by the direct electrochemical detection of the hybridization complex via the microelectrodes in each microchannel. Quantitative determinations of targets concentrations were later obtained by analyzing the electrical chemical signal via the software. The system could obtain a detection limit of 0.2 nM with a RSD% = 6 with when applied to detect the PCR amplified samples.

Wen et al. (2007) and Yang et al. (2009) developed a label-free microfluidic DNA hybridization assay using cationic fluorescent water-soluble polymer and avidin-agarose beads for detecting DNA/mRNA. The fluorescent polymer served as the fluorescent polymeric transducer. The layout of the PDMS microchip is shown in Figure 2-7. The chip has a narrow straight microchannel (20 μm width × 60 μm deep) with a series of micro-chambers (80 μm width × 60 μm deep) on it. The micro-beads (50 μm in diameter) modified with capture probes were transferred into the micro-chambers by a vacuum tweezer first. Then a 100nM fluorescent polymer solution was introduced into the microchannel by gravity-driven flow. After washing away the superabundance polymers, target DNA/ mRNA was added into the microchannel and incubated for 50 min at 50 ℃. Fluorescence images of the micro-beads (probe)-target-polymer complex were captured after the hybridization reaction by an inversed fluorescence microscope for further data analysis. The achieved detection limit is around 50 pM and the detection could be obtained in about one hour.

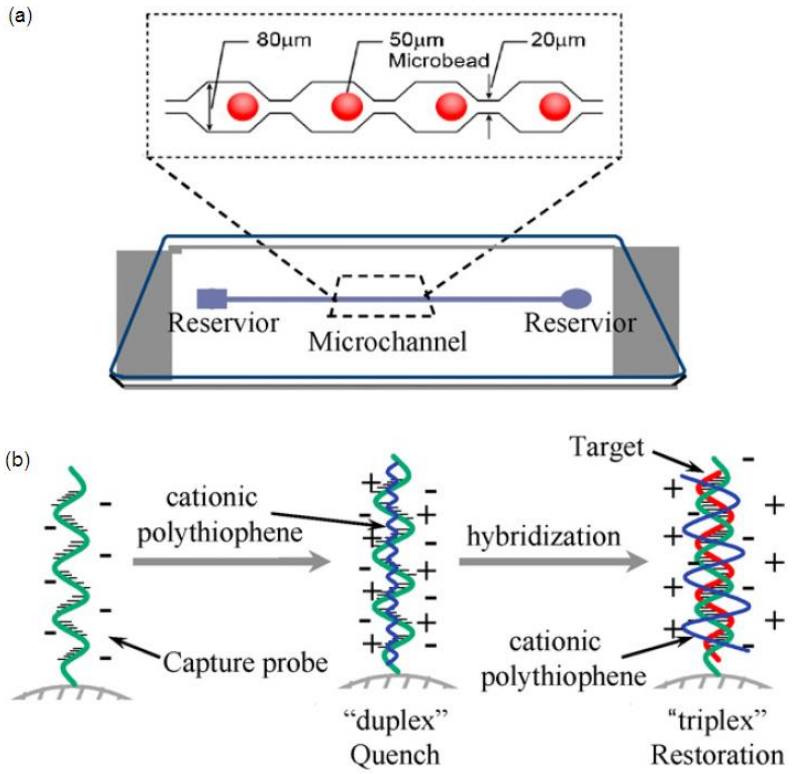

Figure 2-7 (a) Schematic of the DNA detection chip; (b) the process of the interaction between cationic polymer and capture probes modified on the surface of the micro-beads via electrostatic interactions (Yang et al. 2009)

Table 2-2 gives a summary of some representative bead-based DNA hybridization chips. Using beads as solid support for the capture probes in microfluidic DNA hybridization assays has numerous

advantages. The high surface-to-volume ratio of the beads is a main advantage because they can provide more hybridization sites for target DNA and consequently achieve higher sensitivity and the lower detection limit than the surface probe-based hybridization method. In addition, beads offer not only an easier way for coating/ immobilizing probes on their surfaces, but also a more effective solution mixing within the microfluidic channels. However, packed beads may generate a high resistance for pressure-driven flow in microfluidic channels.

Table 2-2 Summary of bead-based DNA hybridization assay

Reference	Bead type	Sample volume	Detection limit	Sample type	Assay time and temperature	Chip materials	Flow method	Detection method
Kwakye et al. (2004)	Superparamagnetic beads & Liposomes	1 μL	10 pmol	RNA	20 min, RT	PDMS & PMMA	Syringe pump	Fluorescence
Seong et al. (2002)	Proactive streptavidin-coated microspheres	_____	_____	Fluorescein-labelled ssDNA	~90 min, RT	PDMS	Pressure/ electrophoresis	Fluorescence
Berti et al. (2009)	Paramagnetic micro-beads	50 μL	0.2 nM	Synthesized DNA	90 min, RT	Commercial microfluidic-based platform, (DiagnoSwiss S.A)	Pumping device and valves	Electrochemical
Senapati et al. (2009)	Carboxylated silica beads	100 μL	100 pM	Fluorescently labelled DNA	1 h, 50 ℃	Glass	Pressure	Fluorescence
Yang et al. (2009)	Avidin–agarose beads	2 μL	0.05 nM	Synthesized DNA & mRNA	1 h, 50 ℃	PDMS	Gravity	Fluorescence
Zaytseva et al. (2005)	Paramagnetic beads	1 μL	_____	RNA	15 min, RT	PDMS	Syringe pump	Fuorescence
Kim et al. (2006)	Super avidin-coated microbeads	2 μL	~0.1n M	Fluorescently labelled DNA	~30 min, 25 ±2 ℃	PDMS	Syringe pump	Fuorescence
Wang et al. (2011)	Magnetic beads	15 μL	10 fg/ μL	DNA of MRSA	~30 min, 63 ℃	PDMS &Glass	Vacuum pump	Absorbance/ optical density analysis

2.4.4 Membrane/ film-based transducer for microfluidic DNA hybridization assays

Recently, membrane-based transducers, one of the chemo-mechanical sensing techniques, have been widely used in biosensors for detecting DNA, enzymes, antibodies and so on (Cha et al., 2008; Kang et al., 2010; Carlen et al., 2006; Satyanarayana et al., 2006). The basic principle of a membrane-based transducer is to convert a change in the concentration of a target sample of a biological reaction into an electronic signal, usually capacitance, via the deflection of the membrane or the changes in the resonance frequency of a sensitive membrane (Schaechter and Lederberg, 2004). The membrane transducer shows highly specific absorption/binding of the corresponding oligonucleotide molecules and the nonspecific absorption/binding can be further reduced by modifying the membrane surface such as altering the electrostatic charge on the membrane surface (Chandler et al., 2004). In their study, the immobilization or bio-molecular reaction can make the membrane deform and consequently the change in measured capacitance. The magnitude of capacitance difference indicates the change in the concentration of the target sample. By applying differential sensing, nonspecific bindings and disturbances such as pressure can be significantly minimized (Cha et al., 2008). The membrane transducers have advantages over many other transducers (microcantilever transducers) such as preventing nonspecific binding, higher sensitivity, better long-term stability, facilitating the integration to miniaturized microfluidic device. However, the production costs of the membrane-based transducers are relative higher.

As an example of the thin membrane transducers (TMT) developed to detect nucleic acid based biomolecular reactions (Cha et al., 2008; Choi et al., 2009; Kang et al., 2010), Kang et al. (2010) integrated a nanocomposite membrane-based chemomechanical transducer into a microfluidic device for DNA hybridization detection. The microfluidic device consists of a nano-membrane transducer with sensor components for capacitive readout, as shown in Figure 2-8. The multi-layer nanocomposite membrane was made by layer-by-layer assembling of polymers and single-walled carbon nanotubes (SWNTs). The SWNTs function as deformable structure responsive to surface stress and electrode for capacitance measurement. The thickness of the membrane is 26 nm. Probe DNA labelled with fluorescence dye was firstly immobilized on the surface of the nano-membranes. The hybridization process could change the surface stresses of the nano-membranes and hence cause a deflection. Consequently, this differential gap compared to the reference state (before the event) could be determined by the capacitance change, thereby the concentration of the target DNA can be evaluated. This nano-membrane transducer-based DNA hybridization assay was able to detect target DNA at the level of 0.1 μM and achieved a short detection time of a few hundred seconds.

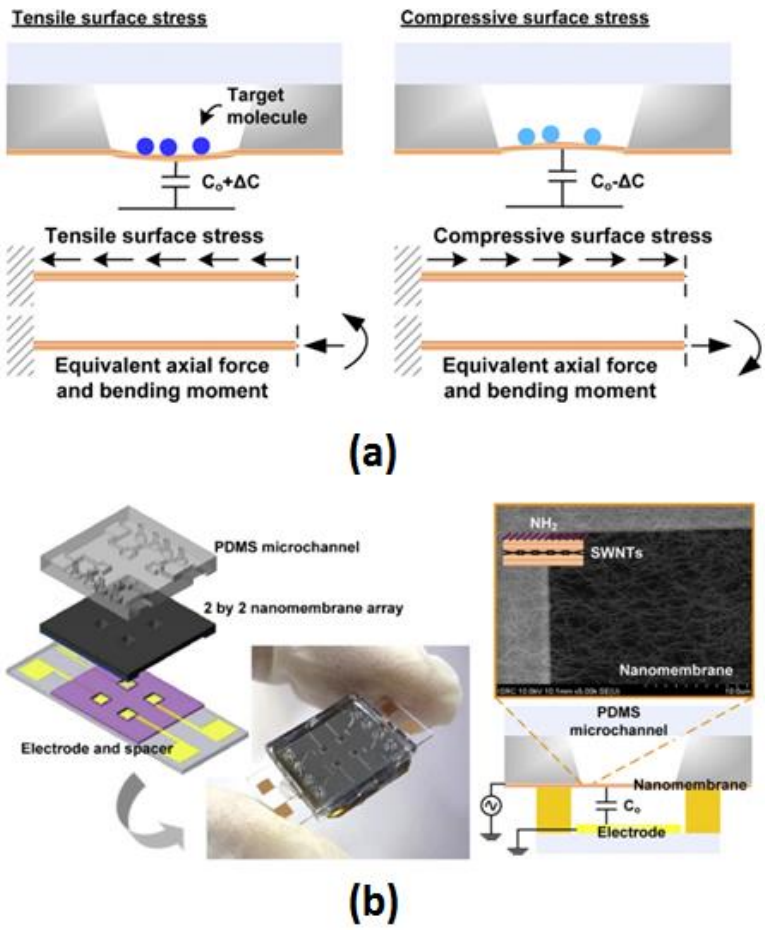

Figure 2-8 (a) The mechanism of the nano-membrane transducer. Deformation of the nano-membrane is actuated by the surface stresses generated by molecular interaction. (b) Schematic and actual picture of the fabricated nano-membrane transducer (Kang et al. 2010)

Misiakos et al. (2009) integrated a monolithic silicon optocoupler into a microfluidic biosensor for DNA and protein molecules detection. The core design of the optocoupler was a silicon nitride (Si_3N_4) film on which DNA probes were spotted. The microfluidic components on the top of the film (membrane) were used for dispensing reagents and target samples. The biochemical reaction (hybridization) could be determined by the changes in optical coupling efficiency and the detector photocurrent of the system. This optical biosensor was used to detect labeled and label-free DNA molecules and could achieve a sensitivity of a few nanomolar of analyte concentration. Hatakeyama et al. (2009) developed a microfluidic device by using a thin film transistor (TFT) photosensor and chemiluminescence detection strategy. Probe DNA molecules were immobilized on the photosensor surface. The use of chemiluminescence method in this DNA chip platform showed advantages over

fluorescence methods as it provided higher sensitivity and required simpler instrumentation. The assay was completed in less than one hour and obtained a detection limit of 0.5 nM.

Although the membrane-based transducers have the advantages of preventing nonspecific binding and achieving high sensitivity, the complicated fabrication process of thin membrane may prevent this method from being a low cost technique for DNA hybridization assays. In addition, the difficulties in miniaturization and integration of the membrane with the microfluidic chips and detection readout system are concerns.

2.4.5 Other methods in microfluidic DNA hybridization assays

In addition to the aforementioned types of microfluidic DNA hybridization assays, there are a couple of other formats. For instance, some researchers (Javanmard and Davis 2011) combined the surface-probe and the bead modification methods with integrated active microfluidic components to shorten the assay procedures; some others (Zhang et al. 2009) utilized hydrogel as the solid support or medium of the hybridization.

Javanmard and Davis (2011) demonstrated an electrical detection of surface/bead hybridized DNA hybridization in a microfluidic chip, see Figure 2-9. During a hybridization process, DNA probes were immobilized on the surface of the microchannel (200 μm wide; 50 μm deep) by physical adsorption firstly. Target DNA sample was then injected into the microchannel and incubated for 30 min. Later, 10 μm streptavidin-modified beads were injected into the microchannel and incubated for 1 min. After washing away the unbound beads, the electric current across the channel was measured via electrodes by a function generator and a current preamplifier. The current signal magnitude would dramatically decrease if the bead attached to the hybridization complex. The detection limit achieved by their system was an order of magnitude better than that of a conventional fluorescent detection system. Additionally, this method does not need for any fluorescent labels.

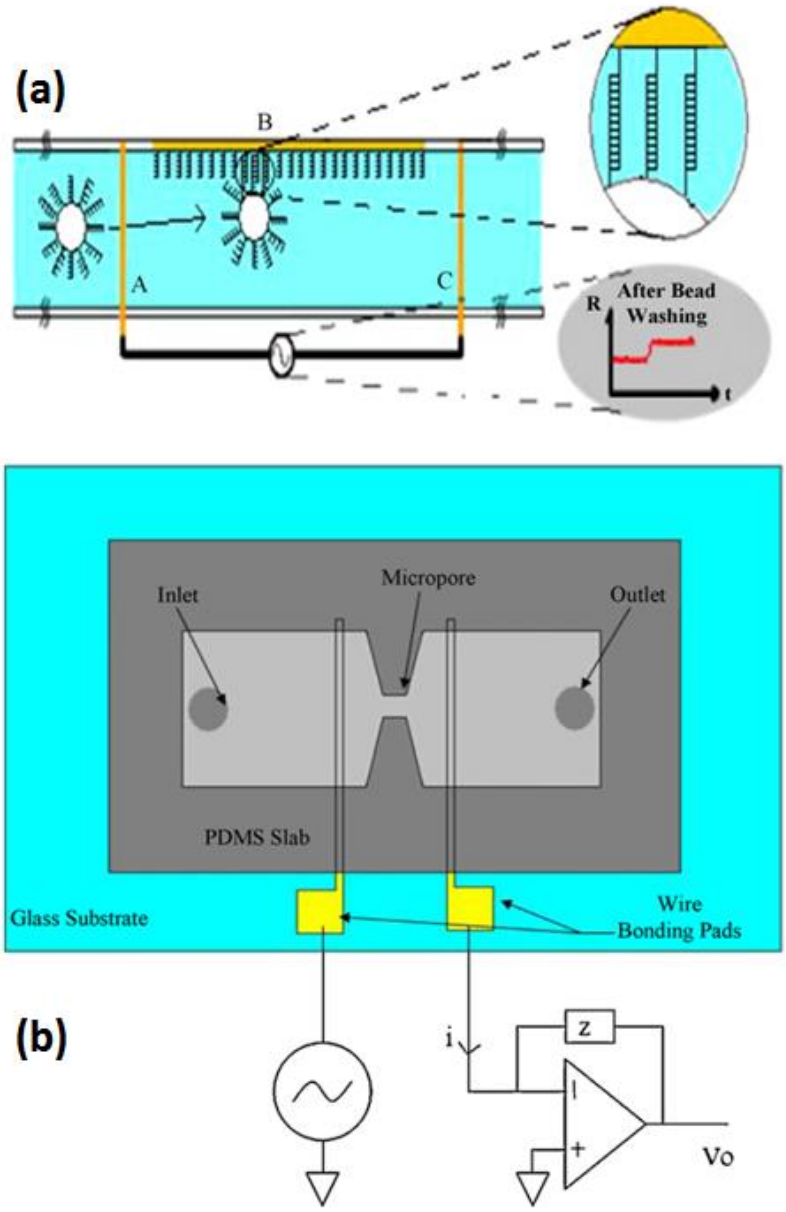

Figure 2-9 (a) Schematic of the microfluidic DNA hybridization biosensor. Biotinilated capture probes are immobilized on the surface of the microchannel. After the hybridization of the target DNAs functionalized with a biotin molecule with the capture probes, streptavidin coated beads are introduced to bind onto the biotinilated target DNA. (b) Schematic of the electrical setup of the microfluidic biosensor for measuring the current across the channel (Javanmard and Davis 2011)

The bio-reaction rate in lab-on-a-chip devices can be enhanced by integrating active microfluidic components such as micropumps and micromixers in the chips. Mai et al. (2007) integrated a micropump, a micro ring mixer and micro-biofilters, into an electrochemical biosensor for rapid pathogen detection. The microfluidic chip consists of two layers, a liquid "flow" layer and a pneumatic "control" layer, the overlap areas of these two layers on the control layer were used as valves or pumps acting on the liquid flow layer. An external electromechanical valve system with pneumatic pressure and a syringe pump was used to control the microvalves and hence the volumetric fluid flow of reagents/ samples. Target 16S rRNA was detected by this system and showed a four-fold improvement in the amplitude of the hybridization signal, when compared to flow through the microfluidic structure without mixing or with manual mixing. Similarly, Wang et al. (2011) developed a microfluidic chip using fluid mixing strategy and demonstrated by experiments that enhanced hybridization efficiency was achieved while the nonspecific adsorption was minimized. It is believed that these improvements were made due to the strong shearing force generated during the mixing process. However, integrating these active pumping and mixing components in microfluidic chips requires complicated microfabrication techniques and are costly.

Hydrogel materials have been widely used in microfluidic devices serving as plugs or valves (Sung et al., 2009; Dhopeshwarkar et al., 2005; Thomas et al., 2006; Wang et al., 2005). Hydrogels can be rapidly created by in-situ photopolymerizing monomer solutions in the microfluidic channel. The nanopores within the polymerized hydrogels are permeable to DNA molecules so that they can be transported through the gel under electrokinetic or pressure driving force. Hydrogel materials have been used in the microfluidic DNA hybridization assays. Olsen and Zangmeister et al. (Olsen et al., 2002; Zangmeister and Tarlov 2004, 2003, 2009) immobilized cross-linked ssDNA probes into hydrogel matrixes via photopolymerization technique to form two separate plugs embedded within a microfluidic channel. The immobilized DNA probes retained activity so that they were able to hybridize with target DNA/RNA strands to form duplexes as they electrophoresed through the hydrogel plugs. Since the DNA probes were fluorescently tagged while the DNA targets were not, the hybridization process could be fluorescently detected by observing the DNA displacement between these two hydrogel plugs. The time scale of this displacement assay was found to increase by decreasing the concentration of the fluorescently-tagged probe DNA, and the limit of detection for complete displacement was 0.5 μM when 20-mer probes were immobilized. The advantages of this approach are the abilities of fast sensing due to the directed electrophoretic transport of reagents/samples and the non-labelled target DNA detection. In addition, this method could achieve multiple targets detection simultaneously by

immobilizing custom-designed probe sequences. The illustration of the principle is shown in Figure 2-10.

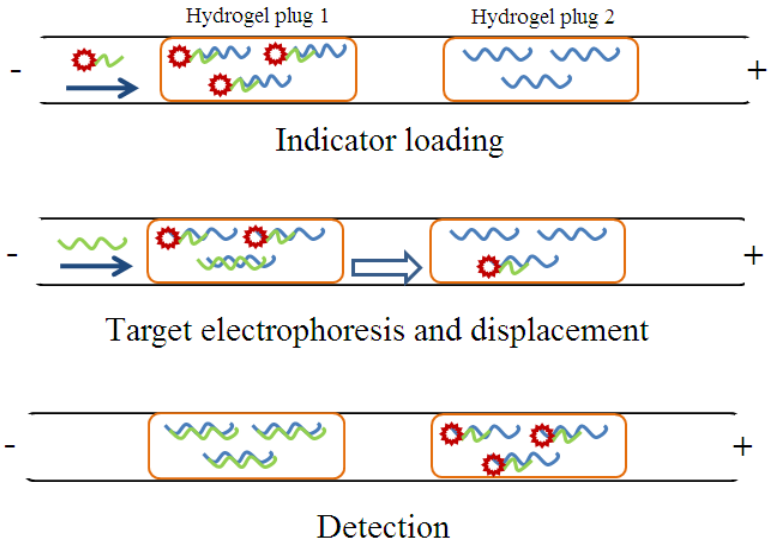

Figure 2-10 Schematic of the principle of the displacement assay. After the two gel plugs (with immobilized probe) are loaded into the channel, a fluorescent tagged 10-mer indicator oligomer is loaded into the first gel plug followed by electrophoretically introducing the unlabeled 20-mer target; during the hybridization, the 10-mer is displaced due to the higher efficiency between the 20-mer target and immobilized probe. At the end of the displacement assay, the displaced indicator is captured and detected in the second gel plug (Zangmeister and Tarlov 2004).

In addition, Lewis et al. (2010) studied the fabrication of uniform DNA-conjugated hydrogel microparticles for the application in rapid and high-throughput DNA hybridization assays. Brennan et al. (2009) proposed a technique of immobilizing probe DNA molecules in a sealed microfluidic system using (3D) hydrogel structures. Photo-initiated prepolymer material poly-ethyleneglycol (PEG) and photo-polymerisation techniques were employed to form the 3D structures covalently attached to the channel surface. A full hybridization assay was conducted to evaluate the selectivity and sensitivity of these hydrogel structures. The results showed significant time advantage over conventional 2D array synthesis techniques.

DNA microarray technology provides a high-throughput analytical tool for DNA hybridization detection. However, the relative long processing time for hybridization reaction is a concern due to the diffusion-limited reaction kinetics of the target samples with the surface-bound probes in the chambers.

When combining the microfluidic techniques with DNA microarray, the hybridization time is significantly reduced as well as the sample consumption due to the large surface-to-volume ratio and the minute diffusion distance (Wang and Li 2011; Benn et al., 2006). Chen et al. (Chen et al., 2011)) demonstrated a CD microfluidic DNA microarray for phenylketonuria (PKU) screening. Reciprocating flow generated by the centrifugal force was employed to operate rapid DNA hybridization. A full hybridization assay could be completed in 15 min by this microfluidic microarray with a sample consumption of 1.5 μl. Penchovsky (2013) presented a fully automated and programmable DNA microarrays on a bead-based microfluidic platform. The microreactors were etched on a silicon wafer. The microfluidic design of cascade chambers in this approach enabled all the procedures of the DNA hybridization detection to be performed fully programmable.

2.4.6 Summary of microfluidic DNA hybridization assays

An overview on the latest development and the applications of microfluidic DNA hybridization assays was presented here. DNA hybridization has been a powerful and versatile technique applied in biomedical diagnostic assays. Combining the microfluidic technology with DNA hybridization assays has proven to have many advantages over the conventional DNA hybridization methods. By coupling with microfluidic methods, sample consumption reduction and decreased non-specific target-probe binding can be achieved. The hybridization kinetics can be enhanced significantly when conducting the hybridization assay in a microfluidic channel due to its small dimensions. By choosing the proper microchannel designs (shapes or physical characteristics) or using active microfluidic pumps and mixers, the kinetic reaction rate can be further enhanced. Moreover, the selectivity and sensitivity can be significantly increased with the improved probe immobilization technique on the solid support. In particularly, the bead-based microfluidic platforms are promising because they can achieve rapid reaction kinetics and enhance the detection limit due to a high surface-to-volume ratio. The microfluidics-based DNA microarrays improved the diffusion-limited reaction kinetics of the conventional static DNA microarrays, meanwhile remain their distinct capability of high-throughput and low-cost.

However, currently, microfluidic DNA hybridization assays are facing some challenges, such as how to develop simpler and low-cost micro-fabrication methods for making the microfluidic DNA hybridization chips, how to simplify the procedures of sample pre-treatment and channel/bead/hydrogel surface modification, and how to develop and improve the integration approaches for facilitating the combination of various functional components into a single miniaturized device. There is no doubt that

with further improvements in the above-mentioned areas, rapid, integrated, high throughput and cost-effective DNA hybridization assay lab-on-a-chip systems with a high selectivity and sensitivity for point-of-care diagnostic detection can be achieved in the future.

2.5 Microvalves in microfluidic application

2.5.1 Mechanical microvalves

- **Active mechanical microvalves**

Mechanical active microvalves traditionally refer to those utilizing MEMS-based bulk or surface micromachining technologies, in which mechanically movable membranes are coupled to certain actuation methods. Various actuation methods have been widely employed in microvalve system, including electronic (Goll et al., 1997; Van der Wijngaart et al., 2002; Teymoori and Abbaspour-Sani, 2004), magnetic (Bae et al., 2002; Fu et al., 2003), thermal (Rich and Wise, 2003; Takao et al., 2005), piezoelectric (Rogge et al., 2004; Goettsche et al., 2005), bistable (Capanu et al., 2000) actuation, and so on. Figure 2-11 shows the principles of the main actuation methods. More information about mechanical active microvalves can be found elsewhere (Kwang and Chong. 2006; Zhang et al., 2007).

Another category in mechanical active microvalves is called the external active microvalves, which are actuated by the external systems, for example, pneumatic means (Kwang and Chong. 2006).

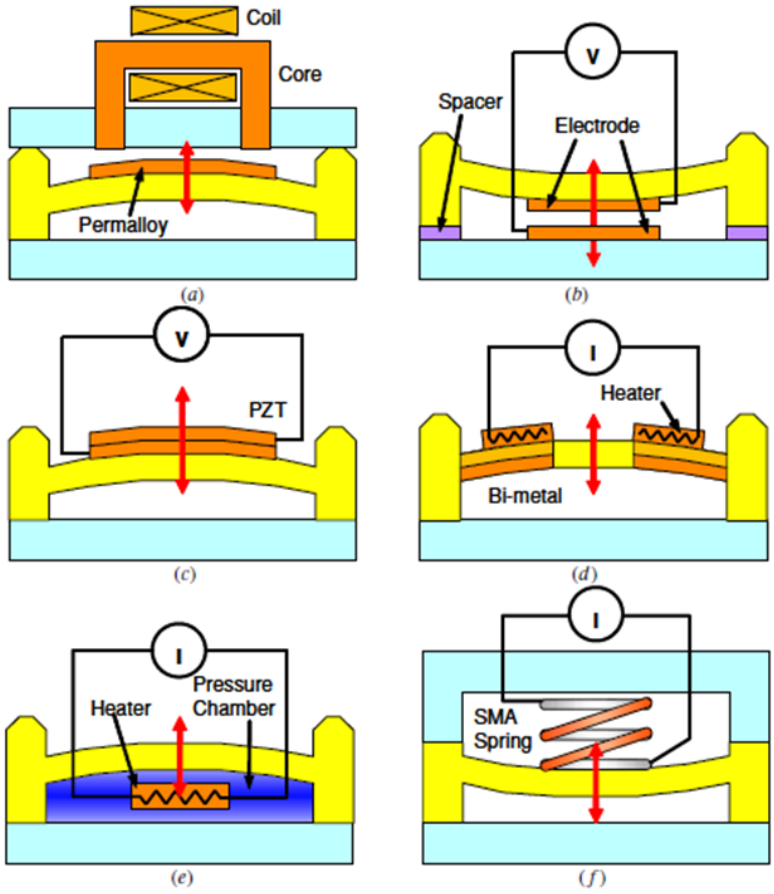

Figure 2-11 Illustrations of the main actuation principles of active mechanical microvalves. (a) eledtromagnetic; (b) electrostatic; (c) piezoelectric; (d) bimetallic; (e) thermopneumatic and (f) shape memory alloy actuation (Kwang and Chong. 2006)

- **Passive mechanical microvalves**

Most passive microvalves, which are regarded as a part of micropumps as well, are usually embedded in inlets and outlets of micropumps as mechanical moving parts (Kwang and Chong, 2006), such as flaps (Sim et al., 2003), membranes (Li et al., 2005), spherical balls (Yamahata et al., 2005) or mobile structures (Pan et al., 2005). These passive mechanical valves can only response to a forward pressure which is known as the diode-like characteristics. However, this one way working mode of these check valves dramatically limits the pumping performance of the micropump (Kwang and Chong, 2006). In addition, leakage in the passive valves is another concern because it reduces backpressure and pumping efficiency of the micropump.

- **External microvalves**

Externally actuated microvalves have been demonstrated for various microfluidic applications such as single cell sorting (Fu et al., 2002) and PCR (Lagally et al., 2004). These externally actuated valving systems, including modular built-in valves (Oh et al., 2005), rotational valves (Hasegawa et al., 2003), thin membrane (Lagally et al., 2004; Baek et al., 2005) or in-line (Studer et al., 2004) microvalves actuated by pressure and vacuum systems, are a significant advancement in microvalve technology, making them highly suitable for usage within a laboratory. Although externally actuated microvalves have the advantage of no leakage flows when applying high input pressures, it is difficult to miniaturize the whole system because additional external systems are required, and hence hinders their application in portable systems. (Kwang and Chong. 2006)

2.5.2 Non-mechanical microvalves

When mechanical microvalves used for the delivery of sample fluids in microfluidics, they normally need electromagnetic, piezoelectric or thermopneumatic actuation, which require high power consumption. In addition, both mechanical active microvalves and passive microvalves have the disadvantages of unavoidable leakage and relatively high cost due to their complicated structures.

Therefore, non-mechanical microvalves are an alternative when energy consumption is a main concern in the microfluidic system. For example, a microfluidic valve based on a stimuli-responsive material, no external power source is necessary. Non-mechanical microvalves refer to those can be realized by employing smart or intelligent materials, or those using the geometries or the surface properties of the microchannels to control flow (Kwang and Chong. 2006).

- **Active non-mechanical microvalves**

Active non-mechanical microvalves refer to those which can be operated by the smart or intelligent materials. Usually such non-mechanical active microvalves hold movable membrane structures which are actuated due to their properties as functionalized smart materials, for example, phase change or rheological materials (Kwang and Chong, 2006).

- **Phase change**

The phase change effect has been considered as a new actuation technique for the development of microvalves. Particularly, phase change microvalves based on the solid-liquid phase transition has been widely adapted to microfluidic applications due to their integrability and compatibility with lab-on-a-

chip device. The principle of phase change microvalves is simply based on the phase change nature of the material. These materials can be hydrogel (Wang et al., 2006), paraffin (Pal et al., 2004, 2005). These materials can be used either as a meltable plug (Felton, 2003) or a deformable membrane (Rich and Wise, 2003) to realize a microvalve.

A special type of hydrogel is the environment- sensitive, stimuli-sensitive, or "smart" hydrogel. These gels are capable of changing their degree of swelling reversibly and reproducibly by more than one magnitude in response to various quantities such as temperature (Richter et al., 2008), pH value (Eddington and Beebe, 2004), ion strength, and exposure to light (Sugiura et al., 2007), influence of electric or magnetic fields (Ghosh et al., 2009), etc.

Song et al. (2008) utilized a low melting point polymer, polyethylene glycol (PEG), to fabricate and operate an electrothermally actuated microvalve based on the large volume change (of up to 30%) upon phase transition of the material. As shown in Figure 2-12, the valve consisted of a gas-permeable elastomeric membrane and the PEG polymer between two etched glass plates, forming a multilayer chip. PEG polymer was in the bottom (control) layer, where Pt/Ti was patterned under the PEG reservoirs to form heating elements. When PEG polymer was heated, the volume expansion was used to actuate the membrane resulting in the seal of the microfluidic channels in the upper etched glass plate. The closing time of this valve could be realized in seconds, however, the opening time required several minutes.

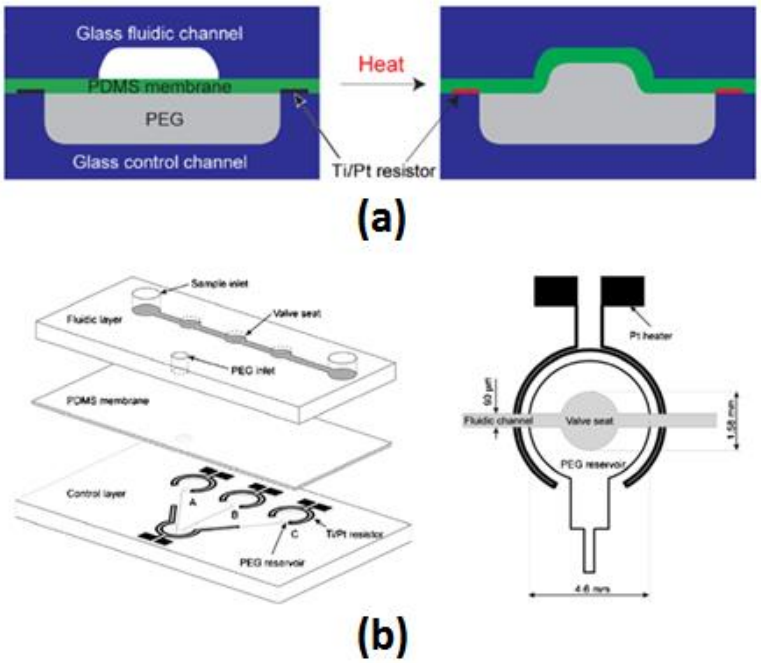

Figure 2-12 An electrothermally actuated microvalve utilizing a low melting point polymer, polyethylene glycol (PEG): (a) side view of the microvalve during the open and closed states (not to scale). When heating, the PDMS membrane deformed to seal the channel by volumetric expansion of the PEG during its phase transition from solid to liquid (b) Schematic of the microfluidic chip structure and the valve dimensions. (Song et al., 2008)

Li Z. et al. (2010) presented an array of thermalresponsive hydrogel-based (poly (N-isopropylacrylamide) (PNIPAAm)) multivalves for microflow injection analysis on a glass microfluidic chip. The thermal-actuated PNIPAAm monolithic plug valves were synthesized inside vinylized glass microchannel within a time interval of 1min via photopolymerization in water-ethanol (1:1) medium by using the hydrophobic initiator. The micro-fluids in microchannels was controlled by the thermal-switchable swell-shrink behavior of PNIPAAm. The moderate tolerating backpressure of such prepared valves was 0.45 MPa.

Ayala et al. (2007) reported a miniaturized pH-sensitive hydrogel-microvalve for implementation in a microfluidic system. The microvalve was fabricated by soft lithographic methods and activated by use of different pH-values. The actuator principle was tested by using a pH 1- and a pH 13-solution successively. They found 16 minutes were the most adequate for polymerizing the hydrogel. The response time of this pH-sensitive hydrogel-valve was 2.5 s.

Baldi et al. (2006) demonstrated a stimuli-responsive hydrogel-based microvalve on a silicon membrane. The silicon membrane carried an array of orifices, where stimuli-sensitive hydrogel was polymerized to function as microvalves. The microvalve was closed when the hydrogel completely occupied the void space of the orifice, resulting the blocking of the pressure-driven fluid flow. The microvalve was open when hydrogel shrank, letting fluid to flow through the opened gap. In their study, temperature, pH, and glucose concentration sensitive hydrogels were tested in the microvalve and the measured response times of which were 10 s, 4 min, and 10 min, respectively.

A microvalve controlled by light irradiation is one of the most attractive components for fluid manipulation on integrated microfluidic device because light irradiation enables non-contact operation and local light irradiation enables independent manipulation of multiple fluids. Several research groups have reported fluid manipulation by means of surface wettability change induced by light irradiation (Liu et al., 2006).

Sugiura et al. (2007) fabricated multiple photoresponsive hydrogel-based microvalves independently controlled by local light irradiation. The photoresponsive hydrogel was developed with the spirobenzopyran chromophore (pSPNIPAAm) functionalized poly (N-isopropylacrylamide) by in situ photo-polymerization in microchannels. The gel was supported by the micropillars fabricated in each branch channel. 18-30 s of the blue light irradiation was found adequate to irradiate the pSPNIPAAm gels to induce their shrinkage, resulting in the microvalves to open. The microvalve control by light irradiation has the advantages of non-contact, independent, and parallel fluid manipulation.

Ghosh et al. (2009) reported an oscillating magnetic field-actuated microvalves. Thermo-sensitive polymer network (-poly (N-isopropylacrylamide) (PNIPAAm)) mixed with tunable magnetic nanoparticles, ferromagnetic nanoparticles (Fe_3O_4), was polymerized inside the micro-capillary tubes as a microvalve for flow regulation. Oscillating magnetic field ranging from 20 to 125 Oe (100-1000 kHz) was used to modulate the magnetically responsive PNIPAAm networks (M PNIPAAm) then the induced heat resulted in the physical swelling and shrinking of the polymer hence the flow motion inside the microchannel. The response time of oscillating field actuation is ~3 s, which is faster than the thermal actuation. Moreover, this microvalve had another advantage of avoiding complicated microfabrication of actuation component such as the embedded heaters or optical integration.

Paraffin is one of the most popular polymers used as the actuator (Lee and Lucyszyn 2006). Yang and Lin (2009) presented a latchable phase-change microvalve by applying low-melting-point paraffin wax and integrated microheater. The multiple-layer chip was composed of chamber layer (350 μm thick), fluid channel layer (12 μm thick) and substrate integrated with microheaters. A pneumatic pressure was used for the open-to-close switching through deformable microchannel ceiling right after the paraffin melt by the heat introduced by microheaters. The valve could switch status within 4-8 s and withstand an inlet pressure of 50 kPa without leakage.

Although paraffin-based microvalves have the advantages of no cross-contamination, high hold pressure, the requirement of several layers makes the fabrication of this chip highly complicated. In addition, almost all reports to date of paraffin-based microvalves involved the patterning of paraffin due to its non-favorable wetting characteristics, hence it is difficult to be filled in microchannels. (Song et al., 2008)

- **Electrochemical**

Electrochemical actuation is very attractive in microfluidic applications and has been drawn a lot interest because of its advantages of simple structural designs and low voltage operation (as low as 1.5V) (Pan et al., 2007).

Lee et al. (2008) reported a microvalve based on reversible electrochemical (ECM) actuation. The microfluidic system and the electrodes were fabricated using multiple UV lithography steps and electroplating techniques with metals. The main components of the valve are an ECM actuator, polydimethylsiloxane (PDMS) membrane and a cured SU-8 polymer made micro chamber. Hydrogen gas bubbles were generated in the valve microchamber with the nanoparticles coated Pt electrodes. The function of the nanoparticles is to enhance the surface-to-volume ratio of the electrode in order to obtain faster reversible electrolysis and valve operation. The amount of the bubbles could cause the motion of the membrane and hence the open or close state of the valve. An approximately 300 μm deflection of membrane could be obtained under a bias voltage of -1.5 V on the electrodes, while the estimated pressure in the valve chamber was about 200 KPa.

- **Rheological**

Niu et al. (2005) introduced a push-and-pull microvalve using a giant electrorheological (GER) fluid which enables the high-pressure changes in GER control channel resulting fully close and open a flow channel. The PDMS multilayer microvalves consisted of GER fluid control channel, the electrode, the flow channel, and the flexible membrane. This GER-fluid-based microvalve could obtain a response time of on-off switching of the flow about 8 ms.

- **Capillary**

In this section, selected examples of passive microvalves without mechanical moving parts will be briefly reviewed.

Several research group studied microvalves with hydrophobic element (Feng et al., 2003), capillary element (Kim et al., 2009) and diffuser/ nozzle element (Wang et al., 2008). Yasuda et al. (2008) presented a microvalve utilizing a superhydrophobic surface to manipulate minute amounts of liquids. This microvalve was fabricated by anodizing the Si surface of a microchannel wall meanwhile making the channel surface partially superhydrophobic in order to inhibit the adsorption of the liquid. The microvalve consists of a superhydrophobic channel and two hydrophilic channels which are fabricated on a Si wafer and covered with a PDMS plate carrying a liquid inlet, liquid outlet and air vent. Liquids

were injected into the hydrophilic channels first and stopped at the boundary between the superhydrophobic and hydrophilic channels. Meanwihile, the air initially in the superhydrophobic channel would separate the two liquids, then the valve was in closed state. In order to open the valve, positive pressure applied from the inlet would make the liquid break into the superhydrophobic channel flowing into the outlet liquid. Conversely, when applied a negative pressure from the inlet, the liquid would be separated again due to the superhydrophobic surface. Consequently, the microvalve was closed again. Experiments conducted by them showed that the microvalve could be opened within 0.5 s by a positive inlet pressure of more than 9 kPa. In addition, they could continue switching the microvalve at 1 Hz for about 3 h (10 800 switching) when adjusting the required inlet pressures.

Capillary valves can be designed actively utilizing different effects such as electrocapillary and thermocapillary to change surface tensions of the meniscus (Chen et al., 2008b; Kim et al., 2009), however, they are more often designed as passive valves by making an abrupt change of geometry in the hydrophobic or hydrophilic microchannels and the trigger of flow can be achieved by centrifugal force or other forces such as electrics and pressure. For example, passive capillary valves have been frequently applied in the regulation of liquid flow in the compact disk (CD)-based centrifugal microfluidics (Madou et al., 2001).

2.5.3 Summary of the various microvalves

The previous section gives a brief introduction to microvalves with respect to various operation mechanisms and their applications. Microvalves can be roughly categorized into active and passive microvalves, furthermore, both groups can be sub-classified into mechanical and non-mechanical microvalves. Non-mechanical active and passive microvalves are paid more attention in this section.

Mechanically actuated microvalves are effective, but are not easy to fabricate, requiring several layers and/or precise integration of metallic/ceramic components such as piezoelectric, magnetic or metallic materials. Magnetic actuation is normally employed for pressure or flow control in the form of solenoids to deflect membranes due to its ability to generate large forces and deflections rapidly. For piezoelectric actuation, large voltages can only introduce very small deflections, though it can yield very high forces. In order to integrate the microvalve with miniaturized structures, electrostatic actuation might be a good choice. However, unlike the magnetic actuation, it is hard to obtain high forces for driving the microvalves because extremely high voltages are required. Thermal actuation is simple and capable of providing large forces, but it is relatively slow. Besides, the heat dissipation is

another concern for thermal actuation. When considering the cost, mechanical active microvalves are mainly reusable and can be assembled into the reusable instruments rather than the disposable microfluidic devices. (Kwang and Chong, 2006)

Non-mechanical active microvalves can be built based on electrochemical, phase change and rheological actuations. The phase change-based microvalves utilize phase changeable materials such as hydrogel, sol-gel and paraffin. Normally, phase change microvalves are actuated by temperature, pH, electric fields or light. The main advantage of low cost makes the phase change microvalves, widely used in disposable microfluidic chip applications. Moreover, the phase change valve can be latched, minimizing the energy required. Electrochemical actuation has the advantage of offering large forces and deflections with low voltage. Rheological materials can be used as movable plugs but cannot provide large forces because of the indirect polarization by the external fields.

Passive mechanical or non-mechanical microvalves can be readily incorporated into microfluidic system to meet integration requirements. These microvalves have several advantages such as simple fabrication, easy operation, perfect sealing and ability to effectively preventing bulk flow of liquid. For example, passive microvalves using capillary effects are often useful in microfluidic PCR applications because the surface properties of the microchannels enable the realization of autonomous and spontaneous valving (Kwang and Chong, 2006). However, the hydrophobic/hydrophilic surface stability associated with these hydrophobic patch microvalves is a problematic issue. Besides, unavoidable leakage flow, complicated fabrication process and relatively high cost are the disadvantages of the passive microvalves. Despite this drawback, passive hydrophobic valves are still considered to be useful for blocking or passing fluidic flows without sealing.

The performance of all kinds of microvalves has been undergoing improvements for recent years, focusing on the power consumption, resistible pressure, leakage flow, response time and biochemical compatibility, etc. However, huge improving room still exists and make them a fully integrated portable microfluidic device and cost effective. It is believed that in the near future microvalves integrated microfluidic devices will make its applications more wide and prevalent.

2.6 Electrokinetics

In a microfluidic system, the two main driving forces are the pressure-driven force and the electrokinetic force. For these two kind of forces, the shortcomings and the strength are obvious. For example, the electrokinetic pumping force is easily integrated and miniaturized while the pressure

pumping force usually needs external mechanical components such as syringe pump. In addition, electro-osmotic pumping force, for instance, is suitable for transporting liquid in microchannels because no moving parts involved in this method and no pulsating flows are produced. Furthermore, electro-osmotic pumping force generates a plug like velocity profile and the average velocity is independent of the microchannel size, all of these features make this force is favorable for sample delivery (Hu et al., 2006). However, the pressure pumping force is a non-destructive method for cell detection. Reversely, the electrical field may kill cells or introduce the photo bleaching of the fluorescent dye which is used to label the cells.

Electrokinetics refers to the motion of bulk fluids or selected particles/cells in the fluids under a applied electric fields. A common source of all these electrokinetic phenomena is the 'double layer' of charges at the interface between two different phases. As known that most solid surfaces obtain certain amount of surface electrical charge when brought into contact with a polar medium. These surface charges will in turn cause the ions redistributing in the polar medium to form the so-called electrical double layer (EDL). For example, the counter-ions of the surface are attracted towards the surface while the co-ions are repelled from the surface. This electrostatic interaction as well as the mixing tendency causing by the thermal motion of the ions, leads to the formation of an electrical double layer (EDL) (Kang and Li, 2009). The EDL consists of the compact layer and the diffuse layer. Because the nearby region of the charged surface contains an excessive of counter-ions over co-ions to neutralize the surface charge, the net charges are therefore generated (Kang and Li, 2009). Under an external electric field, the excess counter-ions in the diffuse layer will move by the electrical force. As the ions move, they will drag the surrounding liquid molecules to move with them due to the viscous effect, resulting in a bulk liquid motion which is so-called electro-osmotic flow (EOF) or electroosmosis. For dispersed particles, an external electric field exerts an electrostatic Coulomb force on the electric surface charge and cause the motion of the particles, which is called electrophoresis. Electroosmosis and electrophoresis are the major effects of electrokinetics (Lyklema, 1995; Hunter, 1989). Other electrokinetic phenomena include diffusiophoresis, capillary osmosis, streaming potential/current, sedimentation potential and so on.

During the last decades, scientists and researchers have been widely applying the electrokinetics technology for the manipulation of particles in biological application, such as blood cells and bacteria. With the booming development of micro/nano-fabrication technologies, microfluidics-based lab-on-a-chip devices become a research focus. These lab-on-a-chip devices successfully miniaturize the

conventional room-sized biomedical instruments into portable devices and contribute to the amazingly fast development of the healthcare industry (Mogensen et al., 2002; Radisic et al., 2006; Chin et al., 2007; West et al., 2008). The main distinctive advantages of the microfluidics-based lab-on-a-chip systems over the traditional methods include: integration of multiple steps of different analytical procedures, the affordable manufacturing and operational costs, large variety of applications, sub-microliter consumption of reagents and samples, and portability. All of these merits enable them to be extremely attractive for fast and effective on-site diagnosis.

Microfluidics-based lab-on-a-chip systems present excellent platforms for many biological manipulations and assays since the biological reagents and particles exist in fluidic natural environment. Extensive research works on biological analysis have been reported, such as PCR, DNA analysis, enzyme assay (Cheng et al., 2001; Yang et al., 2001).

2.7 Biochemical protocol applied in thesis

In this study, a commercial kit (Neogen, Lansing, MI, USA) for foodborne pathogen detection was selected as the research materials. This kit utilizes a novel DNA hybridization technology for rRNA sequence assay. The protocol of the kit is briefly introduced as follow:

The lysed sample firstly obtained by putting the enrichment culture and lysis reagent together, then the sample cells will be disrupted thereby release the nucleic acid target molecules. This assay employs capture and detector DNA probes specific to the ribosomal RNA (rRNA) of pathogens ensuring the highest of specificity. Poly dT coated wells are used as solid phase for capturing the resulting complex. The oligonucleotide capture probe contains polydeoxyadenylic acid (poly dA) at its 3’ end, which is complementary to the poly dT coated on the bottom surface of the wells, facilitating the capturing process. The oligonucleotide detector probe is labelled at its 5’ end with the enzyme horseradish peroxidase (HRP). The hybridization reaction of the probe reagents and the lysed sample is allowed to proceed in the poly dT coated wells for 1 hour. For the assay to yield a positive result, both the capture and the detector probes must bind to the target simultaneously. Meanwhile, the capture probe must also bind to the poly dT coated well. This dual selectivity ensures that only the target pathogen is detected during the assay. After the incubation, a substrate of HRP is added after washing away the unbound probes. Following an incubation of 20 min, the complex solution turned to blue color to indicate the presence of rRNA from the target organism. A sample is considered negative for the presence of target organism if the complex solution has no color change. In order to obtain a colorimetric endpoint for

detection, a stop solution is introduced as the final process. The solution with positive reaction will change color from blue to yellow. Quantitative results can be determined spectrophotometrically at 450 nm by measuring the absorbance value.

There are many distinctive advantages by assaying rRNA sequence. As known that DNA-based sensor has the limitation of non-quantitative result with regard to viable organisms when using DNA as a target (Nugen and Baeumner, 2008). This issue can be overcome by using RNA targets because RNAs are easily decayed after cell death and the presence of RNA suggests the viability of bacterial cells (Heo and Hua, 2009). In addition, the multi-copy nature of rRNA naturally enhances the sensitivity. Table 2-3 compares the performance of applied kit with other available methodologies. From the table, this kit presents superior specificity and sensitivity and faster results. Meanwhile, no costly enzymes are needed.

Table 2-3 Comparison of applied kit with other available methodologies (GeneQuence®, 2008)

Point of Comparison	**Applied kit**	**PCR**	**ELISA**
Technology	DNA hybridization	PCR	Enzyme linked antibody
Enrichment	24 hrs	24-26 hrs	48-72 hrs
Assay time	1 hr 50 min	3 hrs (average)	1 hr 30 min
Specificity	Greater than 99.7%	Greater than 98%	Greater than 96%
Sensitivity	Greater than 98.9%	Greater than 98%	Greater than 98%

Chapter 3

On-Chip RNA-DNA Hybridization Assay with Electrokinetically Controlled Oil Droplet Valves for Sequential Microfluidic Operations

3.1 Introduction

In this RNA-DNA hybridization assay (RDHA) microchip, gravity-based pressure-driven flow was used to generate liquid flow in the microchannels to avoid using syringe pumps, tubing and valves for liquid handling. The pressure difference is generated by the higher liquid level in the reagent wells and the lower liquid level in the waste well. Moreover, in order to obtain a high flow rate and keep the reagent consumption reasonable, the size of reagent wells should be made as large as possible to minimize the change of liquid level in the reagent wells so that a relatively constant pressure difference is maintained, therefore, the flow rate would not decrease significantly during the delivery process. Numerical study was performed to investigate the flow field and concentration field for determining the dimensions of the microchannels. Since the assay involves multiple steps of sequential loading process, another core design is a pair of oil-droplet microvalves. An oil droplet in the control channel was used as a microvalve to open or close a reagent flowing channel by moving the position of the oil droplet in the control channel. Electro-osmotic flow was used to control the valves (the position of the oil droplets) and thereby the sequential loading of different reagents. The size of the control channel is bigger than the main flow channels so that the oil droplets would not incline to move into the flow channel. Positive and negative controls and a *Salmonella* culture were successfully analyzed using the microfluidic chip. This microfluidic approach results in a 10-fold reduction in reagent consumption, assay time reduction from 1 hour 50minutes to 25 minutes, and a detection limit comparable to the conventional assay.

3.2 Numerical study and chip design

Based on the above mentioned considerations, theoretical modeling and numerical simulation were conducted to determine the microchip layout and dimensions. We considered the transient sample transportation within the microchannel network. When the oil-droplet valves are open, the electric field will be stopped applying on the control channels. Therefore, pure pressure driven flow is considered at

each dispensing step. The oil droplets are considered as a fixed insulated solid. The pressures at inlets are considered as a constant for simplicity. Attention is focused upon the washing processing, which is very important to avoid generating false positive signals. Concentration distribution and flow field are studied and comparisons are made based on different chip dimensions. One simplification applied in this numerical simulation is to decrease the dimensionality of the problem from 3-D to 2-D because the physical properties of all the microchannels of the chip can be assumed to be identical and homogenous due to its constant depth and uniform solid walls.

Fluid flow generated by a gravity-based pressure variation in the channel follows the Navier-Stokes equation for incompressible fluid,

$$\boldsymbol{\rho}\frac{\partial \boldsymbol{V}}{\partial \boldsymbol{t}} - \boldsymbol{\eta}\nabla^{\boldsymbol{2}}\boldsymbol{V} + \boldsymbol{\rho V}\cdot\nabla\boldsymbol{V} + \nabla\boldsymbol{P} = \boldsymbol{F} \tag{3-1}$$

$$\nabla\cdot\boldsymbol{V} = \boldsymbol{0} \tag{3-2}$$

Where V is the velocity, ρ is the density of the fluid, η is the dynamic viscosity of the fluid and P refers to the pressure. The volume force F in the equation is considered to be zero because we consider a 2-D model, and the gravity is only in the z direction.

The boundary conditions are given as following,

at inlets, $\boldsymbol{\eta}\left(\nabla\boldsymbol{V} + (\nabla\boldsymbol{V})^{\boldsymbol{T}}\right)\boldsymbol{n} = \boldsymbol{0}, \boldsymbol{P} = \boldsymbol{P_0}$ (3-3)

at outlets, $\left[\boldsymbol{\eta}\left(\nabla\boldsymbol{V} + (\nabla\boldsymbol{V})^{\boldsymbol{T}}\right)\right]\cdot\boldsymbol{n} = \boldsymbol{0}\,, \boldsymbol{P} = \boldsymbol{0}$ (3-4)

at walls, $\boldsymbol{V} = \boldsymbol{0}$ (3-5)

at wells in control channels, $\left[-\boldsymbol{PI} + \boldsymbol{\eta}\left(\nabla\boldsymbol{V} + (\nabla\boldsymbol{V})^{\boldsymbol{T}}\right)\right]\cdot\boldsymbol{n} = \boldsymbol{0}$ (3-6)

Once the flow field is determined, the sample concentration is described by

$$\frac{\partial \boldsymbol{C_i}}{\partial \boldsymbol{t}} + \nabla\cdot(-\boldsymbol{D_i}\nabla\boldsymbol{C_i}) = -\boldsymbol{V}\cdot\nabla\boldsymbol{C_i} \tag{3-7}$$

where $\boldsymbol{C_i}$ is the concentration of the i-th sample, V is the velocity of the sample, $\boldsymbol{D_i}$ is the diffusion coefficient of the i-th sample.

The incoming flow has constant sample concentration at inlets. At outlets, remaining sample molecules leave the system through convection, which follows:

$$\boldsymbol{n}\cdot(-\boldsymbol{D_i}\nabla\boldsymbol{C_i}) = \boldsymbol{0} \tag{3-8}$$

Walls are insulated and the concentration gradients normal to these boundaries are equal to zero,

$$\boldsymbol{n \cdot N = 0; N = -D_i \nabla C_i + C_i V} \quad (3\text{-}9)$$

The above differential equations were solved by using a commercial software package, COMSOL Multiphysics 3.5a, which is based on Finite Element Method.

Different design parameters, i.e., structure of channel, neck width, control channel length, well size, were studied to find out a reasonable design, as shown in Figure 3-1. The dashed borders were the interested regions. In order to reduce the effect of the dispensed liquid on the oil droplet in control channels, and increase the flow rate of the liquid dispensed to the target well, two pairs of converging sections were introduced near the ends of the control channel. The flow rate at the spot 1 and spot 2 was calculated to determine the performance of the chip design. High flow rate at the spot 2 and low flow rate at the spot 1 indicate the majority liquid is flowing into the reaction well rather than the control channels. Studied parameters are listed in the Table 3-1.

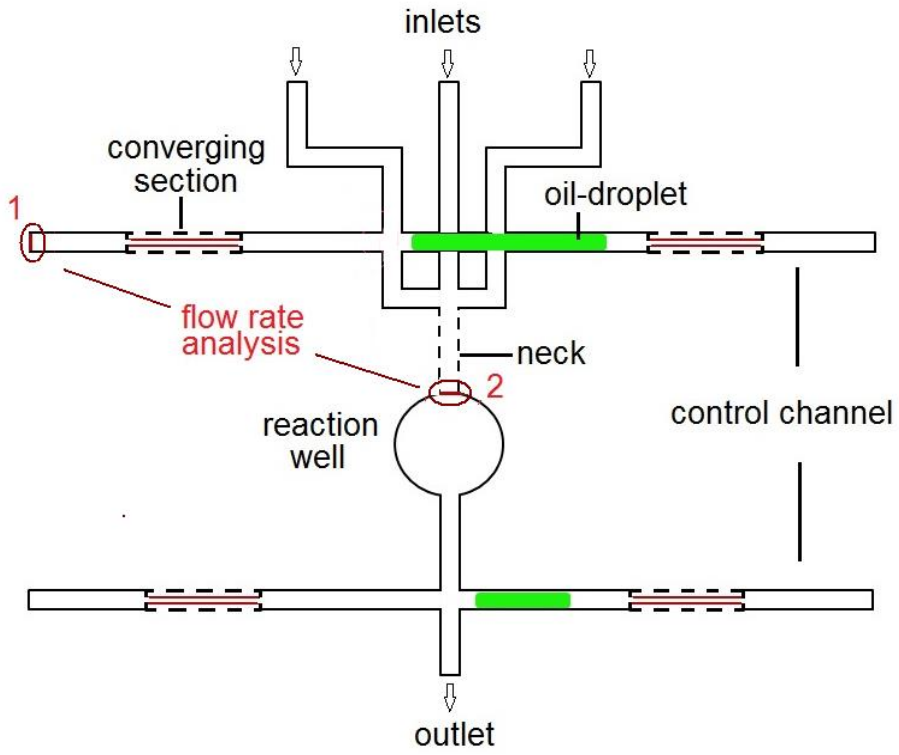

Figure 3-1 Parameter studies in numerical simulation for an optimizing chip layout (not proportional to the exact size). The dashed borders were the studied regions. With and without converging sections were considered. The flow rate was calculated at the spots 1 and 2

Table 3-1 Parameter combinations of chip dimensions studied in numerical simulation

Group	Feature	Geometry dimensions			
		Neck length	**Neck width**	**Control channel length**	**Converging section width**
1	Short/Long neck	2 mm	200 μm	10 mm	------
		1 mm	200 μm	10 mm	------
		250 μm	200 μm	10 mm	------
2	Wide/narrow neck	2 mm	400 μm	10 mm	------
		2 mm	600 μm	10 mm	------
		2 mm	800μm	10 mm	------
3	Converging section in the control channel	2 mm	200 μm	10 mm	80 μm
		2 mm	200 μm	10 mm	50 μm
		2 mm	200 μm	10 mm	20 μm

By numerical simulation, an optimized chip design was obtained. The concentration field profiles in the reaction well are shown in the Figure 3-2. It can be seen that the concentration of the optimized chip comes to equilibrium faster than that in the original chip. Table 3-2 compares the results between the chip designs with and without the converging sections during the washing step under a constant pressure.

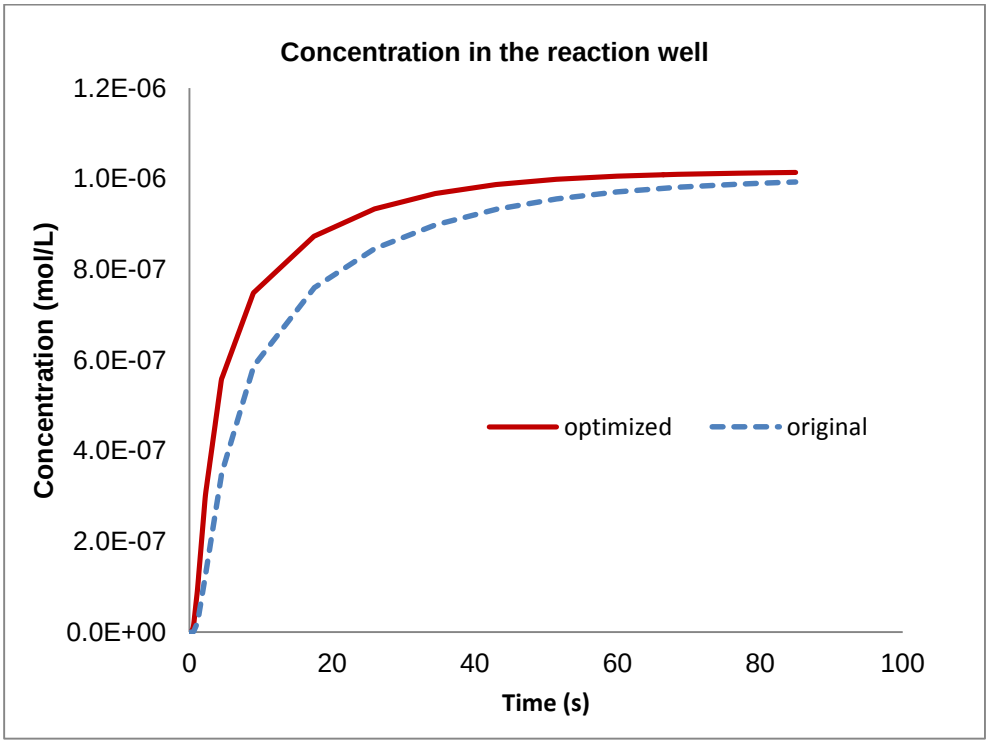

Figure 3-2 Concentration field profiles in the reaction well of the original chip and the optimized chip

Table 3-2 Results of a comparison between the chip designs with and without the converging sections

Chip design	Geometry dimensions [μm]			Flow rate [$\times 10^{-6}$ m^2/s]			Lost%
	converging section	neck width	neck length	spot 1	spot 2	Total (at inlet)	
1	None	200	1000	0.85	0.89	1.86	46%
2	20 (width)	600	250	0.002	1.70	1.77	0.11%

It is found that the converging sections have a dominant effect on the increasing of the flow rate to the reaction well. As we can see in Table 3-2, with these converging sections, the amount of the reagents flowing into the control channel can be reduced from 46% to 0.11%, hence increase the net flow rate to the reaction well. In addition, the flow rate is found ranging from 0 to 0.17 μL/s, 0 to 0.13 μL/s and 0 to 0.10 μL/s for the washing solution, substrate solution and the stop solution, respectively.

The mixing effect in the reaction well was studied as well. As mentioned before, pressure driven flow is used to deliver reagents in our system. When substrate/stop solution is dispensed into the reaction well by pressure, the lower valve is closed, hence the reaction well is a dead end. The flow entering into the reaction well will generate circulations, as shown in Figure 3-3, which can enhance the mixing very well. Therefore, in this method, no extra effort for mixing is needed.

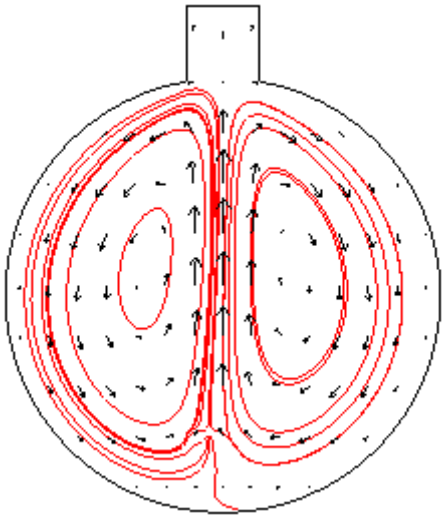

Figure 3-3 Circulations generated by the liquid flowing into the reaction well

Based on the numerical study, a reasonable design of the RNA-DNA hybridization assay (RDHA) microchip is shown in Figure 3-4. The DHA microchip consists of two control microchannels (250 μm wide, 100 μm high) and three separate parallel channels (200 μm wide, 100 μm high) for delivering different reagents. These liquid delivery microchannels are connected to a reaction well and subsequently a waste well. Two pairs of converging sections (20 μm wide, 100 μm high) are embedded in the control channels. As mentioned previously, having these converging sections can dramatically reduce the amount of the reagents flowing into the control channels and increase the rate of liquid transport into the reaction well. The depth of all the wells is approximately 3 mm.

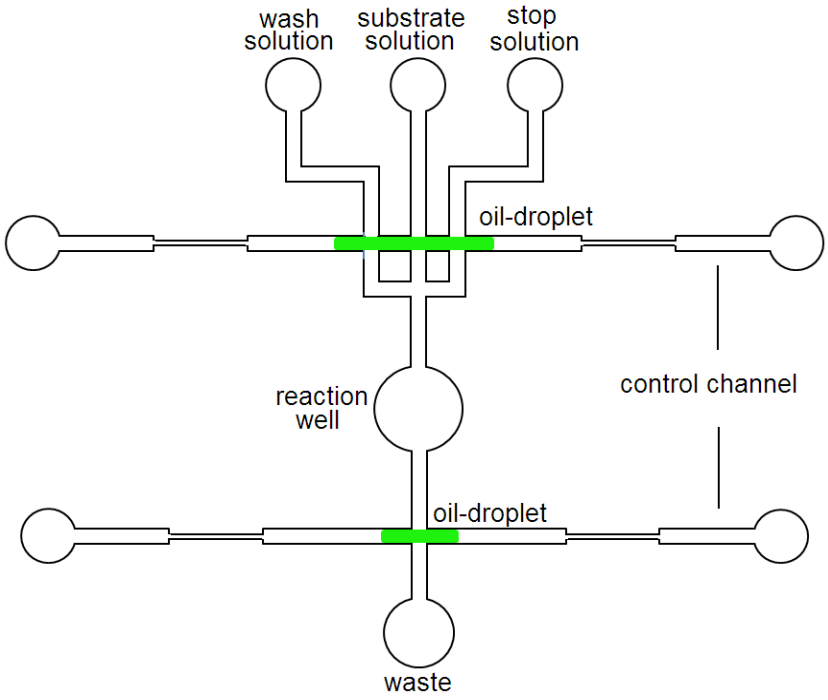
wash solution
substrate solution
stop solution
oil-droplet
reaction well
control channel
oil-droplet
waste

(a)

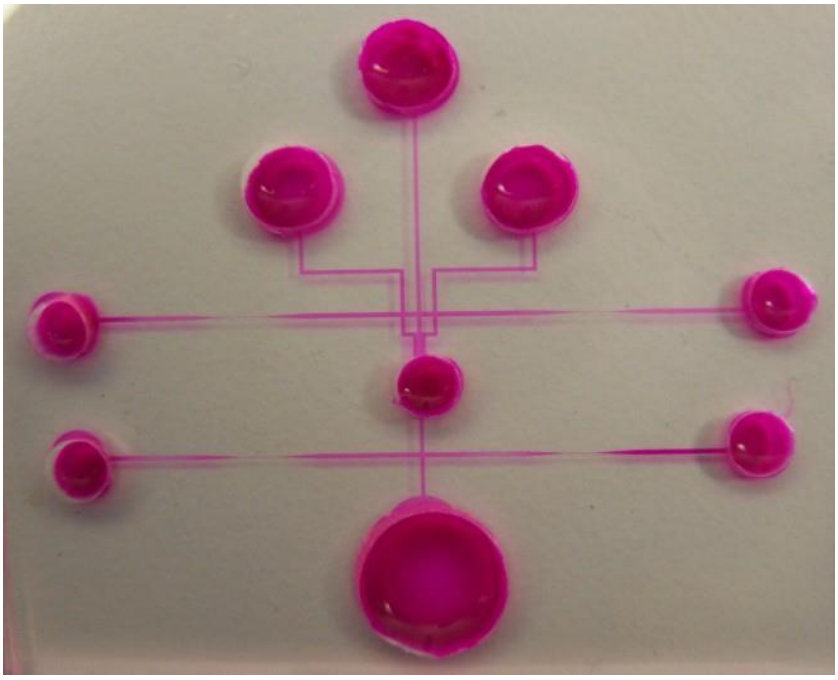

(b)

Figure 3-4 Layout of RNA-DNA hybridization assay (RDHA) microchip. The main flow channels and control channels are 200 μm ×100 μm and 250 μm ×100 μm, respectively. The width of all the converging sections in the control channels is 20 μm. The depth of all microchannels is 100 μm. The diameter of the reagent wells and the waste well is 4.5 mm and 8 mm, respectively. The diameter of the reaction well and all other wells is 3 mm. (a) A schematic illustration of the RNA-DNA hybridization assay (RDHA) (not proportional to the exact size); (b) A picture of the RNA-DNA hybridization assay (RDHA) microchip (The channel is filled with rhodamine B for visualization). Overall outer dimensions of the chip are 50×35 mm^2

3.3 Experiment

3.3.1 Principle of the assay

In this microfluidic RNA-DNA hybridization assay (RDHA), poly dT coated magnetic microbeads (Dynabeads Oligo (dT)25, Invitrogen) are used as a matrix and localized by a magnet in the hybridization reaction well. This assay employs capture and detector DNA probes specific to the ribosomal RNA (rRNA) of *Salmonella*. The oligonucleotide capture probe contains polydeoxyadenylic acid (poly dA) at its 3' end, which is complementary to the poly dT coated on the microbeads, facilitating the capturing process. The oligonucleotide detector probe is labelled at its 5' end with the enzyme horseradish peroxidase (HRP). The probe reagents, poly dT coated magnetic microbeads and the lysed samples are incubated in the reaction well for 10 min. For the assay to yield a positive result, both the capture and the detector probes must bind to the target simultaneously. Meanwhile, the capture probe must also bind to the poly dT coated microbeads which are immobilized in the reaction well by an external magnet. This dual selectivity ensures that only the target pathogen is detected during the assay. After the incubation, a substrate of HRP is added to the reaction well after washing away unbound probes. Following an incubation of 5 min, the complex solution turned to blue color to indicate the presence of *Salmonella*. A sample is considered negative for the presence of *Salmonella* if the complex solution has no color change. In order to obtain a colorimetric endpoint for detection, a stop solution is introduced as the final process. The solution with positive reaction will change color from blue to yellow.

3.3.2 Reagents and solutions

Commercially available reagents from a Salmonella test kit (GeneQuence Salmonella Kit, Neogen, Lansing, MI, USA) were used, which provided lysis reagent concentrate, lysis reagent buffer,

hybridization solution, *Salmonella* probe solution, wash solution, substrate chromogen solution, stop solution and negative control. Instead of the Poly dT coated microwells in the commercial kit, poly dT coated magnetic micro-bead (Dynabeads® (dT) 25, Invitrogen, USA) was used. *Salmonella* bacteria were cultured and quantified the concentration by Laboratory Service, University of Guelph, Canada. Stock cultures of *Salmonella* berta (ATCC8392) were grown for overnight at 37 ℃ in Tryptic Soy Broth (TSB).

The concentration of the sample bacteria sample were estimated by plate counts. The procedure is as below.

1. Prepare sterile 1.5 mL tubes with 0.9 mL PBS in each.
2. Prepare agar plates.
3. Make serial dilution starting with 10-1 (dilution factor) as far as needed: pipet 0.1 mL sample into a tube of 0.9 mL PBS, vortex well. Pipet 0.1 mL of this into another tube of 0.9 mL PBS and vortex. Continue similarly until all dilutions are made.
4. Pipet 0.1 mL of each dilution (starting with 10-3) on duplicate plates (the "real" dilution factor is therefore 10-4). Spread the bacterial suspension over the surface.
5. Incubate all plates in the inverted position at appropriate temperature until colonies appear (usually 1 to 2 nights).
6. Count colonies on a plate containing between 30 and 300 colonies (or an average of duplicate plates) and calculate the number of bacteria per ml using the following formula: CFU/mL= number of colonies × dilution factor × 10 (because only 0.1 mL was plated)

The overnight cultures were killed by boiling in a water bath for 20 min for further use. Different concentration bacteria samples were diluted by PBS (1×) buffer solution (Ricca Chemical, Arlington, TX, USA) into 10^3~10^9 CFU/mL. Lysed sample was prepared by following the procedure specified in the commercial kit. Lysis reagent was added to the *Salmonella* bacteria samples and incubating at 65 ℃ for 5 minutes. *Salmonella* probe hybridization solution was prepared by mixing hybridization solution and *Salmonella* probe solution at a ratio of 4:1. The testing sample was prepared by mixing the lysed sample (or negative control) and the *Salmonella* probe hybridization solution at a ratio of 6:5. Borate buffer solution (Ricca Chemical, Arlington, TX, USA) was used as the buffer solution, and vacuum pump oil (Maxima®C plus oil, Fisher Scientific, Ottawa, ON, Canada) was used to form the oil-droplet

valve, respectively. Food color was purchased from retail stores in Waterloo, ON, Canada and diluted by double distilled water (DDW).

3.3.3 Oil-droplet sequence valve and electrokinetic control

In order to avoid using syringe pumps, tubing and valves for liquid handling, gravity-based pressure-driven flow was used to generate liquid flow in the microchannels. The pressure difference is generated by the higher liquid level in the reagent wells and the lower liquid level in the waste well. Because the assay requires multiple and sequential steps, an oil droplet in the control channel was used as a valve to open or close a reagent flowing channel by moving the position of the oil droplet in the control channel. Electro-osmotic flow was used to move the oil droplet and hence the sequential fluidic operation on the chip. This is referred to as the electrokinetically-controlled oil-droplet sequence valve (ECODSV). Specifically, the movements of both ECODSVs were controlled by the electric fields imposed in the two separate control channels, and the velocities of the ECODSVs were proportional to the strength of the applied electric fields. The two-valve design has two main functions. When both valves are in the open positions, the reagent solution in the corresponding well will flow into the reaction well and then all the way to the waste well, because of the hydrostatic pressure difference. The other function is to hold reaction sample for incubation when both of the valves are closed.

3.3.4 Microfluidic chip fabrication

Microfabrication of the chips was carried out by using the standard soft lithography technique as detailed by Biddiss et al. (2004). Briefly, the master was prepared by first spin coating the film of SU-8 75 negative photoresist onto a silicon wafer followed by prebaking. A photomask bearing certain microchannel geometry was then placed on the top of the film. The photoresist film covered with the mask was then exposed to UV light. After post-baking and developing, the master could be obtained. Next, a 10:1 (w:w) well mixed mixture of PDMS prepolymer and curing agent was poured over the master and cured at 75 ◦C for about 4 h after being degassed under low vacuum. Finally, the PDMS replica was peeled from the master and sealed against a glass slide after oxygen plasma treating for 40 s. Solution reservoirs (wells) were formed by punching holes at each end of the microchannels in the PDMS slab.

3.3.5 Experimental set-up and procedures

The experimental setup is shown in Figure 3-5. Two pairs of platinum electrodes were placed into the solution in the wells of control channels to apply electric field. Two DC-regulated power supplies (CSI12001X, Circuit Specialists Inc., USA) were used to control the voltages on the electrodes. A microscope (Nikon SMZ800, Nikon Instrument Inc., Melville, NY, USA) with a CCD camera (Nikon Digital sight DS-2Mv, Nikon Instrument Inc.) was used to monitor the movements of ECODSV inside the microchannel. The images were captured by the digital camera and digitized by the computer software (NIS-Elements BR 3.0, Nikon Instrument Inc.). A magnet seated on the side of the device localized the magnetic beads in place. Extensive experiments using food color to visualize the flow were conducted on the chips on the RNA-DNA hybridization assay (RDHA) microchip in order to test the feasibility of the ECODSV.

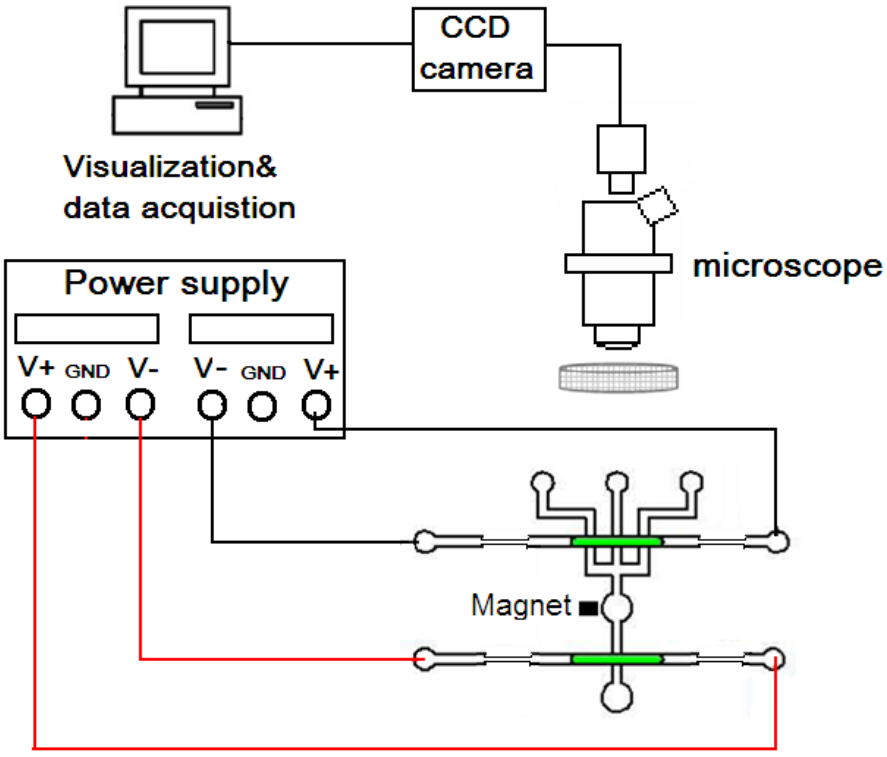

Figure 3-5 Illustration of the experimental system

The experimental procedures are as follows. First of all, borate buffer solution was employed to wet all the channels. The oil droplets were injected into both the control channels from corresponding well at the end, respectively. Turned on the DC power supplies and pumped the oil droplets to the channel

crossing area and then turned off the power to make the oil droplets stop there. Then, the three upper wells of the microchip were each filled with wash solution, substrate solution and stop solution, respectively. This was followed by loading the coated microbeads and the mixture of the testing sample and hybridization reagent into the reaction well and started the assay.

The DNA hybridization assay consists of four steps. In the first step, both of the ECODSVs are in the closed positions for the hybridization reaction and incubation. Ten minutes later, both ECODSVs open at the same time to let the wash solution to wash away the unbound probes. During the third step, the upper ECODSV opens the second channel to let the substrate solution flow into the reaction well, while the lower ECODSV opens for a certain period of time (to let certain volume of the wash solution flow out of the reaction well into the waste well) and is then closed to keep the substrate solution staying in the reaction well for incubation. In the last step, the lower ECODSV is kept closed, and the upper ECODSV is opened for the third channel to dispense the stop solution.

3.3.6 Study of the volume of the reaction sample and incubation time

In order to reduce the sample and reagents consumptions, a series of tests were conducted to investigate the minimum volume which could be qualitatively distinguishable. Tested samples were divided into several groups of different volume of 6 μL, 12 μL and 18 μL. For each group, samples of concentrations ranging from 10^2 CFU/mL to 10^9 CFU/mL were assayed manually in a single PDMS well following the standard procedure. Results were observed by naked eyes. As a result, the volume of 12 μL was found good enough to generate a distinguishable results. Then, this volume was fixed to determine the minimum incubation time. Five, eight, ten and fifteen minutes were studied for the incubation time of the hybridization reaction. It was found that 5 minutes not sufficient to generate acceptable results. For the time of 8 min and 10 min, the results of 10 min showed a better resolution while there was no distinguishable difference between the results of 10 min and 15 min. Therefore, 10 min was determined as the optimized incubation time for the hybridization reaction.

The flow rate of the wash solution, the displacement of the liquid in the reaction well were studied to find out the minimum washing time. Based on the numerical study and the visualization experiments, the average flow rate of the washing solution, substrate solution and the stop solution was 0.08 μL/s, 0.06 μL/s and 0.05 μL/s, respectively. And 8 min was determined as the minimum time for washing. To prove that, this minimum washing time was applied to test negative controls and no false positive signals were found.

3.4 Results and discussion

3.4.1 Feasibility of the microchip design and visualization of the experiment

The experiments demonstrate that the oil-droplet can block the liquid flow from the vertical channels, and also can be well controlled to move forward and backward in the microchannel by switching the polarity of the electrodes placed in the two end wells of the control channel. In addition, the velocity of the oil droplet depends on the magnitude of the applied voltage and the volume of the oil-droplet, Figure 3-6 shows the relationship between the average velocity and the applied voltage for an oil-droplet of 2.5 mm in length.

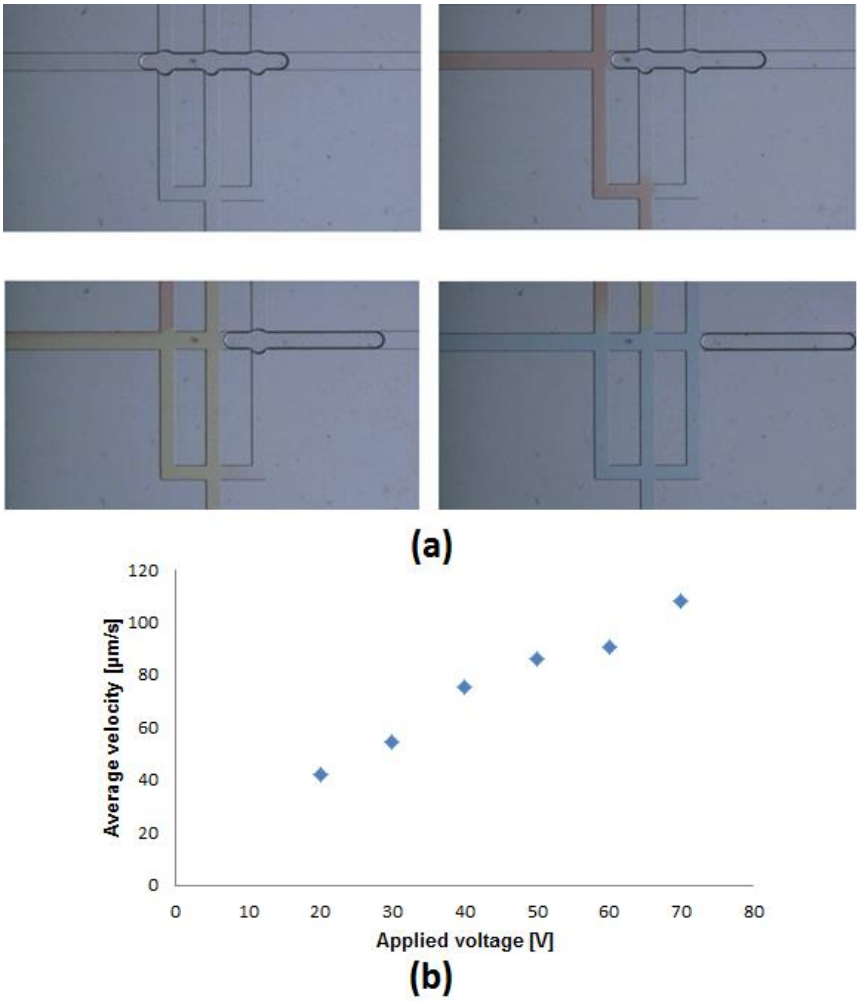

Figure 3-6 (a) The sequential movements of the ECODSV in a 3-channel microfluidic network (b) Average velocity of an ECODSV under different electric fields (for an oil-droplet of 2.5 mm in length)

Figure 3-7 shows an example of the visualized sequential reagents loading processes of the DNA hybridization assay. Three different food colors were used to visualize the reagents involved in the assay. Both of the ECODSVs were controlled at the same time. In the following discussion, for simplicity, we denote the positions of the upstream oil-droplet valve at the three main flow channel exits and the downstream oil-valve position by A1, A2, A3 and B, respectively. Table 3-3 describes the operation steps and the status of the oil-droplet valves at each step for a complete on-chip DNA hybridization assay. The DNA hybridization assay consists of four steps. The first step is the hybridization reaction and incubation of a test sample. In this step, both ECODSVs are closed. The second step is the washing of the unbound probes. During this step, valve A1 and B are opened. The following step is the dispensing of the substrate solution and incubation. In this step, valve A2 opens while valve B opens for 30 s and then is closed. The last step is the dispensing of the stop solution. In this step, valve A3 opens and valve B is closed. The realization of these steps of operations and the ECODSVs status at each step are illustrated in Figure 3-7. Furthermore, it is shown in Figure 3-7, by controlling the dispensing time of the liquid flowing in the 1st channel, the pressure difference between the liquid level in the 1st upper well and the waste well diminished gradually so that the flow in the 1st channel eventually stopped. Therefore, when the second or the third flow channel was opened, the higher pressure flow would cut off the low-pressure flow, and only the flow in the currently opened channel would flow into downstream, which helped to avoid cross-contamination when two or three channels were in open status at the same time. Figure 3-7 (a) shows the reaction well during the hybridization reaction and incubation of the sample. Figure 3-7 (b) shows the washing of the unbound probes. Figure 3-7 (c) is the dispensing and incubation of the substrate solution. Figure 3-7 (d) is the dispensing of the stop solution.

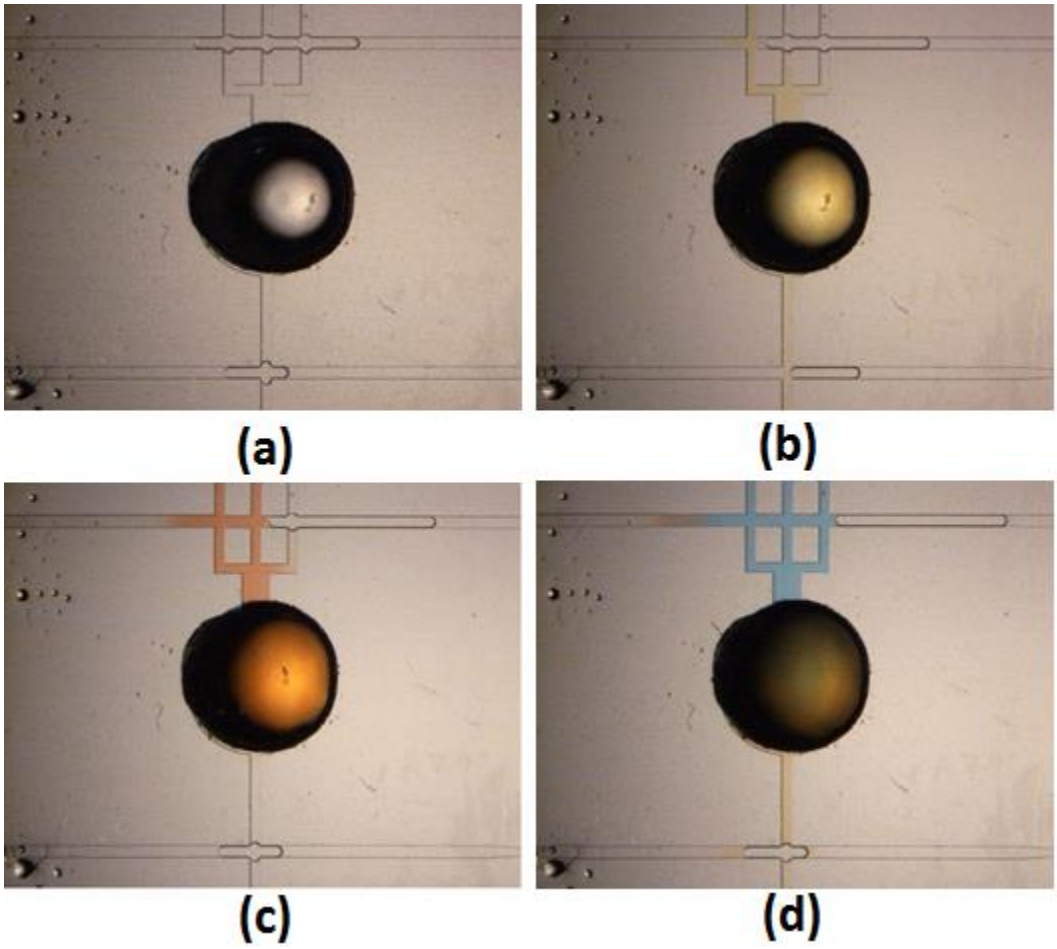

Figure 3-7 The visualized sequential steps of the RNA-DNA hybridization assay. Yellow, red and blue food colors represent wash solution, substrate solution and stop solution, respectively. (a) The initial positions: both ECODSVs were closed; (b) The visualized washing process to remove the unbound probes, valves A1 and B were opened; (c) The visualized process of dispensing substrate solution and incubation, valve A2 was opened, valve B stayed opened for a while to pump out wash solution and then was closed; (d) The visualized process of dispensing stop solution, valve A3 was opened and valve B stayed closed.

Table 3-3 Sequential steps and controlling parameters in the electrokinetically-controlled RNA-DNA hybridization assay

No.	Steps	Status of the ECODSVs (Open = O Closed = C)			
		A1	A2	A3	B
1	Hybridization reaction/ Incubation	C	C	C	C
2	Washing	O	C	C	O
3	Dispensing substrate solution/ Incubation	O	O	C	C
4	Dispensing stop solution	O	O	O	C

3.4.2 RNA-DNA hybridization assay on *Salmonella*

In this study, the RNA-DNA hybridization assay (RDHA) was applied to detect *Salmonella* samples of known concentrations ranging from 10^9 to 10^3 CFU/mL. All experiments were carried out at room temperature. The sequential hybridization operations were achieved by controlling the movements of the ECODSVs and the corresponding operation parameters are provided in Table 3-4. Sixty volts voltage was firstly applied when ECODSVs needed to be moved as desired and then turned off right after the flow channel was open or close. In order to test the performance of the assay, negative control and *Salmonella* samples were tested by this RNA-DNA hybridization assay (RDHA) microchip. A blank was used to be compared with the test results. The complete assay took approximately 25 min.

Figure 3-8 shows an example of the RNA-DNA hybridization assay to detect a *Salmonella* sample of 10^9 CFU/mL. These pictures were taken by a CCD camera under a microscope. The images illustrate the status of the ECODSVs as captured during the main steps. Figure 3-9 shows the results from the assay of *Salmonella* samples of concentration 10^2, 10^3, 10^5, 10^7 and 10^9 CFU/mL and negative control, respectively. All images in Figure 3-8 were taken by a common digital camera. The *Salmonella* sample produced distinguishable yellow color under the observation of both microscope and naked eyes.

Table 3-4 Operation steps and controlling parameters for a full RNA-DNA hybridization on-chip assay

Steps	**Applied potentials in the control channels (V)**		**Time**
	Upper	**Lower**	
1.Hybridization reaction/ Incubation	0	0	10 min
2.Washing	60(0)*	60/0*	8 min
3.Dispensing substrate solution/ Incubation	60(0)*	-60(0)**	5 min
4.Dispensing stop solution	60(0)*	0	2 min

*60 V is the driving voltage, 0 V is the holding voltage.

**The sign "-" illustrates that the direction of the applied electric field is switched.

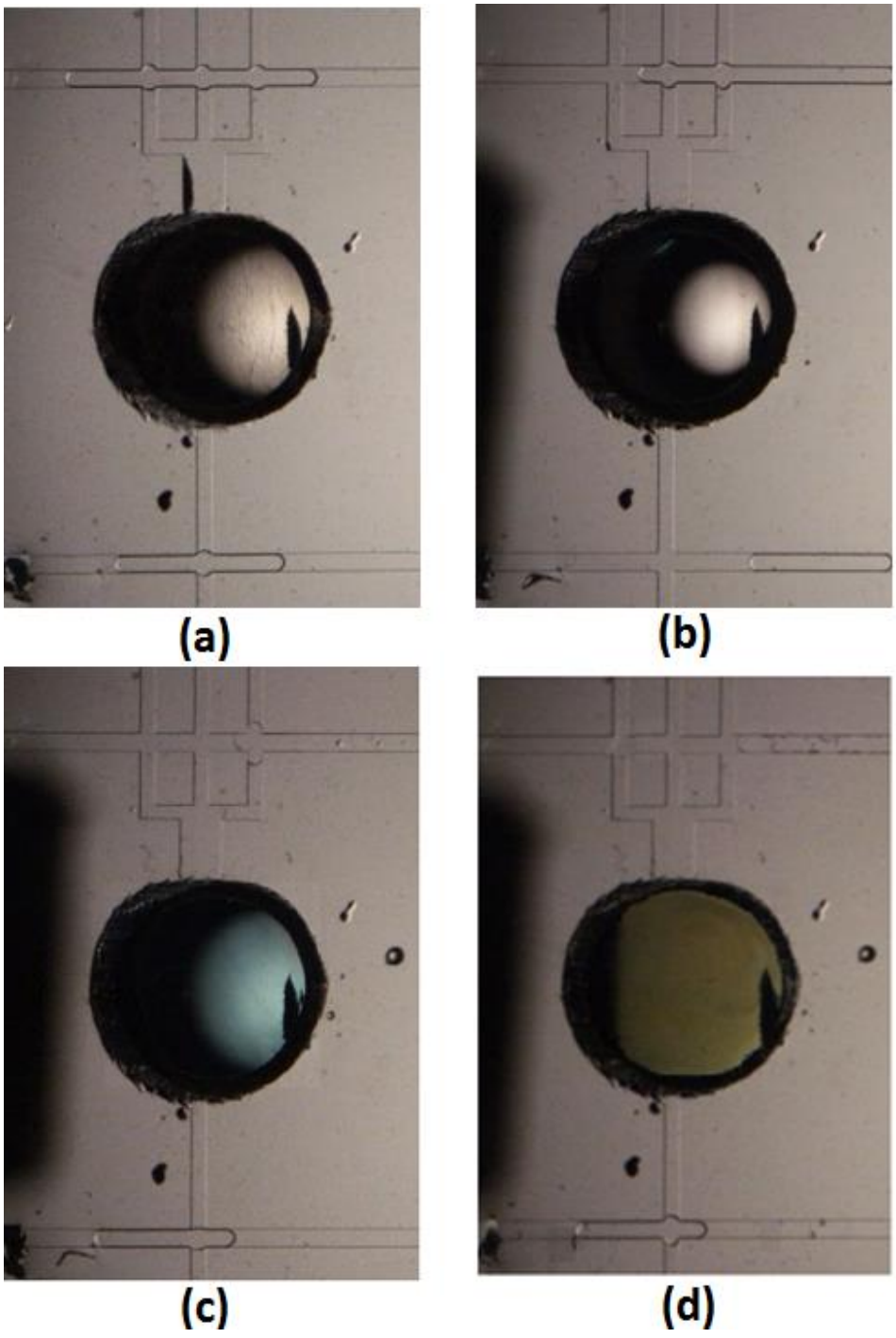

Figure 3-8 The images of the sequential processes in the positive control tests and the detection results of the negative control and *Salmonella* sample. (a) Hybridization reaction and incubation; (b) Washing; (c) Dispensing substrate solution and incubation; (d) Dispensing stop solution

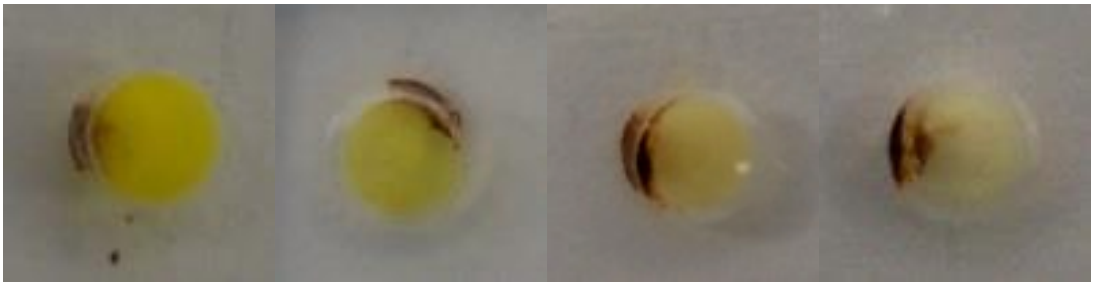

10^9 **10^7** **10^5** **10^3**

10^2 **Negative control** **Blank**

Figure 3-9 Images of the detection results of negative control and the *Salmonella* samples of concentration 10^9, 10^7, 10^5, 10^3 and 10^2 CFU/mL, blank was used as comparative sample. All pictures were taken by a common digital camera (Kodak EasyShare V803, Eastman Kodak Company, USA) (Black circles indicate the positions of the reaction wells)

It is can be seen from Figure 3-9, by using this microfluidic RNA-DNA hybridization assay chip, the yellow color of the final complex becomes lighter and lighter with the decrease in the concentrations of *Salmonella* samples. For the samples with a concentration higher than 10^3 CFU/mL, distinguishable yellow color can be observed by naked eyes in comparison with blank. However, no color difference is visible for the sample of 10^2 CFU/mL. Table 3-5 compares our present DNA hybridization assay chip with the conventional assay (a popular commercial kit: GeneQuence *Salmonella* Microwell assay). In the experiment, 12 μL reaction sample (mixing solution of lysed sample and the *Salmonella* probe hybridization solution) and 48 μL wash solution, substrate solution and stop solution were preloaded into the reagent wells. It clearly shows that our chip-based assay achieves shortened assay time and significantly reduced reagent consumption and a comparable detection limit to many commercial kits (For example, MicroSEQ® Food Pathogen Detection Solution).

Table 3-5 Comparison between the microfluidic RNA-DNA hybridization assay and conventional assay

		On-chip Assay	**Conventional**
Total assay time		25min	1hr 50min
Consumption	Reaction sample*	12 μL	275 μL
	Microbeads	7 μL	—
	Wash solution	48 μL	200 μL
	Substrate solution	48 μL	150 μL
	Stop solution	48 μL	50 μL
Sampling mode		Semi-automatic	Manual pipetting
Detection limit		10^3 CFU/mL	10^3 -10^4 CFU/mL

*Reaction sample was prepared by mixing the lysed sample (or positive control, negative control) and the *Salmonella* probe hybridization solution at a 6:5 ratio.

3.5 Summary

An RNA-DNA hybridization assay (RDHA) microchip based on the electrokinetically-controlled oil-droplet valves was developed. Based on the parameters obtained from the numerical simulation study, we designed a novel microchip for DNA hybridization assay. A pair of electrokinetically-controlled oil-droplet sequence valves (ECODSVs) was employed to control the sequential fluidic processes. Four converging sections were embedded in the control channels to obtain better control of the flow field and oil-droplet positions. With effective control of the valves movements by adjusting the voltages imposed in the control channels, the sequential assay operations can be achieved in 25 min. It is demonstrated that *Salmonella* bacteria sample can be detected down to 10^3 CFU/mL by this microfluidic DNA hybridization assay. The microfluidic chip has shortened assay time from 1hr 50mins to 25 min, and reduced reagent consumption by 3~20 times, as compared to the conventional assay.

Chapter 4

Automatic On-Chip RNA-DNA Hybridization Assay with Integrated Phase Change Microvalves

4.1 Introduction

In the previous section, a microfluidic system with electrokinetically controlled oil-droplet valves was used to realize the sequential loadings of the DNA hybridization assay. Although it worked, it has some drawbacks. For example, the sealing of the oil-droplets involves sophisticated operations. The movements and the positions of the oil-droplets have to be monitored in real time, which does not facilitate the automation of the system.

In this section, the study of an automatic DNA hybridization assay in a microfluidic chip with electrothermally actuated phase-change microvalves for pathogen detection is described. As the hybridization assay involves sequential loading and washing processes, magnetic beads coated with poly dT are used to immobilize the captured target RNA. In order to avoid using syringe pumps and mechanical valves, gravity force is used to generate the flow in the microchannels, while electrothermally actuated phase-change microvalves using the low melting point paraffin wax as the phase-changing material are designed to achieve the sequential loading processes. To achieve quantitative detection, light absorption is analyzed by an optical module to record the transmitted light intensity passing through the hybridization complex which is a function of the *Salmonella* concentration in the tested sample. LabVIEW program is coded to implement the automatic operations of the assay, including the sequential operation of the four phase-change microvalves, the activation of the light source and the recording of the outputs of the photo-detector. All assays are carried out at room temperature. Compared with the conventional methods based on microbiological culture and many commercial test kits, the approach presented in this paper can realize a rapid detection within approximately 26 min with a sample /reagents consumption reduction up to 20 folds.

4.2 Experiment

4.2.1 Principle of the assay

The principle of the assay has been demonstrated in the Chapter 3. Briefly, capture and detector DNA probes specific to the ribosomal RNA (rRNA) of target organism, poly dT coated magnetic microbeads

(Dynabeads Oligo (dT)25, Invitrogen) used as the matrix are employed. During an assay, the probe reagents, poly dT coated magnetic microbeads and the lysed samples are incubated in the reaction well for 10 min. A positive result will be yielded when both the capture and the detector probes bind to the target simultaneously. Meanwhile, the capture probe must also bind to the poly dT coated microbeads which are immobilized in the reaction well by an external magnet. After the incubation, a substrate of HRP is added to the reaction well after washing away unbound probes. Following an incubation of 5 min, the complex solution turned to blue color to indicate the presence of target. In order to obtain a colorimetric endpoint for detection, a stop solution is introduced as the final process. The final reaction complex has a differential absorption to the light of 450 nm. And the absorption is dependent on the concentration of the target sample and can be quantified by measuring the light intensity passing through the complex.

4.2.2 Materials and sample preparation

Lysis reagent concentrate, lysis reagent buffer, wash solution, hybridization solution, *Salmonella* probe solution, substrate chromogen solution, stop solution, positive and negative control were obtained from a commercial *Salmonella* test kit (GeneQuence *Salmonella* Kit, Neogen, Lansing, MI, USA). Poly dT coated magnetic micro-beads (Dynabeads® (dT) 25) were purchased from Invitrogen (Carlsbad, CA, USA).

Low-melting-point paraffin wax (Sigma-Aldrich, melting point: 44 ~ 46 ℃) was used as the material of the electrothermally actuated phase-change microvalves. Low melting point (46 ℃) paraffin wax is selected out of two main reasons: minimum energy consumption and avoid the damage to the reagents by heating. Low voltage flexible film heaters (KHLV-0502, 10W/in^2) from Omega (Stamford, CT, USA) were used to provide heating actuation.

Salmonella bacteria were prepared by Laboratory Service, University of Guelph, Canada. The procedures were summarized as follows. *Salmonella* berta (ATCC8392) cultures were grown overnight at 37 ℃ in Tryptic Soy Broth (TSB). The concentration of the bacteria was estimated by plate counting, the procedure can be found in Chapter 3.

After that, the overnight cultures were placed in boiling water bath for 20 min to kill the *Salmonella* bacteria for further use, the concentration of the cultures was 10^9 CFU/mL. The procedure for preparing *Listeria monocytogenes* was as follows. Stock cultures of *Listeria monocytogenes* (ATCC19115) strain were grown for overnight at 37 ℃ in LB Broth. The overnight cultures were killed by boiling in a

water bath for 20 min for further use. These original *Salmonella* and *Listeria monocytogenes* bacteria were diluted by PBS (1×) buffer solution (Ricca Chemical, Arlington, TX, USA) into samples of various concentrations ranging from 10^8 to 10^4 CFU/mL for testing.

Salmonella bacteria samples were obtained by diluting the culture into 10^2~10^7 CFU/mL with PBS (1×) buffer solution (Ricca Chemical, Arlington, TX, USA). Lysed *Salmonella* bacteria samples were prepared by the following specified procedure of the commercial *Salmonella* test kit: adding lysis reagent to the *Salmonella* bacteria samples followed by incubating at 65℃ for 5 min. *Salmonella* probe/hybridization mixture was prepared by *Salmonella* probe solution and hybridization solution at a mixing ratio of 1:4. The reaction sample was prepared by mixing the lysed *Salmonella* bacteria samples (controls) and the *Salmonella* probe/ hybridization mixture at a ratio of 6:5. Lysed *Listeria monocytogenes* samples were prepared by following the similar procedure. Lysis reagents were added into the *Listeria monocytogenes* bacterial samples of different concentrations ranging from 10^4~10^8 CFU/mL for incubation at 37 ℃ (*Listeria monocytogenes* samples for 5 min. *Listeria monocytogenes* probe/hybridization solution was prepared by mixing the *Listeria monocytogenes* probe solution and hybridization solution at a ratio of 1:3. The reaction samples were prepared by mixing the lysed *Listeria monocytogenes* samples (controls) and the *Listeria monocytogenes* probe/ hybridization mixture at a ratio of 6:5.

A self-made lysis buffer for *Listeria monocytognes, LB2* (prepared by Laboratory Service, University of Guelph, Canada) was tested to compare its performance with the lysis reagent of the commercial kit.

4.2.3 Microfluidic chip design and fabrication

The RNA-DNA hybridization assay (RDHA) microfluidic chip consists of a cross-shaped microchannel (400 μm wide, 100 μm high) and five reservoirs. The centre reservoir at the junction is the reaction reservoir for hybridization reaction. The diameter of the reaction reservoir is 3 mm. Three of the branch microchannels and the connected reservoirs were used for dispensing and containing the washing solution, the substrate solution and the stop solution, respectively. Another branch microchannel was connected to a waste reservoir. The diameters of the reagent holding reservoirs and the waste reservoir are 4.5 mm and 8 mm, respectively. The height of all the reservoirs is approximate 3 mm. A schematic illustration of the DHA chip (not proportional to the exact size) is shown in Figure 4-1.

The above design of the microfluidic chip is based on the following considerations. Firstly, gravity force, using the pressure difference generated by the liquid level difference between the reagent holding wells and the waste well, is employed as the driven force to generate flow in the microchannels to get rid of the use of external, bulky pumping systems. Secondly, a high flow rate must be obtained in order to reduce the assay time. Therefore, the dimensions of the microchannel cross-section cannot be too small, while the size of the reagent wells should be made as large as possible to generate a relatively constant pressure difference during the dispensing processing. However, the size of the reagents wells cannot be too large in order to minimize the reagents consumption. Theoretical modeling and numerical simulation (COMSOL Multiphysics 3.5a) were conducted to evaluate the effects of the microfluidic chip layout and dimensions on the flow and concentration fields. In addition, the core design requirement of the DHA microfluidic chip is to realize the sequential loading and washing processes involved in the assay; hence microvalves should be integrated into the DHA microfluidic chip for this purpose. For easy microfabrication and operation control, electrothermally actuated phase-change microvalves are chosen in this design. Because there are multiple microvalves on the same chip, the structure of the microchannel network must be optimally designed to minimize the mutual interference of the electric heating during the activation. The details of the electrothermally actuated phase-change microvalves are discussed later.

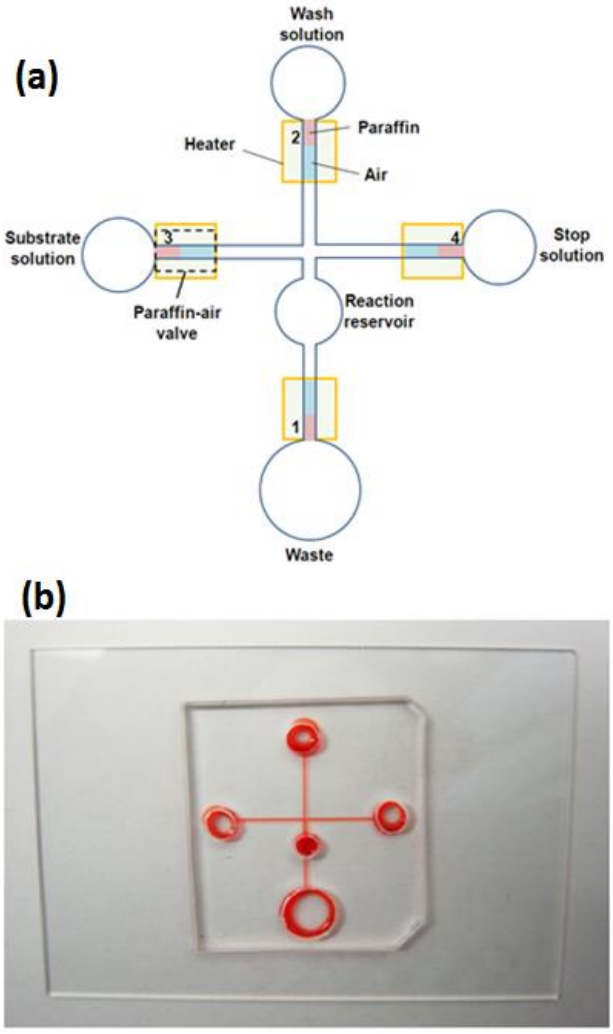

Figure 4-1 (a) Schematic of the RNA-DNA hybridization assay (RDHA) chip with integrated phase-change microvalves. The dimensions of the four branch channels are 400 μm (w) ×100 μm (h) ×10mm (l). The diameters of the reagent reservoirs and the waste reservoir are 4.5 mm and 8 mm, respectively. The depth of all the reservoirs is approximately 3 mm. The red sections represented the sealed paraffin which formed the microvalves, while the blue sections are the sealed air during the liquid loading process. Thin film heaters are placed at the bottom of the glass slide and aligned with the positions of the paraffin microvavles. (b) A picture of the microfluidic RNA- DNA hybridization assay chip (The channel is filled with a food color for easy visualization)

The microfluidic chip was made of a PDMS plate and a glass slide (25×75×1 mm, VWR International, Suwanee, GA, USA) following the standard soft lithography protocol as detailed by Biddiss et al. (2004). The master was fabricated by first spin coating a layer of SU-8 75 negative photoresist onto a

silicon wafer followed by pre-baking. A photomask carrying designed microchannel geometry was then placed on the top of the SU-8 layer and exposed to UV light. The master was ready for use after post-baking and developing. Next, a 10:1(w/w) well-mixed PDMS prepolymer and curing agent mixture was poured over the master and cured at 75 ℃ for 4 h after being degassed under low vacuum. Finally, the PDMS replica was peeled off from the master, punched holes for reservoirs (wells) and bonded onto a glass slide after oxygen plasma treating for 40 s. When bonding was conducted, a position marker was used to facilitate the alignment of the paraffin microvalves and corresponding heaters.

4.2.4 Microvalve design and operation

Phase-change microvalves based on the solid-liquid phase transition has been widely adapted to microfluidic applications (Pal et al. 2004; Lee and Lucyszyn 2007; Yang and Lin 2009). In our study, electrothermally actuated phase-change microvalves were chosen for this DHA microfluidic chip. Low melting point paraffin wax was employed as the phase change material and four separate thin film heaters were used for heating actuators. After the PDMS slab was bonded onto a glass slide, a small amount of melting paraffin was placed by a syringe at the entrance of the microchannel connecting to the reagent well. When the paraffin wax was solidified, the channel entrance was blocked, i.e., the valve was closed. Once paraffin wax was heated above its melting point, the molten paraffin wax flew into the reagent well and would solidify as the heating was stopped, then the valve was opened.

Electric thermal is employed to provide the heating for actuate the paraffin wax valve. To minimize the negative effect on the reagents in the reagent wells by heating, the power-on time should be the shorter the better. The melting point of the paraffin wax is 44 ~ 46 ℃. The time must be long enough to provide enough heating to make the paraffin wax melt. Voltage applied on the film heater and duration were studied to find out the actuation condition for the paraffin wax valve. Figure 4-2 shows the time required for different voltage applied on heater to actuate the paraffin wax valve. By doing the experiments, for an applied voltage of 5V, the heating generated by the film heater could not provide sufficient heat to melt the paraffin wax valve. When increased the magnitude of the applied voltage, the time needed for actuating the valve decreased linearly. It is found that when applied a voltage of 20 V on the heater, the paraffin wax could melt in 7 s. However, the instantaneous temperature generated was too high and the glass slide of the microchip could be damaged. Therefore, a voltage of 18 V is selected for the actuation voltage and power-on time is 15 s.

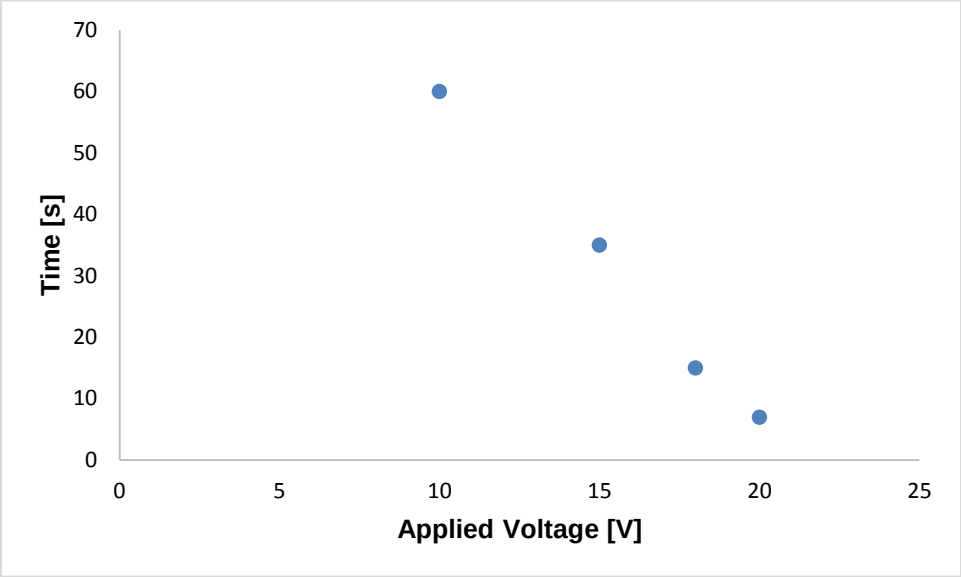

Figure 4-2 Relationship between the applied voltage on the film heater and the time required to actuate the paraffin wax valve

In the experiments, no leakage was found by using the paraffin valves. An image of a paraffin microvalve under a microscope in closed and open states is shown in Figure 4-3.

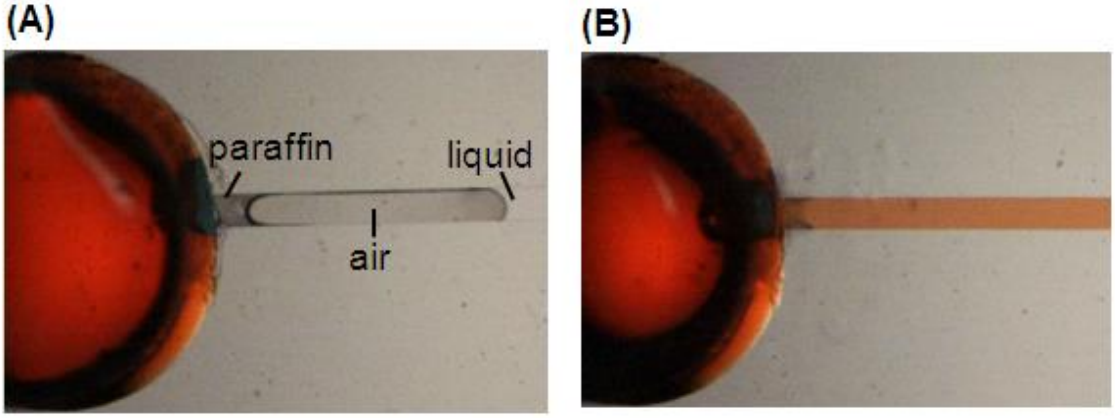

Figure 4-3 Top-view images of a paraffin microvalve under morcoscope. (A) Closed paraffin microvalve. (B) Opened paraffin microvalve

Following the experimental procedure, microbeads and buffer solution were introduced first into the reaction reservoir (see Figure 4-1). During the process, some air was inevitably sealed in the microchannels because the ends of all the microchannels were closed by the paraffin wax. However,

the sealed air will not affect the efficiency of the paraffin microvalves. In contrast, the expansion of the air under heating helps to push the molten paraffin wax into the reagent well.

Biochemical compatibility tests of the paraffin wax and the reagents involved in the assay were conducted in the commercial wells provided in the commercial test kit. Positive control, negative control and *Salmonella* samples were tested with and without the presence of paraffin wax, there was no visual difference can be detected. In addition, paraffin wax has the property of insolubility in water. All these indicated that paraffin wax would not cause any contamination.

4.2.5 Detection and signal analysis

The detection is based on the preferential absorbability of the hybridization reaction product to 450 nm wavelength light. Consequently, the transmitted light intensity is dependent on the *Salmonella* concentration of the tested samples. The schematic diagram of the detection module based on light intensity measurement is shown in Figure 4-4. The detection module consists of an illumination unit, a sample platform for holding the microfluidic chip, a photo-detector and a signal acquisition & processing unit. The illumination unit includes a blue LED (Luxeon®, San Jose, CA, USA) with a collimated lens and a 448/20 nm wavelength band-pass filter (BrightLine®, Semrock Inc., Rochester, New York, USA). A high sensitivity Si photodiode (S8745-01, Hamamatsu, Bridgewater, NJ, USA) is employed to detect the light intensity. The control of the LED, signal acquisition via the photodiode, signal storage and display is achieved by a DAQ board (USB-6259, National Instruments, Austin, TX, USA) and a LabVIEW program.

Principle verification experiments were conducted by light intensity detection using a digitized CCD camera (Retiga 2000R, QImaging®, Surrey, BC, Canada) mounted on an inverted microscope (Nikon Eclipse Ti, Nikon Instrument Inc.) instead of the photodiode, as shown in the dashed frame in Figure 4-4. Images were taken to record the transmitted light intensities passing through the hybridization complex, which were dependent on the *Salmonella* concentration of the samples, to see whether the differences could be distinguished or not. Images were analyzed by software NIS-Elements BR 3.0.

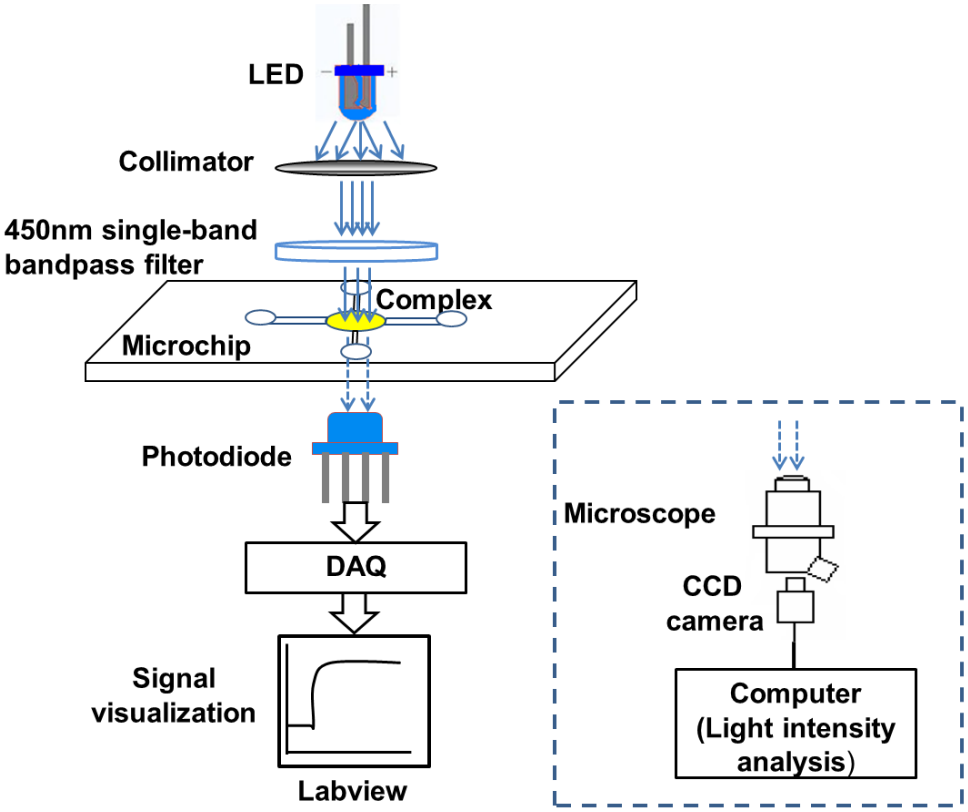

Figure 4-4 Schematic of the detection system based on light absorption measurement

4.2.6 Experimental procedures and setup

The light source, microfluidic chip holder, heaters and the photodiode were integrated in a custom designed holder box (approximately 10×8×6 cm). In the chip holder, the thin film heaters were fixed on the top of a glass slide with prefixed positions aligned to the paraffin microvalves in the microfluidic chip. The microfluidic chip was placed on the top of the glass slide with the heaters. Twenty volts was applied to the heaters sequentially by the LabVIEW program for 15s to activate a paraffin microvalve via a DC-regulated power supply (CSI12001X, Circuit Specialists Inc., USA). After running the hybridization assay, the microbeads were attracted aside to the reaction reservoir edge by a magnet to avoid the interfering the optic detection. The light source was activated by the LabVIEW program and then the output voltage of the photodiode was recorded by the LabVIEW as well via the data acquisition system (DAQ).

The typical DNA hybridization assay on this microfluidic chip followed the following procedures. First, the entrances of all the four branch channels are sealed by paraffin wax to form the phase-change

microvalves as described previously. Then, reagents reservoirs are filled with wash solution, substrate solution and stop solution, respectively. Afterwards, the coated microbeads and buffer solution are introduced into the reaction reservoir followed by loading the testing sample to start the assay.

For a complete DNA hybridization assay, four steps are involved. The first step is the hybridization reaction and incubation during which all the four paraffin microvalves are closed. The second step is the washing. In this step, the microvalves 1 and 2 as indicated in the Figure 4-1 are opened sequentially in order to wash away the unbound probes. In the third step, the microvalve 3 is opened to dispense the substrate solution. The substrate solution will replace the most volume of the wash solution in the reaction reservoir and then undergo incubation. The last step is the opening of the microvalve 4 for dispensing the stop solution.

The experimental system consists of light source, microfluidic chip, heaters, microscope, CCD camera, power supplies and computer, as shown in Figure 4-5. Flexible heaters are fixed on the bottom of the glass slide, which aligned to the positions of the paraffin microvalves. Eighteen volts is imposed on the heater sequentially for 10~15 s to activate corresponding paraffin microvalve via a DC-regulated power supply (CSI12001X, Circuit Specialists Inc., USA). After running the hybridization assay, the light source provided by the illumination system as aforementioned is lighted on, meanwhile a microscope mounted with a CCD camera and the computer software are used to capture and digitized the image of the reaction reservoir followed by the intensity analysis. A magnet seated on the bottom of the glass slide will localize the magnetic beads to the side of the reservoir to avoid the interference error when the detection was undergoing.

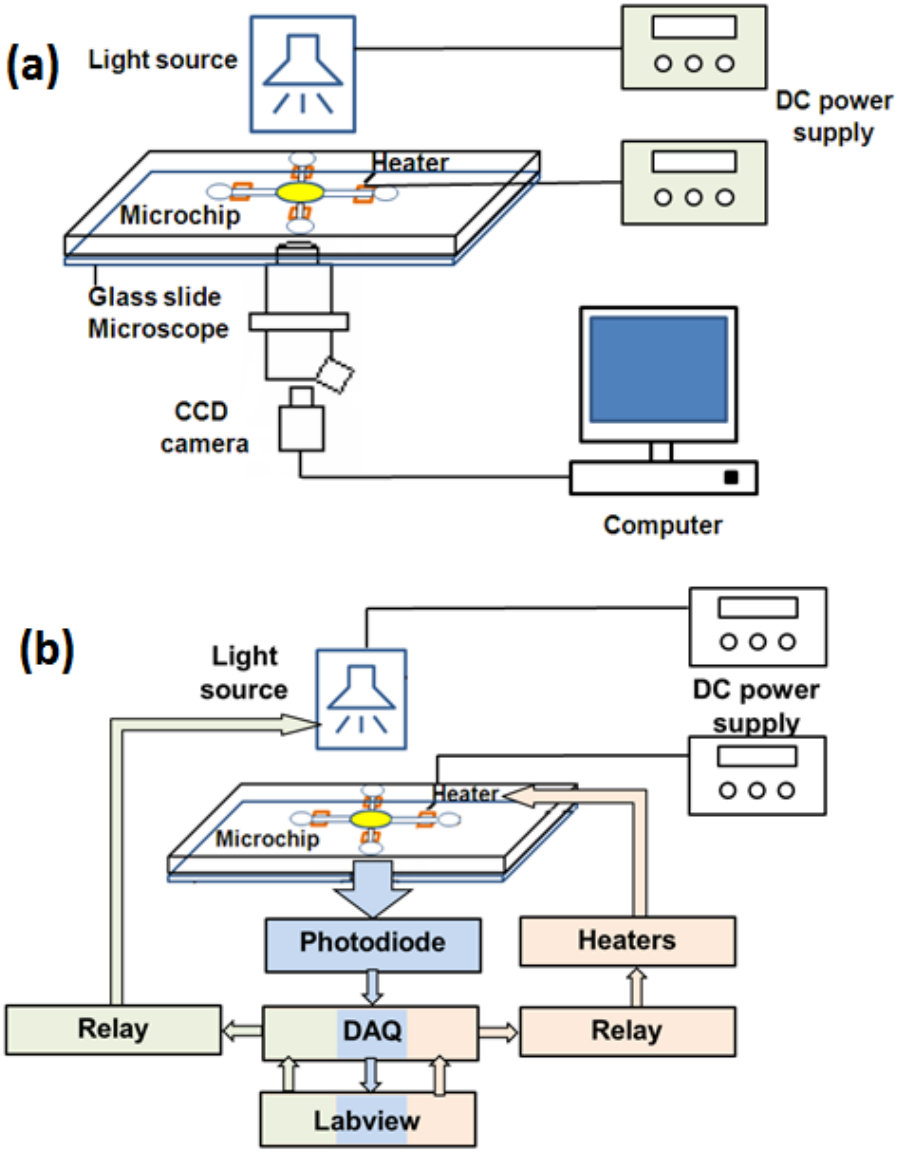

Figure 4-5 Schematic of the experimental setup for the microfluidic RNA-DNA hybridization assay. (A) the experimental setup of verification experiments; (B) the experimental setup based on the miniaturized optical detection

4.3 Results and discussion

4.3.1 Visualization experiment of the RDHA microfluidic chip

In this study, efforts were made to determine reasonable time for the washing step to prevent the false positive signal, while reducing the overall assay time as much as possible. The flow rate of the wash solution and the displacement process of the liquid in the reaction reservoir were studied by numerical simulations and by experimental verification. The duration for each step is summarized in Table 4-1. V1~V4 in Table 4-1 represent the paraffin microvavles 1 to 4 in the four branch channels.

Table 4-1 Operation steps for the RNA-DNA hybridization on-chip assay

Valve operation	**Steps**	**Time**
All closed	Incubation (hybridization reaction)	10 min
V1 opened	Washing	2 min
V2 opened		6 min
V3 opened	Dispensing and incubation(substrate solution)	5 min
V4 opened	Dispensing (stop solution)	2 min
All opened	Detection	30 s
Total assay time		~26 min

An example picture of the visualized sequential reagents loading processes of the DNA hybridization assay is shown in Figure 4-6. The full DNA hybridization assay consists of four steps as mentioned previously. For the first step, all four paraffin microvalves were closed for the hybridization reaction and incubation (Figure 4-6 (a)). During the second step — washing, paraffin microvlave 1 and 2 were opened sequentially to remove the unbound probes (Figure 4-6 (b)): open the microvalve 1 makes the major reaction sample flow to the waste reservoir firstly due to the pressure difference; afterwards, microvalve 2 was opened to flush the reaction reservoir by washing solution (Figure 4-6 (c) and (d)). The sequential opening operation of these two microvalves was critical since the wash efficiency can be enhanced compared to the way that opening the two microvalves at the same time. The following two steps were the loading of the substrate solution and the stop solution as the opening of the microvalve 3 and 4. As mentioned previously, gravity-based pressure-driven flow was used to generate

liquid flow in the microchannels. The flow was generated due to the pressure difference between reservoirs, as time went, the liquid level difference diminished gradually until came to a uniform level hence the flow eventually stopped. Since liquid level in the next-opened reservoir was always higher than that of the balanced liquid, i.e., the liquid level in the reaction reservoir and the former opened reservoir, it could generate flow to the relative low-pressure reservoirs, as well as avoided the cross-contamination of reagents.

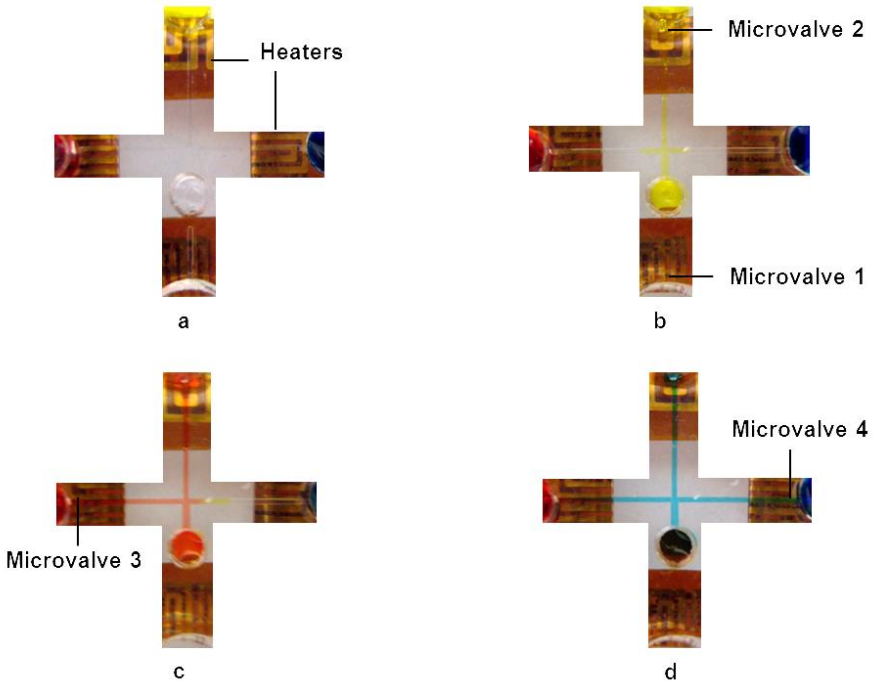

Figure 4-6 The visualized sequential loading processes of a full RNA-DNA hybridization assay. Yellow, red and blue food colors represent wash solution, substrate solution and stop solution, respectively. (a) The visualized hybridization reaction step: all four paraffin microvalves were closed. (b) The visualized washing step to remove the unbound probes: microvalves 1 was open firstly for 2 min and subsequently microvalve 2 for 8 min. (c) The visualized step of loading substrate solution and incubation: microvalve 3 was opened. (d) The visualized step of loading stop solution: microvalve 4 was opened

4.3.2 RNA-DNA hybridization assay on *Salmonella*

Salmonella samples of known concentrations ranging from 10^9 to 10^2 CFU/mL, positive control and negative control were tested on presented RDHA microfluidic chip. The experimental procedures and

controlling parameters were provided in Table 4-1. Briefly, the sequential loading of reagents was achieved by opening the paraffin microvalves one by one. Twenty volts were applied on the flexible heaters for 15 s to actuate the paraffin microvalve. After dispensing the stop solution, illumination system was lighted up followed by recording the voltage output of the photodiode (the image and intensity analysis in the verification experiments). The total time for a full assay on presented DHA microfluidic chip was approximately 26 min.

Experiments were repeated five times for reaction sample of each studied concentration. A set of representative experimental results with intensity measurement of final hybridization complex is shown in Figure 4-7. The intensity profile of the reaction samples of different concentrations is shown in Figure 4-8. As seen in the Figure 4-8, the detection limit can be achieved as low as 10^2 CFU/mL by this DHA microfluidic chip.

The experiments were repeated five times for each concentration by the miniaturized optical module. As an example, Figure 4-9 shows the detected light intensity in terms of the voltage output of the photo-detector. The transmitted light intensity of the final hybridization complex decreases with the concentration of the original bacterial concentration in the tested samples. The voltage output as a function of *Salmonella* concentration is shown in Figure 4-10. As seen in the figure, the detection limit can be achieved as low as 10^3 CFU/mL by this DHA microfluidic chip with miniaturized optical detection system.

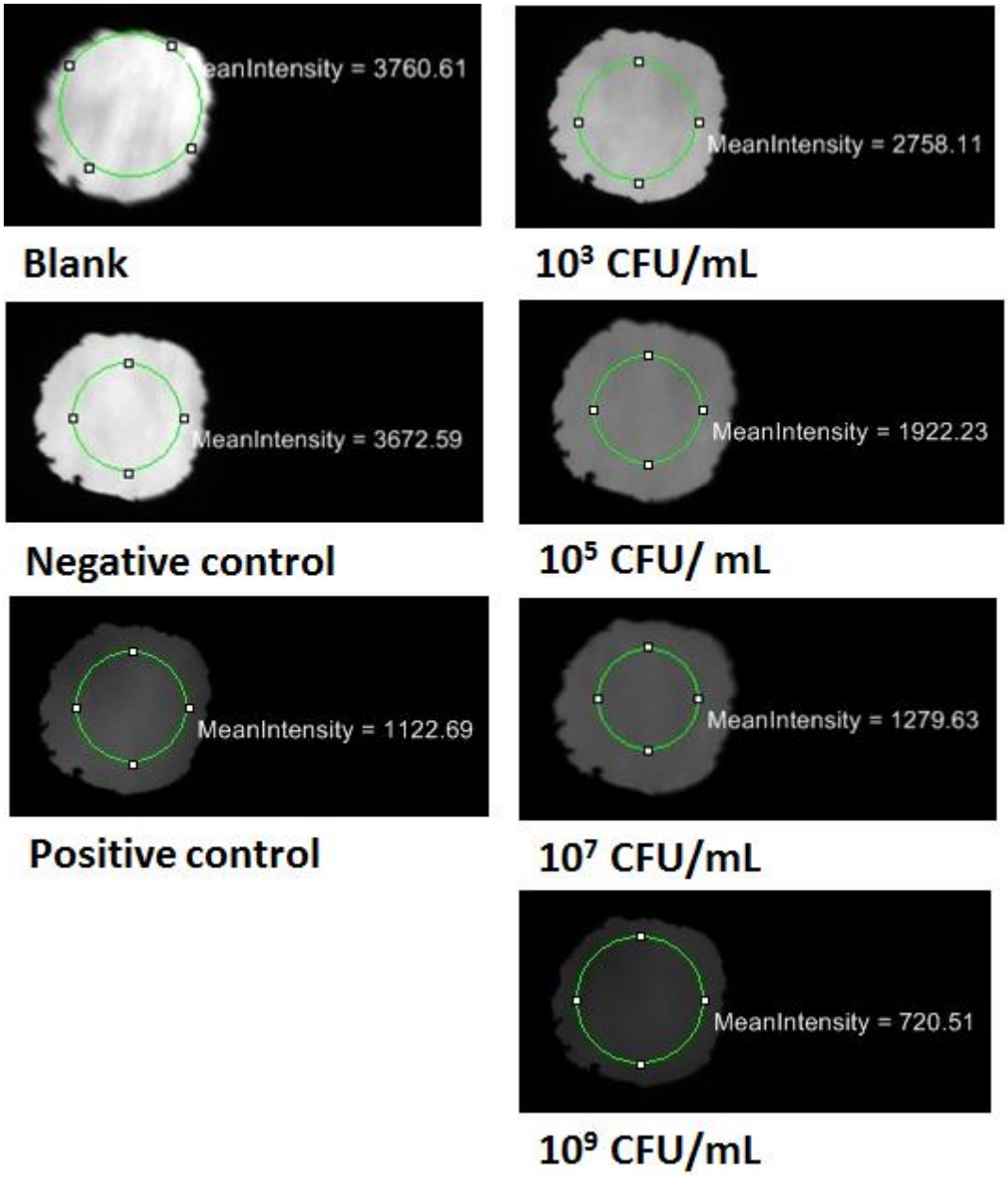

Figure 4-7 An example of light intensity images of samples with different concentrations

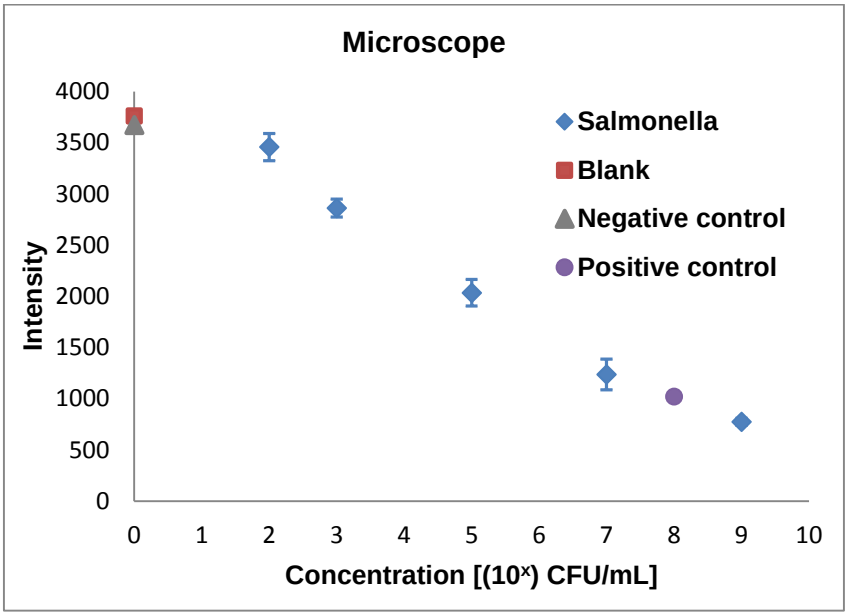

Figure 4-8 Intensity profile detected by microscope depending on concentrations of *Salmonella* bacteria, negative control, positive control and blank

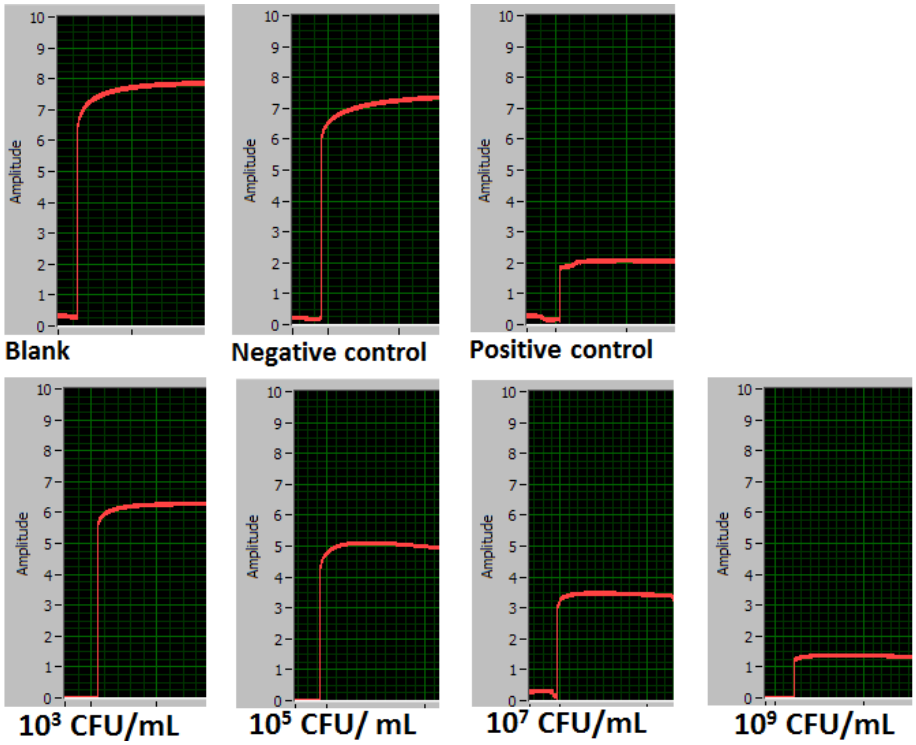

Figure 4-9 An example of voltage output detected by photodiode of different concentration samples

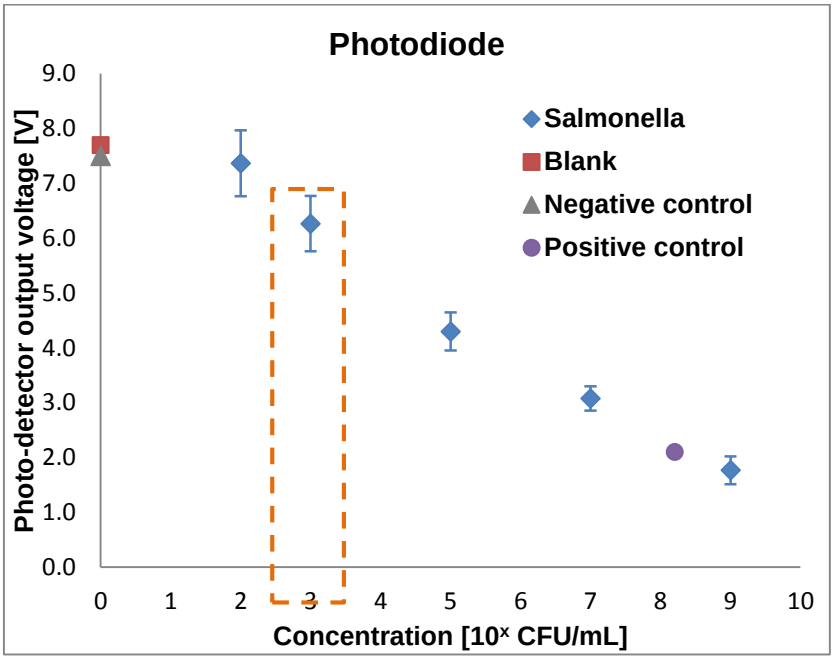

Figure 4-10 Voltage profile detected by photodiode depending on concentrations of *Salmonella* bacteria, negative control, positive control and blank

4.3.3 RNA-DNA hybridization assay on *Listeria monocytognes*

The results of the DHA microfluidic system in the detection of *Salmonella* bacteria shown in the previous section have proven that the method worked well and the performance of the miniaturized optical detection module was excellent. Then *Listeria monocytogenes* bacteria was tested by this microfluidic system. Commercial lysis reagent and self-made LB2 lysis reagents were applied.

Listeria monocytogenes bacteria sample were diluted into various concentrations ranging from 10^2 CFU/mL to 10^8 CFU/mL. The detection for each concentration sample was repeated 2~3 times. Clearly, the transmitted light intensity of the final hybridization complex decreased with the concentration of the bacterial concentration in the tested samples. The voltage output of the photo-detector as a function of *Listeria monocytogenes* concentration is shown in Figure 4-11 and Figure 4-12. Figure 4-11 is the result by using commercial lysis buffer, while Figure 4-12 shows the result by using LB2 lysis buffer.

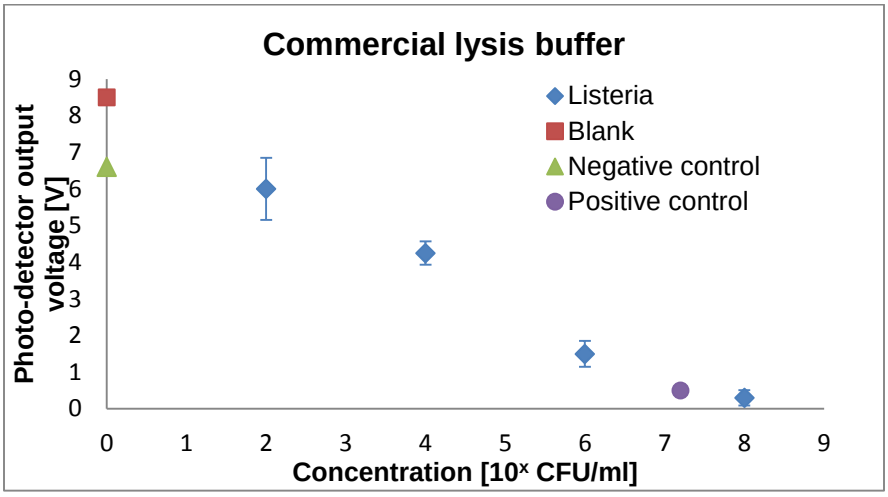

Figure 4-11 Dependence of the voltage output detected by photodiode on the concentrations of *Listeria monocytogenes*, negative control, positive control and blank (commercial lysis buffer)

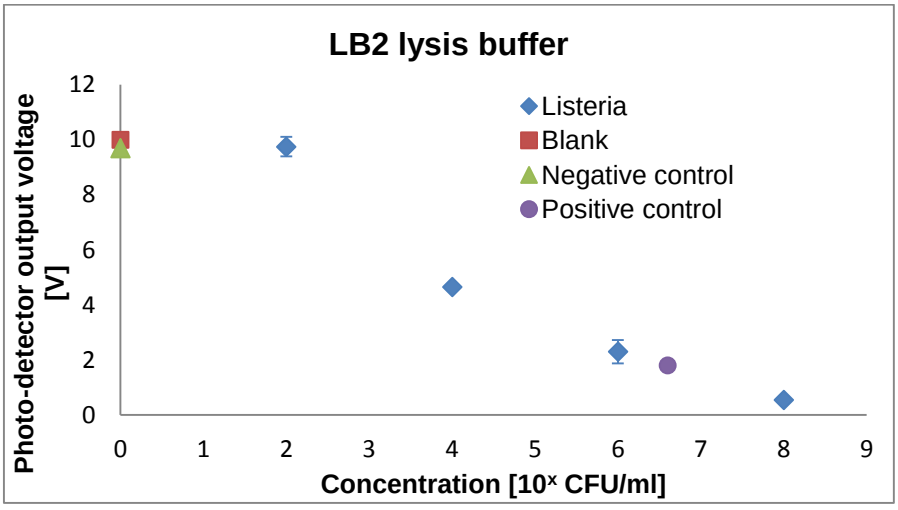

Figure 4-12 Dependence of the voltage output detected by photodiode on the concentrations of *Listeria monocytogenes*, negative control, positive control and blank (LB2 lysis buffer)

When compared to the popular commercial test kit, as shown in Table 4-2, the presented DNA hybridization assay chip has distinguished advantages, such as the shortened assay time (from 1hr 50 min to 26 min), significantly reduced reagent consumption (from 275 μL to 14 μL) and a better detection limit to many commercial kits (For example, MicroSEQ® Food Pathogen Detection Solution).

Table 4-2 Comparison between the microfluidic RNA-DNA hybridization assay and commercial kits

		On-chip Assay	Commercial kit
Total assay time		26 min	1 hr 50 min
	Reaction sample [a]	14 μL	275 μL
	Microbeads	7 μL	—
Consumption	Wash solution	48 μL	200 μL
	Substrate solution	48 μL	150 μL
	Stop solution	48 μL	50 μL
Sampling mode		Automatic	Manual pipetting
Detection limit		10^3 CFU/mL	10^3 ~ 10^4 CFU/mL

[a] Reaction samples were prepared by mixing the lysed *Salmonella/ Listeria monocytogenes* bacterial samples (controls) and the *Salmonella/ Listeria* probe/ hybridization mixture at a ratio of 6:5.

4.4 Summary

This study has demonstrated an automatic microfluidic DNA hybridization assay chip for *Salmonella* and *Listeria monocytogenes* bacteria detection. Electrothermally actuated phase-change microvalves were applied in this DHA microfluidic chip to achieve the sequential multistep assay operations. Miniaturized optical detection system was employed to determine the bacterial concentration quantitatively based on the transmitted light intensity measurement. LabVIEW program was coded to implement the automatic operations of the complete assay. Significantly shortened assay time (~26 min) and reagent/sample consumption reduction (up to 20-folds) were achieved. In addition, the detection limit in *Salmonella* bacteria detection is as low as 10^3 CFU/mL, which is comparable to or even better than many commercial test kits. The presented DHA microfluidic chip has the potential to facilitate the development of a handheld device for point-of-testing applications. Furthermore, this DHA microfluidic chip, as a general fluidic operation system, can be readily expanded its applications in detecting other bacteria by employing corresponding reagents and probes.

Chapter 5

Automatic Electrokinetically-controlled RNA-DNA Hybridization Assay for Foodborne Pathogens Detection

5.1 Introduction

The microfluidic RNA-DNA hybridization assay chip was further improved by using fully electrokinetic control method. The biggest advantage of this method is no microvalves and tubes are required. The automatic sequential reagent dispensing and washing processes are realized by a programmable DC (direct current) voltage sequencer. The electro-osmotic pumping force is employed to drive the liquid. What we need to do is to provide and manage the electric fields along the microchannels at each step via electrodes. The management of the potentials on the electrodes is realized by the programmable DC voltage sequencer. The required electric potentials and duration on the electrodes are pre-set as a sequence in the voltage sequencer. It was found that the substrate solution is unstable under the electric field, thus a novel method of generating electrokinetically-induced pressure-driven flow in the T-shape microchannel is developed. This way may eliminate the chance for the substrate to expose to the electric field directly. Similarly, the miniaturized light absorption detection module is applied to get the quantitative result. The numerical model was studied to investigate the flow field of the microchip. Then Salmonella bacteria and Listeria monocytogenes of different concentrations are assayed. Compared to the previous designed microfluidic system, no complicated microvalve fabrication process is involved, the chip layout is much simpler while significant reduction in the sample and reagent consumption, and substantially shorten assay time are still achieved. The detection limit for the Salmonella and Listeria monocytogenes bacteria with this microfluidic system is 10^4 CFU/mL. This automatic-operating DNA hybridization assay microfluidic system is promising for the on-site pathogens detection applications.

5.2 Principle of the flow control

In this approach, the electro-osmotic flow (EOF) is applied to drive the liquid. The principle of the electro-osmotic flow can be briefly demonstrated as follow. When an electric field is applied along a microchannel, the ions in the liquid will move by the electrical force. Then moving ions can drag the surrounding liquid molecules to move with them because of the viscous effect thus generating a bulky

liquid motion. This bulky liquid motion is so called the electro-osmotic flow. This flow can be used as the pump to drive liquid. As mentioned that the electrokinetically-induced pressure-driven flow is used to dispense the substrate solution.

5.3 Numerical study

5.3.1 Theoretical analysis

The schematic diagram of the proposed method is shown in Figure 5-1. The microfluidic system is placed horizontally on a lab table. The microchip consists of a T-shaped rectangular channel and four cylindrical reservoirs initially with the same liquid level. The assay procedure is composed of three steps: hybridization reaction and incubation (step 1), washing (step 2) and substrate solution dispensing (step 3).

In the numerical simulation, the liquid in the microchannel is assumed as an incompressible, Newtonian, symmetric electrolyte with constant density and viscosity. All the four reservoirs, 1, 2, 3 and 4 are open to air and have atmospheric pressure. The channel wall is uniformly charged with the zeta potential, ζ. The channel 2-4 is used as an electro-osmotic pump which can be generated by applying the DC power among the reservoirs 2, 1 and 4. The different applied voltages for step 2 and step 3 are shown in Figure 5-1. In the step 2, the direction of the EOF (electro-osmotic flow) is required to flow from the reservoir 2 to the reservoir 4. In the step 3, the direction of the EOF (electro-osmotic flow) is required flow from the reservoir 1 to both the reservoir 2 and 4. Due to the flow continuity, reservoir 1 has the negative pressure that induces a flow from the reservoirs 3 to the reservoir 1 thus generates a continuous pressure-driven flow.

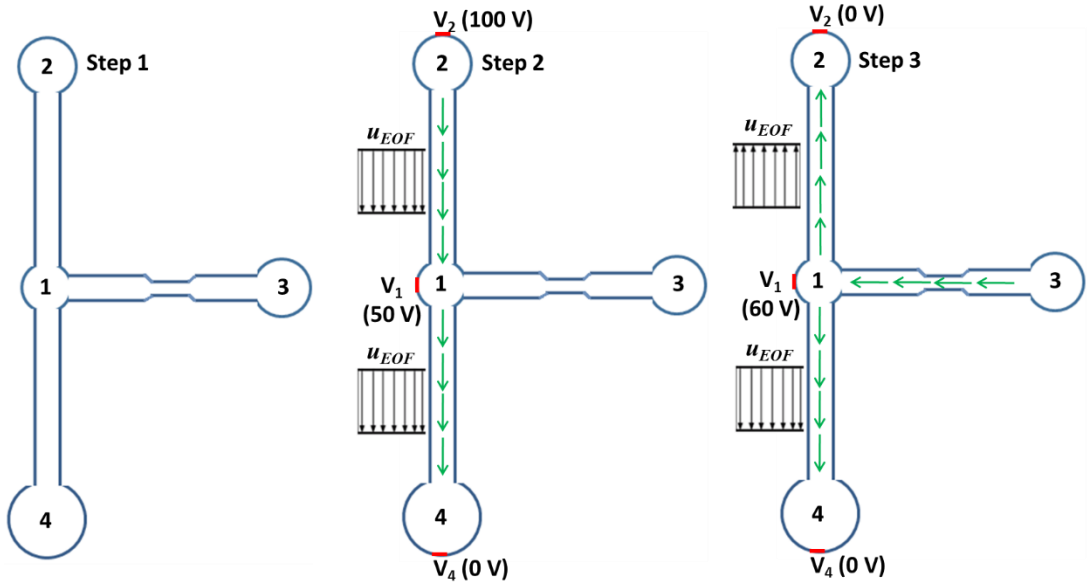

Figure 5-1 Schematic diagram of the assay procedure and proposed method for flow control. Electro-osmotic flow and electrokinetically-induced pressure-driven flow were employed in the second step and the third step, respectively. The green arrows indicates the flow direction. The red lines indicates the position of the electrodes

In the step 2 of washing, the liquid is pumped out of the reservoir 2 and all the way to the reservoir 4 by the electro-osmotic force via the electric field applied along the microchannel 2-4. In the step 3, once the electric field is applied on the vertical microchannel, the liquid is sucked out from the reservoir 1 and flows into both the reservoir 2 and 4 due to the EOF resulting in a negative pressure in the reservoir 1. According to the fluidic continuity, the liquid in the horizontal channel will move into the reservoir 1 to fill it. Thus, a pressure gradient is generated between the reservoir 1 and reservoir 3 resulting in a continuous electrokinetically-induced pressure-driven flow in the horizontal channel. By this novel method, it is clearly shown that without any moving parts and syringe pumps, the pressure-driven flow is generated in the proposed microfluidic chip. When loading the substrate solution in the reservoir 3, the substrate solution will flow into the horizontal microchannel hence the reservoir 1 by electrokinetically-induced pressure-driven flow without being exposed to the electric field directly.

There is a concern here must be noticed. Since it takes a period of time for the first two steps, during the time period the substrate solution may flow into the reaction well or the reaction sample may flow into the reservoir of substrate solution. This is unacceptable because the substrate solution may react with the detector probes (both bond and unbound to the target organism) coated with enzyme HRP thus

fails the test. This unexpected flow causes by two reasons. One is the diffusion and the other is the pressure difference due to the liquid level between the reservoirs 1 and 3 which introduced by the error when loading reagents manually. The second factor is dominant. In order to avoid this flow, a narrow section of 30 μm can be added onto the horizontal channel. This narrow section is supposed to generate a big resistance to reduce the unexpected pressure-driven flow.

5.3.2 Physical modeling

Numerical study was conducted to prove the theoretical analysis. In the numerical simulation, COMSOL MULTIPJHYSICS was used to solve this numerical model. 200,000 elements or more were used in all the simulations to avoid the grid dependence. The numerical studies were done by three main parts. In the first part, the step 2 was studied to investigate the washing process. In the second part, the effectiveness of the proposed electrokinetically-induced pressure-driven flow in the T-shaped channel was studied. In the third part, the comparison of the concentration fields between the designs with narrow section on the substrate solution dispensing channel and without this section was illustrated.

- *Electric field*

When electrical potential, $\emptyset_e$, is applied at reservoir 2, 1 and 4, the applied potential through the system is governed by Laplace's equation.

$$\boldsymbol{\nabla^2 \emptyset_e = 0} \tag{5-1}$$

Once the electrical field is known, the local electric field strength can be calculated by

$$\boldsymbol{\vec{E} = \vec{\nabla} \emptyset_e} \tag{5-2}$$

The zeta potential at the non-conducting channel wall ζ_w is a constant and the value depends on the properties of the solid material and the liquid. According to Helmholtz–Smoluchowski equation, the velocity of the electro-osmotic flow is expressed as

$$\boldsymbol{\vec{u} = \vec{u}_{eo} = -\frac{\varepsilon_0 \varepsilon_r \zeta_w}{\mu} \vec{E}} \tag{5-3}$$

where ε_0 and ε_r are the dielectric constant in vacuum and the dielectric constant of the solution, respectively. The electro-osmotic velocity boundary condition is applied at the walls of the vertical channe and non-slip velocity boundary condition is applied at the other walls where the flow is generated by the induced pressure. The boundary conditions of the electric field are

$$\begin{cases} \emptyset_{e1} = \emptyset_1, \ \textbf{at reservoir 1} \\ \emptyset_{e2} = \emptyset_2, \ \textbf{at reservoir 2} \\ \emptyset_{e4} = \emptyset_4, \ \textbf{at reservoir 4} \end{cases} \quad (5\text{-}4)$$

- *Velocity field*

The velocity field is governed by the continuity equation and the Navier-Stokes equations.

$$\boldsymbol{\nabla \cdot \vec{u} = 0} \quad (5\text{-}5)$$

$$\boldsymbol{\rho \vec{u} \cdot \nabla \vec{u} = -\nabla P + \mu \nabla^2 \vec{u}} \quad (5\text{-}6)$$

where ρ and μ are the density and viscosity of the liquid, u is velocity, P is the pressure gradient.

- *Concentration field*

The concentration field of species is described by

$$\boldsymbol{\frac{\partial C}{\partial t} + \nabla \cdot (-D \nabla C) = -\vec{u} \cdot \nabla C} \quad (5\text{-}7)$$

where C is the concentration, D is the diffusion coefficient, u is the velocity.

The boundary conditions are

$C = C_0$ at reservoir 3 , (5-8a)

$C = 0$ at reservoir 1, 4 (5-8b)

$\frac{\partial C_{t\geq 0}}{\partial n} = 0$ at all the walls (5-8c)

and the initial concentration in the microchannel is

$C_{t=0} = 0$

For analysis, the following parameters are used in the numerical simulation:

- For convenience, the channel depth is fixed at 40 μm;
- The length of vertical channel is 1.2 cm; the width of the vertical channel is 500 μm.
- The width and length of horizontal channel are 250 μm and 6 mm, respectively;
- The width of the narrow section is 30 μm;

- The work solution is DI water. The density of DI water ρ is 1000 kg/m^3, the viscosity of DI water μ is 10^{-3} kg/m·s, the relative permittivity of water ε is 80;
- The zeta potential ζ is -98 mV (Lee and Li, 2006).

Figure 5-2 shows the simulation model of the proposed microfluidic chip. Equations (5-1), (5-2) and (5-3) subjected to boundary conditions were solved to find the electric potential in the system. At the reservoir 1, a plane with the dimension 100 μm × 40 μm was assumed to be an electrode ($Øe_1$). It was also assumed that the boundaries (reservoirs) 2 and 4 have the potential value $Øe_1$ and $Øe_4$. In order to obtain the velocity field, Equations (5-5) and (5-6) subjected to boundary conditions must be solved. The open boundary condition (inlet and outlet) was assumed for boundaries (reservoirs) 2 and 4. The electro-osmotic slip velocity was considered on the walls of channel 2-4 while the walls in the rest of the walls have no-slip velocity conditions due to the pressure driven flow.

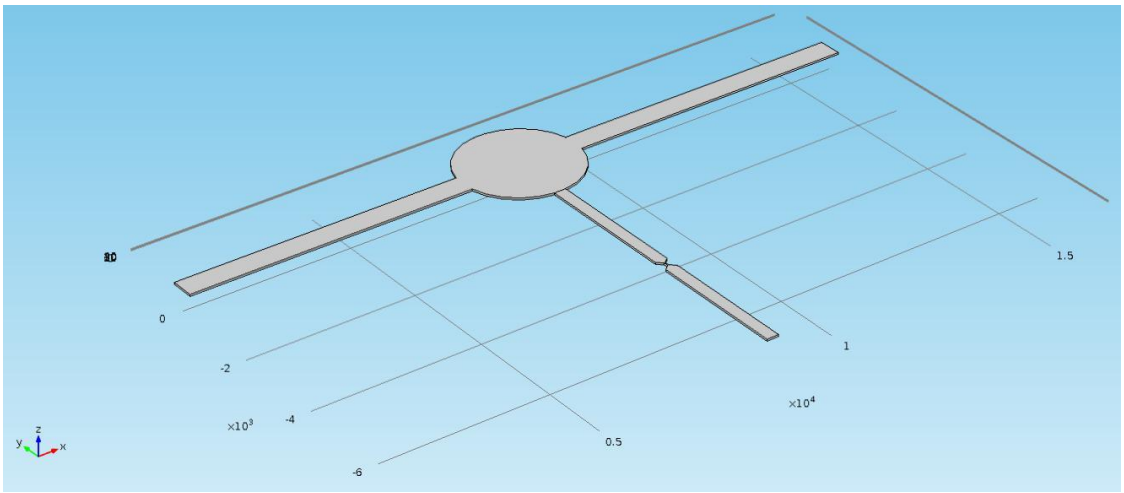

Figure 5-2 The simulation model of the proposed microfluidic chip

5.3.3 The flow field in the microchannel during washing step

By applying the electric potentials 100 V, 50 V and 0 V at the reservoirs 2, 1 and 4, the EOF flow was generated in the channel 2-4 and consequently the washing step was implemented in the mcirochannel 2-4.

Figure 5-3 (a) shows the electric potential distribution in the T-shaped microchannel. As mentioned before, when applying the electric potentials 100 V, 50 V and 0 V at the reservoirs 2, 1 and 4, the electro-osmotic flow is generated in the vertical channel and consequently the washing step is

implemented. In Figure 5-3 (a), the result clearly shows that there is no electric potential in the channel 3-1 (the electric potential at the inlet 3 is the same as at the reservoir 1). Figure 5-3 (b) shows the details of the flow field in the microchannel. The red vectors demonstrates the flow direction in the channel 2-4. It is clearly seen that the liquid flows in the channel 2-4 due to the EOF. The flow rate is about 1.03×10^{-11} m^3/s at the outlet 4. The average velocity at the outlet 4 is about 515 μm/s, which is very close to the velocity of the EOF (approximately 560 μm/s). The simulation result agrees with the theoretical prediction. It should be noted that there is no flow motion in the microchannel 3-1, which indicates that the liquid is stationary in the microchannel 3-1 during the washing step.

From Figure 5-3, it can be seen clearly that the dominant flow is the electro-osmotic flow near the walls thus the net flow is from the inlet 2 towards the end of channel 4. There is no flow motion generated in the microchannel 3-1. This means the narrow section in the middle of the channel works well because it will generate a big pressure resistance preventing it diffuse into the reservoir 1. This is very important. Because the substrate solution must not contact with the probe reagent in the reaction reservoir prior to the washing step otherwise it will be oxidized by the enzyme HRP and cause false positive signal.

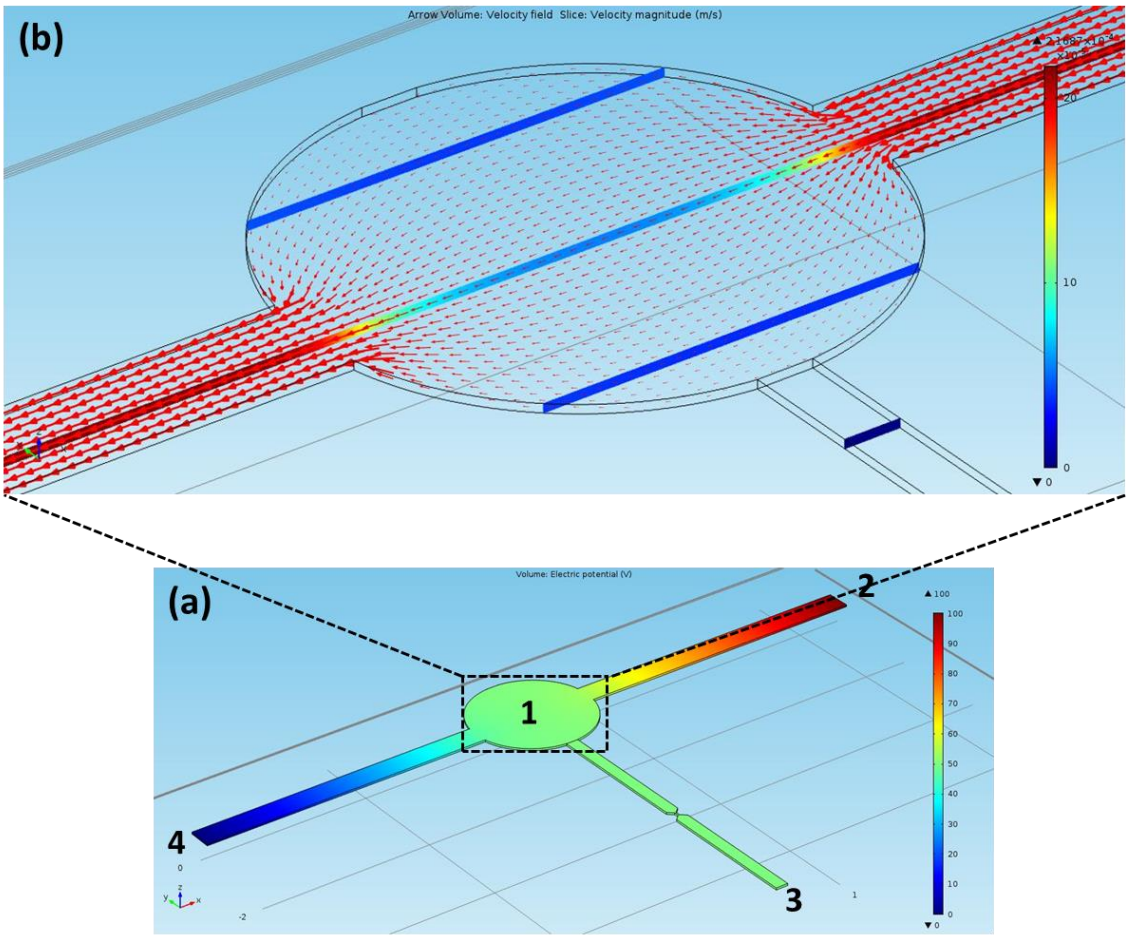

Figure 5-3 (a) Electrical potential distribution in the T-shaped microchannel. (b) The details of the flow field in the T-shaped microchannel (100 V, 50 V and 0 V at the reservoirs 2, 1 and 4)

5.3.4 The flow field in the microchannel during substrate solution dispensing step

In step 3, the substrate solution needs to be dispensed to the reaction reservoir (reservoir 1). However, it is found that it is unstable when expose to electric field for a period of time hence it cannot driven by the EOF directly. Therefore, the electrokinetically-induced pressure-driven flow is introduced to address the issue. In this way, the substrate solution is driven by the pressure-driven flow so that avoid being damaged (oxidized) by the electric filed.

According to generating the required flow, the applied voltages on the reservoirs need to be changed. In the numerical study for this step, the electric potentials 60 V, 0 V and 0 V were imposed at the reservoirs 2, 4 and 1, respectively. After applying the voltages at the reservoirs, the EOF flow is

generated in both the microchannel 1-4 and 1-2. These two microchannels are used as the electro-osmotic pumps to suck the liquid out of the reservoir 1. As mentioned before, this electro-osmotic pumping force will cause an electrokinetically-induced pressure-driven flow in the microchannel 1-3.

Figure 5-4 (a) shows that there is no electric potential in the vertical channel (the electric potential at the inlet 3 is the same as at the reservoir 1), which indicates that only the pressure-driven flow exists in the microchannel 1-3. Figure 5-4 (b) shows the velocity vectors in the microchannels. In the microchannel 1-2 and microchannel 1-4, the liquid near the channel walls flows out of reservoir 1 towards the both ends of the microchannel due to the electro-osmosis flow, meanwhile, it is found that there is also a backward flow in the middle of the microchannel due to the pressure gradient between the reservoirs (2 and 4) and the reservoir 1. It should be noted that this static pressure gradient is generated by the motion of liquid. From this figure, it can be clearly seen that the dominant flow is the electro-osmotic flow near the walls and hence the net flow is from the reservoir 1 to the ends of channel. Meanwhile, in Figure 5-4 (c), the red vectors demonstrated the velocity of the pressure-driven flow from the reservoir 3 to the reservoir 1. It is clearly shown that the continuous electrokinetically-induced pressure-driven flow is generated in the channel 3-1. From the simulation result, the average velocity is approximately 214 μm/s.

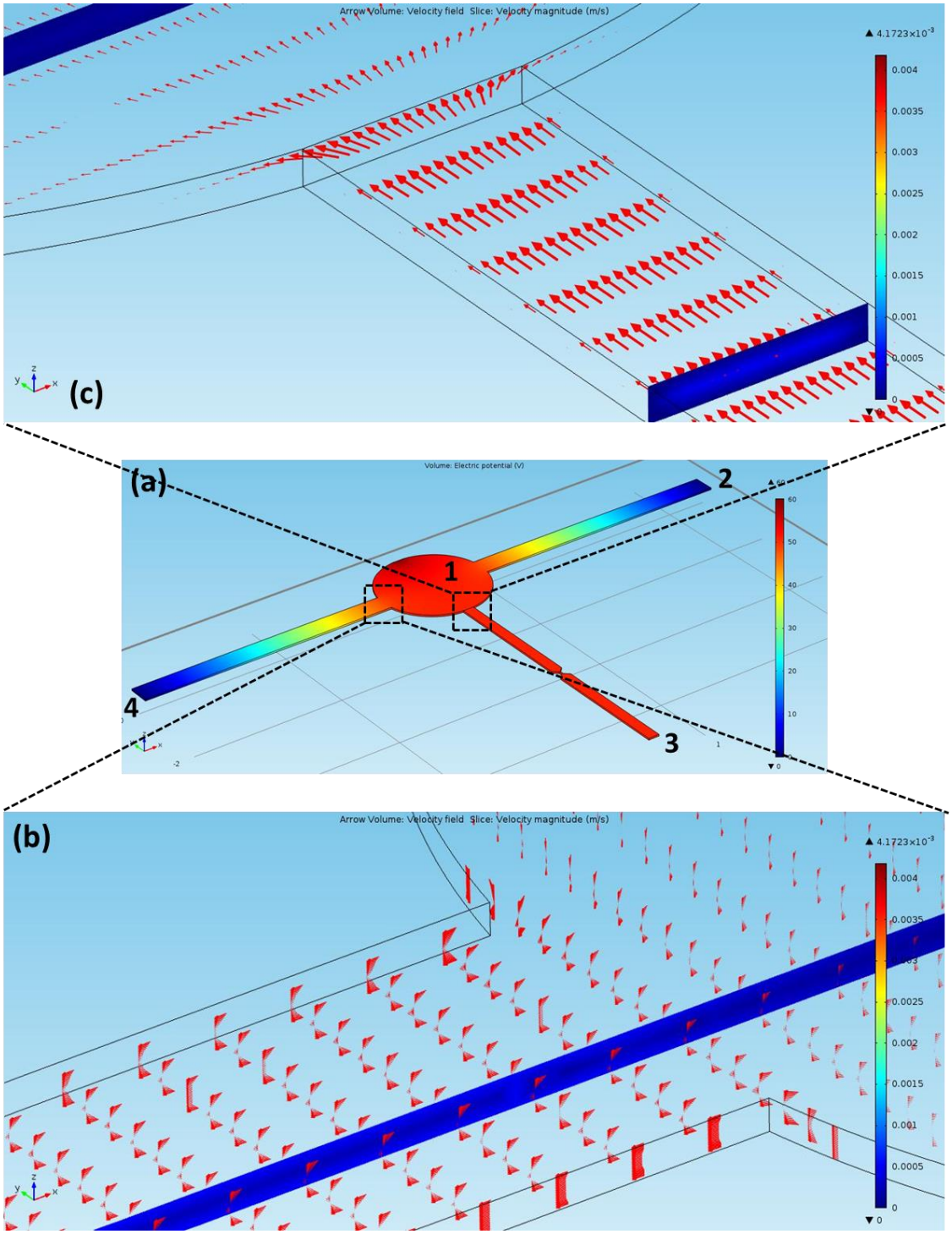

Figure 5-4 (a) Electrical potential distribution in the T-shaped microchannel (b) The details of the flow field in the T-shaped microchannel (0V, 60 V and 0 V at the reservoirs 2, 1 and 4) (c) Velocity of the pressure-driven flow from the reservoir 3 to the reservoir 1

5.3.5 Performance of the design of narrow section on the microchannel

As mentioned in the theoretical analysis, the flow between the reservoir 1 and reservoir 3 due to the diffusion and pressure-driven flow during the hybridization reaction step and washing step must be avoided. A narrow section of 30 μm on the horizontal channel is designed. The time-dependent concentration field during the first step and the second step was calculated to investigate its performance. In this numerical simulation, a height difference of 100 μm thus a pressure difference of 1 Pa between reservoir 3 and reservoir 1 was assumed. A total time of 900 seconds for step 1 and step 2 was studied. The results are shown in the Figure 5-5 and Figure 5-6.

As we can see from the Figure 5-5, within a time of 360s, the liquid in the reservoir 3 has already flew into the reservoir 1 (Figure 5-5 (a)) but for the design with the narrow section, only a little liquid flows out of the reservoir 3 and enters into the channel (Figure 5-5 (b)). As time goes on, the washing step proceeds, which is shown in the Figure 5-6 (a), a big amount of liquid is observed to flow into the reservoir 1. However, there is no liquid flowing into the reservoir 1 with the design of narrow section during the whole washing step, as shown in Figure 5-6 (b). The simulation result is the case we assume that the liquid level of the reservoir 3 is higher than that of the reservoir 1. Similar result can be obtained for the situation in which the liquid level of the reservoir 3 is lower than that of the reservoir 1, which indicates the liquid in the reservoir 1 will not leak to the reservoir 3 with the design of narrow section.

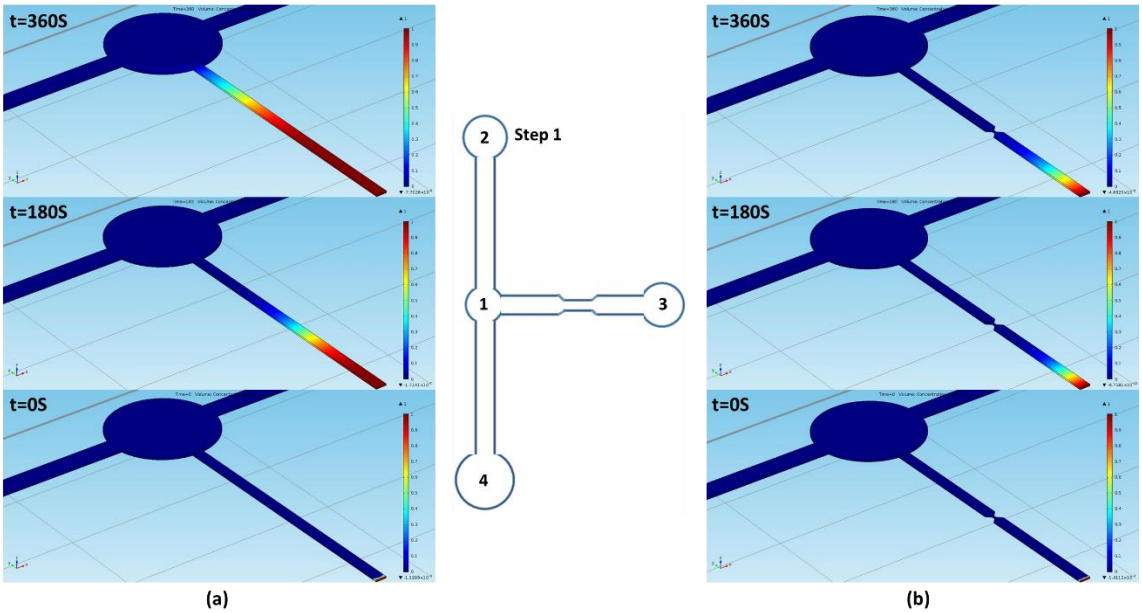

(a) (b)

Figure 5-5 (a) Concentration field in the microchannel without a narrow section on the channel 1-3 at t=0, t= 180 s and t=360 s during the step 1 for hybridization reaction. (b) Concentration field in the microchannel with a narrow section of 30 μm on the channel 1-3 at t=0, t= 180 s and t=360 s during the step 1 for hybridization reaction.

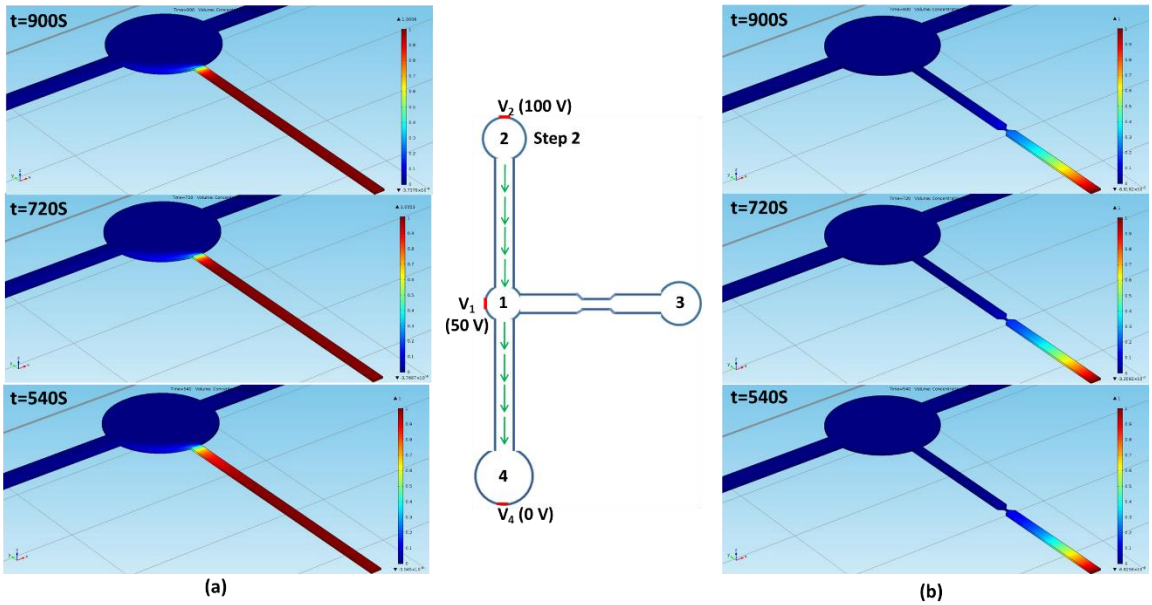

Figure 5-6 (a) Concentration field in the microchannel without a narrow section on the channel 1-3 at t=540 s, t= 720 s and t=900 s during the step 2 for washing. (b) Concentration field in the microchannel with a narrow section of 30 μm on the channel 1-3 at t=540 s, t= 720 s and t=900 s during the step 2 for washing.

The above are the numerical simulation results. These results verifies the theoretical analysis. Based on these results, the microchip was designed and fabricated to conduct the experiments, which is introduced in the following section.

5.4 Experiment

5.4.1 Parameters studies

To determine the minimum volume of reaction sample which can be assayed by the optical module. A series of tests were done by detecting different volume of reaction sample. Tested samples were divided into several groups. For each group with the same volume, samples of different concentrations ranging from 10^3 CFU/mL to 10^9 CFU/mL were assayed by following the procedure in a single PDMS

manually, then the resultant complex was measured by the self-made optical module to investigate if the samples can be differential. As a result, the volume of 5.5 μL was found the minimum volume that could be assayed distinguishingly with an acceptable resolution. Once the volume of the reaction sample was found out, the time for washing was then determined by the estimated flow rate obtained by the numerical study. Consequently, the volumes of the wash buffer and substrate solution could be determined accordingly. The optimized parameters are summarized in the Table 5-1. To prove that all these parameters are appropriate. Negative control was assayed firstly to test the washing efficiency by this electrokinetics method. By applying the operation parameters shown in the Table 5-1, no false positive signal was detected, which verified the parameters were effective.

Table 5-1 Operation parameters of the electrokinetically-controlled RNA-DNA hybridization on-chip assay

Step	**Applied potentials at reservoirs (V)**			**Duration of the step (min)**	**Volume (μL)**
	Φ1	**Φ2**	**Φ4**		
Hybridization reaction (Reaction sample)	0	0	0	6	5.5
Washing (wash solution)	50	100	0	8	25
Dispensing and incubation (substrate solution)	60	0	0	6	8

5.4.2 Chip design and fabrication

Based on the results of the numerical simulation, the DNA hybridization assay microfluidic chip was made as shown in Figure 5-7. The microfluidic chip consists of a T-shaped microchannel and four reservoirs. The vertical channel is 500 μm wide and 12 mm long, and is used as the washing channel. The horizontal channel is 250 μm wide and 6 mm long, with a narrow section (30 μm width) in the middle. All the microchannels are 40 μm in depth.

The PDMS microfluidic chip was fabricated by using the standard soft lithography technique (Biddiss et al., 2004). The master mold for the microfluidic chip was made by spin coating a film of SU-8

negative photoresist onto a silicon wafer firstly. After the pre-baking, a photomask bearing the T-shaped microchannel geometry was placed on the top of the film and then exposed to UV light. After post-baking and developing, the master mold was obtained. PDMS (10:1(w/w) PDMS prepolymer : curing agent) was poured over the master mold and cured for about 4 hours at 75 ℃ after being degassed under low vacuum. The PDMS replica was peeled from the master and the holes of required diameters were punched through the PDMS to make the reservoirs (wells). Finally, the PDMS slab was aligned and bonded onto a glass slide after oxygen plasma treatment for 30 s.

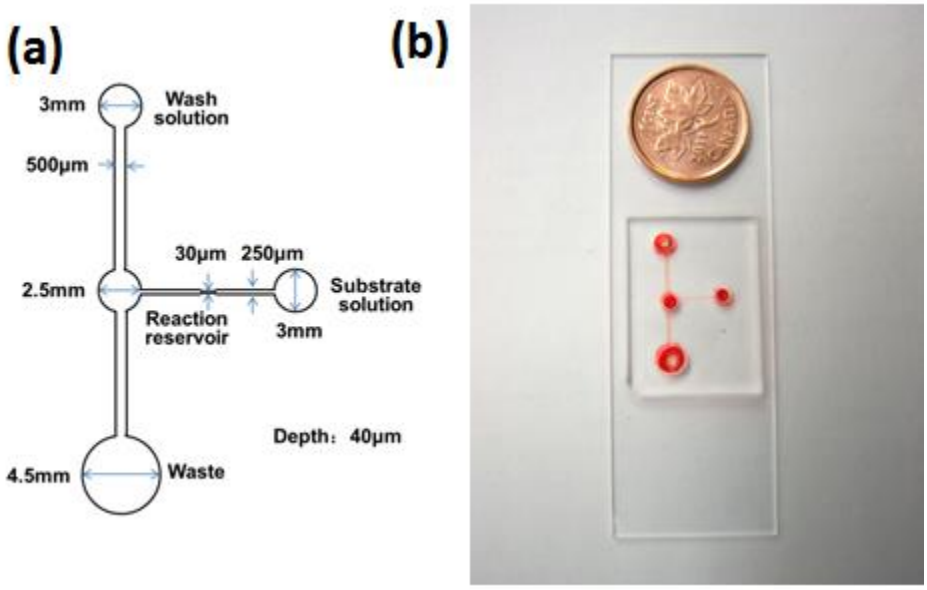

Figure 5-7 (a) An illustration of the microfluidic RNA-DNA hybridization assay chip. (b) A picture of the microfluidic RNA-DNA hybridization assay chip (The channel is filled with a food color for easy visualization)

5.4.3 Reagents and sample preparation

Lysis reagent, hybridization solution, probe solution, substrate chromogen solution, positive and negative controls for *Salmonella* and *Listeria monocytogenes* bacteria were obtained from the commercial *Salmonella* and *Listeria monocytogenes* test kits (GeneQuence® Salmonella & L. monocytogenes Kit, Neogen, Lansing, MI, USA). Poly dT coated magnetic micro-beads (Dynabeads® (dT) 25) were purchased from Invitrogen (Carlsbad, CA, USA). Borate buffer solution (Ricca Chemical, Arlington, TX, USA) was used as the wash solution.

The *Salmonella* and *Listeria monocytogenes* bacteria were obtained from Laboratory Service, University of Guelph, Canada. The procedure for preparing *Salmonella* bacteria was described previously (Weng et. al, 2011). Briefly, *Salmonella* berta (ATCC8392) cultures were grown at 37 ℃ in Tryptic Soy Broth (TSB) for overnight. The concentration of the bacteria was estimated by plate counting, the procedure can be found in Chapter 3. The overnight cultures were placed in boiling water bath for 20 min to kill the *Salmonella* bacteria for later use, the estimated concentration of the *Salmonella* culture was 10^9 CFU/mL. The procedure for preparing *Listeria monocytogenes* was as follows. Stock cultures of *Listeria monocytogenes* (ATCC19115) strain were grown for overnight at 37 ℃ in LB Broth. The concentration of the bacteria was estimated by plate counting, the procedure can be found in Chapter 3.The overnight cultures were killed by boiling in a water bath for 20 min for further use. These original *Salmonella* and *Listeria monocytogenes* bacteria were diluted by PBS (1×) buffer solution (Ricca Chemical, Arlington, TX, USA) into samples of various concentrations ranging from 10^4 to 10^8 CFU/mL for testing.

Lysed *Salmonella* and *Listeria monocytogenes* samples were prepared following the procedure specified in the commercial kits. Lysis reagents were added into the bacteria samples for incubation at 65 ℃ (*Salmonella* bacteria samples) and 37 ℃ (*Listeria monocytogenes* samples) for 5 min, respectively. *Salmonella* probe/hybridization solution was prepared by mixing the *Salmonella* probe solution and hybridization solution at a ratio of 1:4. *Listeria monocytogenes* probe/hybridization solution was prepared by mixing the *Listeria monocytogenes* probe solution and hybridization solution at a ratio of 1:3. The reaction samples were prepared by mixing the lysed *Salmonella/ Listeria monocytogenes* samples (controls) and the *Salmonella/ Listeria monocytogenes* probe/ hybridization mixture at a ratio of 6:5, respectively.

5.4.4 Electrokinetically-driven RNA-DNA hybridization assay

The principle of the assay has been demonstrated in the section 4.2.1. In order to avoid using mechanical pumps and valves, electro-osmotic flow is used in this study to transport liquid through the microchannels. To start an on-chip assay, 4 μL microbeads was introduced into the reaction reservoir first and then sucked out its buffer immediately. 5.5 μL reaction sample and 8 μL substrate solution were then added into the reaction reservoir and the substrate solution reservoir at the same time. The wash solution reservoir and the waste reservoir were filled with 8 μL and 17 μL wash solution, respectively. In order to apply electric field and generate electro-osmotic flow, platinum electrodes were placed into the wash solution reservoir, reaction reservoir and the waste reservoir.

The DNA hybridization assay was simplified by us into three main steps. The first step was the hybridization reaction and incubation after the four reservoirs were filling with reaction sample, wash solution and substrate solution respectively. The second step was washing, during which the wash solution was dispensed from the wash solution well (reservoir 2 as indicated in Figure 5-8) to the reaction well (reservoir 1 as indicated in Figure 5-8) and from there to the waste well (reservoir 4 as indicated in Figure 5-8), to flush out the unbound probes. The last step was to dispense the substrate solution into the reaction well and incubation. It was found that the substrate solution was unstable when it was directly exposed to an electric field. Therefore, to avoid the direct electrical field driven flow (electro-osmotic flow) of the substrate solution, an electrokinetically-introduced pressure-driven flow was used to dispense the substrate solution. As shown in Figure 5-8 (c), the electro-osmotic flow path was from the reservoir 1 to the reservoir 2 and the reservoir 4. As the liquid in the reservoir 1 was draining out, the liquid in the horizontal channel was pulled into the reaction reservoir, resulting the substrate solution flowing into the reaction reservoir (as the orange arrow indicated in the Figure 5-8 (c)).

It is found that, while dispensing the substrate solution into the reaction well, the pH value near the positive electrode in the reaction well decreased due to the electrolysis effect of the water under the electric field for a period of time. The chemical equation of electrolysis is shown as follows:

$$\textbf{Anode:} \quad 4OH^- - 4e = O_2\uparrow + 2H_2O$$

This effect was favorable for the assay because the hybridization reaction should be stopped and come to a colorimetric endpoint for signal detection due to the decreased pH value. Therefore, no stop solution was required and no extra step needed in this assay. These sequential processes in the microfluidic DNA hybridization assay chip are illustrated in Figure 5-8. For each step, the applied electric potentials and duration on the electrodes were pre-set as a sequence in the DC Voltage Sequencer (Labsmith, Livermore, CA, USA) via the Sequence software. When starting an assay by running the sequence program, the sequential operations as illustrated above (in Figure 5-8) were carried out automatically during the assay. At the end of the assay, the microbeads were attracted aside to the reaction reservoir edge by a magnet to avoid the interfering the further optic detection.

5.4.5 Light absorption detection module

The hybridization reaction product has a preferential absorbability of 450 nm wavelength light, and the transmitted light intensity is dependent on the bacterial concentration in the tested samples. An optical

detection module is developed to detect the light absorption of the hybridization reaction product. It consists of a light source, filter and photo-detector. The light source is a blue LED (Luxeon®, San Jose, CA, USA) with a collimated lens. The filter is a 448/20 nm wavelength band-pass filter (BrightLine®, Semrock Inc., Rochester, New York, USA) and placed on the LED light path to obtain the light of 450 nm wavelength light. The photo-detector is a high sensitivity Si photodiode (S8745-01, Hamamatsu, Bridgewater, NJ, USA), which is placed below the chip under the reaction reservoir to detect the transmitted light intensities. At the end of the assay, the light source was automatically turned on by a LabVIEW program. Light from the LED passes through the band pass filter and reaches the hybridization reaction product; then the transmitted light is captured by the photo-detector. The signal is recorded by a computer via a data acquisition card (USB-6259, National Instruments, Austin, TX, USA).

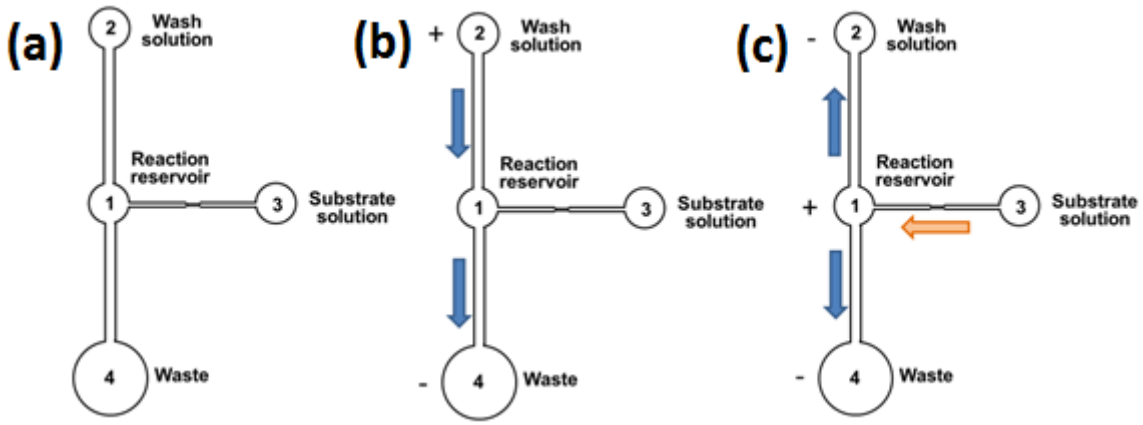

Figure 5-8 The sequential steps of the electrokinetically-controlled RNA-DNA hybridization assay on a microfluidic chip. Three electrodes are placed in the reservoir 1, 2 and 4. The arrows indicate the flow direction. (a) hybridization reaction and incubation; (b) washing of the unbound probes; (c) dispensing the substrate solution by pressure-introduced flow, incubation and stop the reaction

5.4.6 Experimental setup

Figure 5-9 schematically shows the experimental setup of the DNA hybridization assay test system. After loading the sample and reagent solutions in the corresponding wells, the assay was conducted automatically by the DC voltage sequencer. The output channels of the sequencer were connected with the platinum electrodes and used to apply the electric potentials in different wells of the microfluidic chip. After the hybridization reaction, the LED and photo-detector were turned on by a LabVIEW

program to detect and record the light absorption of the hybridization reaction product. The controlling parameters for every step of the assay are shown in Table 5-1.

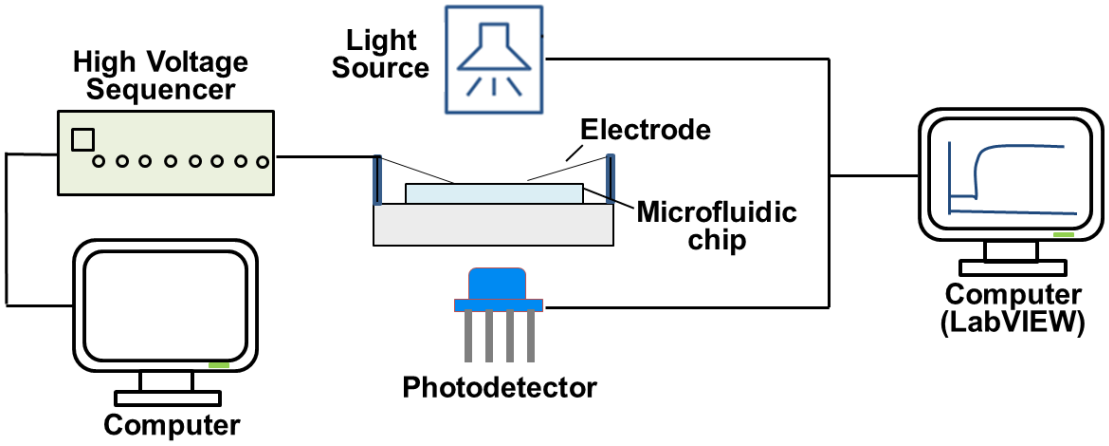

Figure 5-9 A schematic of the experimental setup of the electrokinetically-controlled RNA-DNA hybridization assay system

5.5 Results and discussion

Numerical simulation based on the theoretical prediction was performed to determine the structure and dimensions of the microchip as well as the operation parameters of the assay. A minimum volume of 5.5 μL reaction sample and incubation time 6 min for hybridization reaction were firstly determined by a series of tests in a single PDMS well. In the numerical study, the flow fields of different steps were calculated, then an estimated times for washing and dispensing substrate solution were decided based on the numerical results. In the step of dispensing substrate solution, the approach of electrokinetically-induced pressure-driven flow was put forward to address the unstable problem of the substrate solution when driven by the electro-osmotic flow directly. Considering that in a practical experiment, the substrate solution is supposed to stay in its reservoir for a period of time. However, the liquids in the reservoir may diffuse into the associated channel with time. In addition, the pressure driven flow between reservoirs caused by the liquid level difference due to error introduced in process of manual reagents loading simultaneously. These two flow motions have negative effects to the assay and may fail an assay. To solve the problem, a design of narrow section on the substrate solution dispensing channel is used. The time-dependent concentration fields with or without this narrow section were investigated, respectively. From both the numerical and experimental studies, it is found that this design

is important and effective. Without the narrow section, the liquid may easily flow out even under a tiny liquid level difference. In contrast, the liquid will not flow through the narrow section due to the big resistance.

After obtaining the parameters from the numerical study, the washing efficiency and whole assay process were verified by experiments. *Salmonella* and *Listeria monocytogenes* bacterial samples of known concentrations ranging from 10^4 to 10^9 CFU/mL were successfully assayed on the electrokinetically-controlled microfluidic DNA hybridization assay chip. Negative control and positive control from the commercial kits were tested as well to obtain a reference value for comparison. The DNA hybridization assays were conducted at room temperature. For each concentration, three independent runs were tested. Figure 5-10 and Figure 5-11 are the plots of the results of the photo-detector outputs depending on the concentrations of the *Salmonella* and the *Listeria monocytogenes* bacterial samples. It can be seen in the Figure 5-10 that *Salmonella* bacteria could be reliably detected in the concentration range between 10^4 and 10^9 CFU/mL. Similarly, Figure 5-11 shows that *Listeria monocytogenes* bacteria could be reliably detected in the concentration range between 10^3 and 10^8 CFU/mL. The detection limit of this electrokinetically-controlled microfluidic DNA hybridization assay chip is 10^3~ 10^4 CFU/mL which is comparable to that of many commercial kits (For example, MicroSEQ® Food Pathogen Detection Solution).

In addition, comparison between the electrokinetically-controlled microfluidic DNA hybridization assay chip of this study and the commercial kits (GeneQuence® *Salmonella* / L. monocytogenes Kit, Neogen, Lansing, MI, USA) sharing the same protocol is shown in Table 5-2. The presented microfluidic DNA hybridization assay chip has shortened assay time significantly and reduced reagent consumption dramatically.

By applying the electrokinetic method in this microfluidic DNA hybridization assay, no moving parts and bulky and expensive components are involved to achieve the sequential steps. The method removes the obstacles that get in the way of developing a real portable microfluidic device. Meanwhile, the fully automatic procedure is realized. In this study, further effort should be focused on achieving lower detection limit and high-throughput capability. The selectivity test should also be conducted.

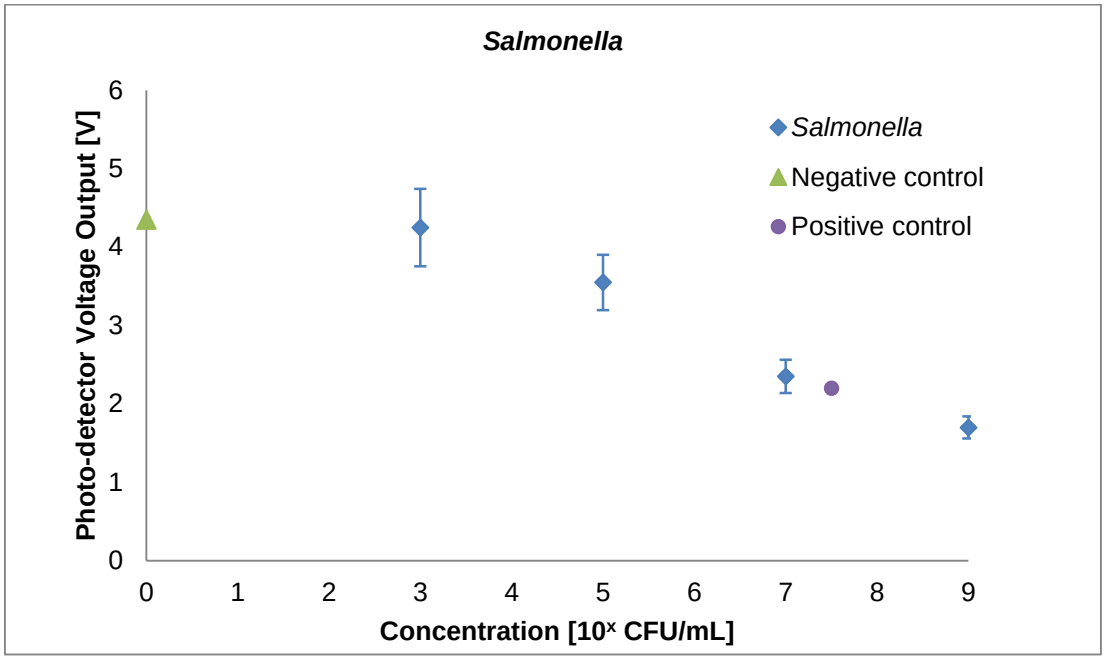

Figure 5-10 The dependence of voltage output of the photo-detector on the concentration of the *Salmonella* bacteria

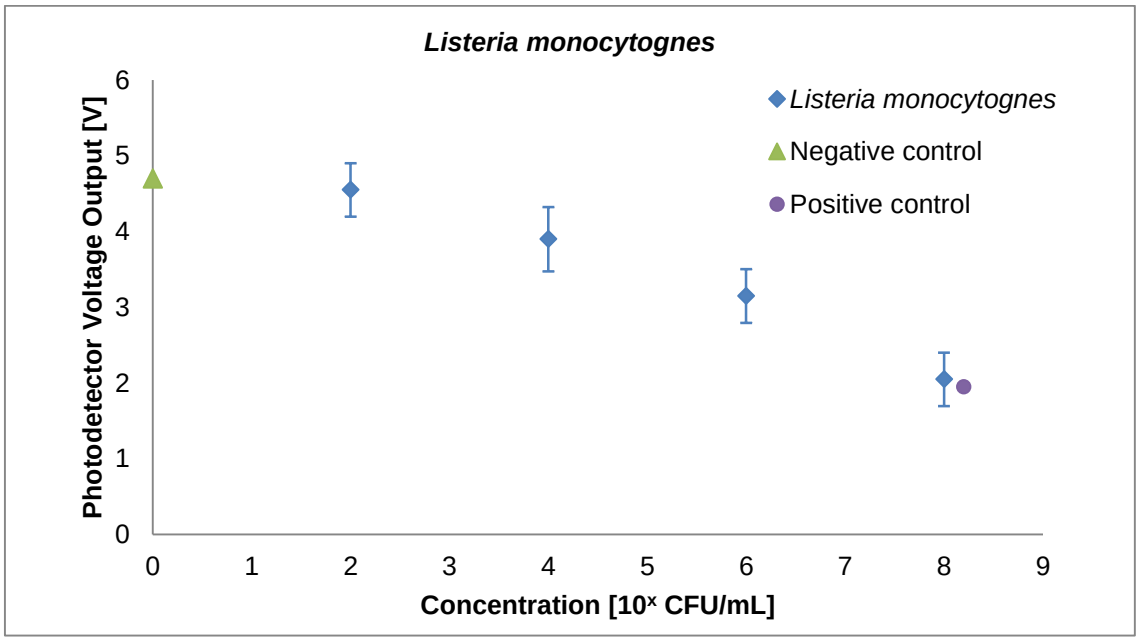

Figure 5-11 The dependence of voltage output of the photo-detector on the concentration of the *Listeria monocytogenes*

Table 5-2 Comparison between the electrokinetically-controlled on-chip assay and a commercial kit*

		On-chip Assay	**Commercial kit***
Consumption	Reaction sample**	5.5 μL	275 μL
	Microbeads	4 μL	—
	Wash solution	25 μL	200 μL
	Substrate solution	8 μL	150 μL
	Stop solution	—	50 μL
Reagent delivery		Automated electrokinetically-driven	Manual pipetting
Total assay time		~20 min	1 hr 50 min

* GeneQuence® *Salmonella* / *L. monocytogenes* Kit, Neogen, Lansing, MI, USA

**Reaction samples were prepared by mixing the lysed *Salmonella/ Listeria monocytogenes* bacterial samples (controls) and the *Salmonella/ Listeria* probe/ hybridization mixture at a ratio of 6:5.

5.6 Summary

In this chapter, we have demonstrated the ability of an electrokinetically-controlled DNA hybridization assay microfluidic chip to detect the foodborne pathogens, *Salmonella* and *Listeria monocytogenes*. Numerical simulation was performed to determine the structure and dimensions of the microchip as well as the operation parameters of the assay. Applying the electrokinetic microfluidic method, an assay could be completed within 20 min automatically. This presented microfluidic method significantly reduced the sample and reagent consumption, up to 30-folds in comparison with that of the commercial kits. The quantified experimental results show that the detection limit of the bacterial sample concentration is approximate 10^3~10^4 CFU/mL. In addition, the microfluidic chip presented in this paper does not require any external valves or mechanical pumps. Therefore, this microfluidic system has potential to be further developed to a portable device for on-site pathogen detection.

Chapter 6

Conclusions and Future Work

6.1 Summary of thesis

Foodborne pathogens are responsible for million cases of foodborne diseases over the world every year, costing billions of dollars in medical care and lost productivity. The ongoing research for improved methodologies is particularly important since conventional identification methods of pathogens sensing usually require not only tedious enrichment and pre-selection steps, but also the time-consuming, labor-intensive and high-consumption assay procedures.

Therefore, the instrumental development of portable and robust devices for rapidly providing information on pathogens is of considerable significance. It is an effective manner in prevention and control of the foodborne diseases so as to reduce mortality rates, hospitalization in case of infectious pathogens. In the past two decades, a numerous of biosensors have been developed, however, miniaturized, low-cost or disposable devices capable of rapid detection, sensitive and accurate identification of a wide variety of pathogens are still an inevitable trend and undergoing.

In this thesis, we proposed to develop a microfluidic system towards a portable device for pathogens detection based on DNA hybridization assay technology. Since the assay involves multiple steps for the sequential loading and washing process, syringe pumps, tubing and valves for liquid handling must be avoided from the miniaturization point of view. In this thesis, three distinctive microchip designs are developed to realize the pathogen detection. In the first two designs, gravity-based pressure driven flow is used flow handling in the microchannels and two different kinds of microvalves are made in each design to realize the on-chip sequential procedure. A pair of electrokinetically-controlled oil droplet valves and electrothermally actuated phase change microvalves are used in these two microfluidic system, respectively. However, for the first two designs, they both have some limitations. For example, the manipulation of making oil-droplet valve, sealing and control of the oil-droplet in the microchannel need skilled operator, which is not good for a practical application. The phase change microvalve is easier in fabrication than the oil-droplet valve. It is in solid form under the room temperature and more easy for mass production. In the final design, fully electrokinetic control method is applied to drive the flow, thus the sequential reagents loading. What we need to do is to provide and manage the electric fields along the microchannels at each step via electrodes. The biggest advantage

of this method is no microvalves are required. The management of the potentials on the electrodes is realized by a programmable DC voltage sequencer. The required electric potentials and duration on the electrodes are pre-set as a sequence in the Voltage Sequencer. Since no microvalves are required, this valveless electrokinetics-based assay further simplifies the preparation process of the microfluidic chip and the on-chip procedure. The following table shows the features of these three microchip designs and their performance when doing the assay. In the last two microfluidics systems, a low cost, miniaturized light detection module based on the differential light absorbability of the hybridization complex to the light of 450nm wavelength is developed to obtain the quantitative results. In the system, the sequential triggers of the film heaters, LED and the photodiode, as well as the data acquisition are achieved by homemade circuit and coded LabVIEW program thus the automatic operations of the assay is achieved.

Table 6.1 Summary of the features of the three developed microchips

		Microchip 1	Microchip 2	Microchip 3
Consumption	Reaction sample**	12 μL	14 μL	5.5 μL
	Microbeads	7 μL	7 μL	4 μL
	Wash solution	48 μL	48 μL	25 μL
	Substrate solution	48 μL	48 μL	8 μL
	Stop solution	48 μL	48 μL	—
Microvalve		oil-droplet valve	phase change valve	valveless
Result		qualitative	quantitative	quantitative
Reagent delivery		semi-automatic	automatic	automatic
Total assay time		25 min	26 min	~20 min

**Reaction samples were prepared by mixing the lysed *Salmonella/ Listeria monocytogenes* bacterial samples (controls) and the *Salmonella/ Listeria* probe/ hybridization mixture at a ratio of 6:5.

In the research of this thesis, the three methods of on-chip DNA hybridization assay have successfully detected the signals from the positive/ negative control and the real pathogen samples, *Salmonella*

bacteria and *Listeria monocytogenes*. Significantly shortened assay time and reagent/sample consumption reduction are achieved. In addition, the detection limit in *Salmonella* bacteria and *Listeria monocytogenes* detection is as low as 10^3~10^4 CFU/mL.

6.2 Novelty statement and contributions made by this study

Compared to many commercial kits (MicroSEQ®, 2013; AccuProbe®, 2011; GENE-TRAK®, 2008; GeneQuence®, 2008), the total assay time is significantly shortened from hours to approximate 20 min, the sample/ reagent consumptions are reduced by 20 folds, meanwhile a comparable detection limit is maintained. Compared to current microfluidic DNA hybridization assays (Liao et al., 2006; Javanmard and Davis 2011; Wang et al., 2011; Senapati et al., 2009), external pumps, valves, tubing and expensive optical instruments are avoided, which is favorable for the system integration and miniaturization. In addition, the development of the miniaturized optical detection module make this system cost-effective and capable of quantitative detection. With extra effort to integration strategy, it would be possible to make this microfluidic system a commercial product. All of these efforts can be very useful in future development of a real portable DNA hybridization assay lab-on-a-chip device for point-of-care detection with a number of advantages including rapidity, low sample and reagent consumption, low power consumption, automation, compactness, disposability, and low cost.

6.3 Publications in peer-reviewed journals resulting from this thesis

Several publications in peer-reviewed journals have resulted from this research as follows:

1. **Xuan Weng**, Hai Jiang, Dongqing Li. Electrokinetically-Controlled RNA-DNA Hybridization Assay for Foodborne Pathogens Detection. Microchimica Acta, 2012, 178 (3-4): 381-387.

2. **Xuan Weng**, Hai Jiang, Junsheng Wang, Shu Chen, Honghe Cao, Dongqing Li. Automatic On-Chip RNA-DNA Hybridization Assay with Integrated Phase Change Microvalves. Journal of Micromechanics and Microengineering, 2012, 22(7): 075003.

3. **Xuan Weng**, Hai Jiang, Chan Hee Chon, Shu Chen, Honghe Cao, Dongqing Li. An RNA-DNA Hybridization Assay Chip with Electrokinetically Controlled Oil Droplet Valves for Sequential Microfluidic Operations. Journal of Biotechnology, 2011, 155 (3): 330-337.

4. **Xuan Weng**, Hai Jiang, Dongqing Li. Microfluidic DNA hybridization assay. Microfluidics and Nanofluidics, 2011, 11(4): 367-383.

5. **Xuan Weng,** Hai Jiang, Dongqing Li. A miniaturized system for rapid and quantitative detection of Cocaine metabolite by homogeneous enzyme immunoassay. Instrumentation Science & Technology, 2013, 41 (5): 512-523.

6.4 Suggestions for future work

In the chapter 5 of this thesis, the electrokinetics method is found a promising way in the development of the portable biomedical microdevices. My research will continue to find out how this microfluidic system can be applied in other biomedical diagnosis. More specifically, in the technological perspective, study the optimization design of the electrokinetics-based microfluidic system, make the integration design; in the application perspective, take this microfluidic system as a general platform for biological detection to find out more practical applications.

Based on the results obtained in this study, future research will be focused on the following aspects:

- From the technology point of view, effort can be made to further improve the current microfluidic system. On one hand, integration strategy can be selected for the portable device development. Chip layout, dimension of the microchannel, flow & concentration fields, optical detection module need to be studied deeply to enhance the performance of the microfluidic chip, such as the selectivity, sensitivity and detection limit of the system. On the other hand, the protocol of the DNA hybridization assay can be improved to further increase the sensitivity and specificity, and so on.
- From the application point of view, the microfluidic system presented in this study could not be restricted to the DNA hybridization assay. As a general platform, many other biomedical assays could be achieved by simply modifying the design of the microfluidic chip. For instance, ELISA, two more branch channels and two more reagent dispensing step and washing step could be added to realize the assay. As a future work, the sample preparation procedure can be integrated into the microfluidic system for an automated, portable platform with raw-sample-to-result capabilities.

Appendix A

List of Publications in Refereed Journals

Papers from the results of this thesis:

1. **Xuan Weng**, Hai Jiang, Dongqing Li. Electrokinetically-Controlled RNA-DNA Hybridization Assay for Foodborne Pathogens Detection. Microchimica Acta, 2012, 178 (3-4): 381-387.

2. **Xuan Weng**, Hai Jiang, Junsheng Wang, Shu Chen, Honghe Cao, Dongqing Li. Automatic On-Chip RNA-DNA Hybridization Assay with Integrated Phase Change Microvalves. Journal of Micromechanics and Microengineering, 2012, 22(7): 075003.

3. **Xuan Weng**, Hai Jiang, Chan Hee Chon, Shu Chen, Honghe Cao, Dongqing Li. An RNA-DNA Hybridization Assay Chip with Electrokinetically Controlled Oil Droplet Valves for Sequential Microfluidic Operations. Journal of Biotechnology, 2011, 155 (3): 330-337.

4. **Xuan Weng**, Hai Jiang, Dongqing Li. Microfluidic DNA hybridization assay. Microfluidics and Nanofluidics, 2011, 11(4): 367-383.

Papers from other research work：

5. **Xuan Weng,** Hai Jiang, Dongqing Li. A miniaturized system for rapid and quantitative detection of Cocaine metabolite by homogeneous enzyme immunoassay. Instrumentation Science & Technology, 2013, 41 (5): 512-523.

6. Hai Jiang, **Xuan Weng**, Dongqing Li. Dual-wavelength fluorescent detection of particles on a novel microfluidic chip. Lab Chip, 2013, 13, 843-850.

7. Hai Jiang, **Xuan Weng**, Chan Hee Chon, Xudong Wu, Dongqing Li. A microfluidic chip for blood plasma separation using electro-osmotic flow (EOF) control. Journal of Micromechanics and Microengineering, 2011, 21 (8): 085019.

8. Hai Jiang, **Xuan Weng,** Dongqing Li. Microfluidic whole-blood immunoassays. Microfluidics and Nanofluidics, 2011, 10 (5): 941-964.

9. **Xuan Weng**, Chan Hee Chon, Hai Jiang, Dongqing Li. Rapid detection of formaldehyde concentration in food on a polydimethylsiloxane (PDMS) microfluidic chip. Food Chemistry, 2009, 114: 1079-1082.

Appendix B

License Agreement for Chapter 2

This is a License Agreement between Xuan Weng ("You") and Springer ("Springer") provided by Copyright Clearance Center ("CCC"). The license consists of your order details, the terms and conditions provided by Springer, and the payment terms and conditions.

All payments must be made in full to CCC. For payment instructions, please see information listed at the bottom of this form.

License date	Sep 05, 2013
Licensed content publisher	Springer
Licensed content publication	Microfluids and Nanofluids
Licensed content title	Microfluidic DNA hybridization assays
Licensed content author	Xuan Weng
Licensed content date	Jan 1, 2011
Volume number	11
Issue number	4
Type of Use	Thesis/Dissertation
Portion	Full text
Number of copies	6
Author of this Springer article	Yes and you are the sole author of the new work
Order reference number	
Title of your thesis / dissertation	A Microfluidic System for RNA-DNA Hybridization Assay
Expected completion date	Sep 2013
Estimated size(pages)	130
Total	0.00 USD

Appendix C

License Agreement for Chapter 3

This is a License Agreement between Xuan Weng ("You") and Elsevier ("Elsevier") provided by Copyright Clearance Center ("CCC"). The license consists of your order details, the terms and conditions provided by Elsevier, and the payment terms and conditions.

All payments must be made in full to CCC. For payment instructions, please see information listed at the bottom of this form.

Supplier	Elsevier Limited The Boulevard,Langford Lane Kidlington,Oxford,OX5 1GB,UK
Registered Company Number	1982084
Customer name	Xuan Weng
Customer address	Apt.8, 431 Hazel Street Waterloo, ON N2L3P7
License date	Sep 05, 2013
Licensed content publisher	Elsevier
Licensed content publication	Journal of Biotechnology
Licensed content title	An RNA–DNA hybridization assay chip with electrokinetically controlled oil droplet valves for sequential microfluidic operations
Licensed content author	Xuan Weng,Hai Jiang,Chan Hee Chon,Shu Chen,Honghe Cao,Dongqing Li
Licensed content date	20 September 2011
Licensed content volume number	155
Licensed content issue number	3
Number of pages	8
Start Page	330
End Page	337
Type of Use	reuse in a thesis/dissertation
Intended publisher of new work	other

Portion	full article
Format	both print and electronic
Are you the author of this Elsevier article?	Yes
Will you be translating?	No
Order reference number	
Title of your thesis/dissertation	A Microfluidic System for RNA-DNA Hybridization Assay
Expected completion date	Sep 2013
Estimated size (number of pages)	130
Elsevier VAT number	GB 494 6272 12
Permissions price	0.00 USD
VAT/Local Sales Tax	0.0 USD / 0.0 GBP
Total	0.00 USD

Appendix D

License Agreement for Chapter 5

This is a License Agreement between Xuan Weng ("You") and Springer ("Springer") provided by Copyright Clearance Center ("CCC"). The license consists of your order details, the terms and conditions provided by Springer, and the payment terms and conditions.

All payments must be made in full to CCC. For payment instructions, please see information listed at the bottom of this form.

License date	Sep 05, 2013
Licensed content publisher	Springer
Licensed content publication	Microchimica Acta
Licensed content title	Electrokinetically-controlled RNA-DNA hybridization assay for foodborne pathogens
Licensed content author	Xuan Weng
Licensed content date	Jan 1, 2012
Volume number	178
Issue number	3
Type of Use	Thesis/Dissertation
Portion	Full text
Number of copies	6
Author of this Springer article	Yes and you are the sole author of the new work
Order reference number	
Title of your thesis / dissertation	A Microfluidic System for RNA-DNA Hybridization Assay
Expected completion date	Sep 2013
Estimated size(pages)	130
Total	0.00 USD

Bibliography

AccuProbe® *Listeria Monocytogenes* culture identification test package insert-Rev. Gen-Probe Incorporated, San Diego, CA, 2011

AFNOR Validation, 2010. http://www.afnor-validation.com

Ali MF, Kirby R, Goodey AP, Rodriguez MD, Ellington AD, Neikirk DP, McDevitt JT (2003) DNA hybridization and discrimination of single-nucleotide mismatches using chip-based microbead arrays. Anal. Chem. 75: 4732-4739.

AOAC (Association of Official Analytical Chemists) (1984) Official methods of analysis of the Association of Official Analytical Chemists, 14th edn.. Arlington. V.A., Association of Official Analytical Chemists Inc.

AOAC International (2009) J. AOAC Int. 92 (6): 1840-1901.

Ayala VC, Michalzik M, Harling S, Menzel H, Guarnieri FA, Büttgenbach S (2007) Design, construction and testing of a monolithic pH-sensitive hydrogel-valve for biochemical and medical application. J. Phys. Conference Series 90: 012025.

Bae B, Kim N, Kee H, Kim SH, Lee Y, Lee S, Park K (2002) Feasibility test of an electromagnetically driven valve actuator for glaucoma treatment. J. Microelectromech. Syst. 11: 344-542.

Baek JY, Park JY, Ju JI, Lee TS, Lee SH (2005) A pneumatically controllable flexible and polymeric microfluidic valve fabricated via in situ development. J. Micromech. Microeng. 15: 1015-1020.

Baldi A, Lei M, Gu Y, Siegel RA, Ziaie B (2006) A microstructured silicon membrane with entrapped hydrogels for environmentally-sensitive fluid gating. Sens. Actuators B-Chem. 114: 9-18.

Basuray S, Senapati S, Aijian A, Mahon AR, Chang HC (2009) Shear and AC field enhanced carbon nanotube impedance assay for rapid, sensitive, and mismatchdiscriminating DNA hybridization. ACS Nano. 3 (7): 1823-1830.

Becker H, Gärtner C (2008) Polymer microfabrication technologies for microfluidic systems. Anal. Bioanal. Chem. 390: 89-111.

Benn JA, Hu J, Hogan BJ, Fry RC, Samson LD, Thorsen T (2006) Comparative modeling and analysis of microfluidic and conventional DNA microarrays. Anal. Biochem. 348: 284-293.

Benoit V, Steel A, Torres M, Yu Y, Yang H, Cooper J (2001) Evaluation of three-dimensional microchannel glass biochips for multiplexed nucleic acid fluorescence hybridization assays. Anal. Chem. 73: 2412-2420.

Ben-Yoav H, Dykstra PH, Bentley WE, Ghodssi R (2012) A microfluidic-based electrochemical biochip for label-free diffusion-restricted DNA hybridization analysis. Biosens. Bioelectron. 38: 114-120.

Berti F, Laschi S, Palchetti I, Rossier J S, Reymond F, Mascini M, Marrazza G (2009) Microfluidic-based electrochemical genosensor coupled to magnetic beads for hybridization detection. Talanta 77(3): 971-978.

Betanzos-Cabrera G, Harker BW, Doktycz MJ, Weber JL, Beattie KL (2008) A comparison of Hybridization Efficiency between Flat Glass and Channel Glass Solid Supports. Mol. Biotechnol. 38: 71-80.

Biddiss E, Erickson D, Li D (2004) Heterogeneous surface charge enhanced micromixing for electrokinetic flows. Anal. Chem. 76: 3208-3213.

Blackburn CW (1993) Rapid and alternative methods for the detection of *Salmonellas* in foods. J. Appl. Bacteriol. 75: 199-214.

Bolton ET, Mccarthy BJ (1962) A general method for the isolation of RNA complementary to DNA. Proc. Natl. Acad. Sci. U S A. 48: 1390-1397.

Brennan D, Dillmore S, Moore E, Galvin P (2009) A rapid polymerisation process realizing 3D biocompatible structures in a microfluidic channel suitable for genetic analysis. Sens. Actuators B-Chem. 142: 383-388.

Britten RJ, Kohne DE (1968) Repeated Sequences in DNA. Science, 161 (3841): 529-540.

Cano RJ, Torres MJ, Klem RE, Palomares JC, Casadesus J (1992) Detection of *Salmonella*s by DNA hybridization with a fluorescent alkaline phosphatase substrate. J. Appl. Bacteriol. 72: 393-399.

Cao W, Su M, Zhang S (2010) Rapid and sensitive DNA target detection using enzyme amplified electrochemical detection based on microchip. Electrophoresis 31: 659-665.

Cao YC, Jin R, Mirkin CA (2002) Nanoparticles with raman spectroscopic fingerprints for DNA and RNA detection. Science 297: 1536-1540.

Capanu M., Boyd JG Hesketh PJ (2000) Design, fabrication, and testing of a bistable electromagnetically actuated microvalve. J. Microelectromech. Syst. 9: 181-189.

Carlen ET, Weinberg MS, Dube CE, Zapata AM, Borenstein JT (2006) Micromachined silicon plates for sensing molecular interactions. Appl. Phys. Lett. 89: 173123.

CDC (Centers for Disease Control) (2007) *Salmonella* typhimurium infection associated with raw milk and cheese consumption-Pennsylvania, MMWR Morb. Mortal. Wkly. Rep., 56: 1161-1164.

Cha M, Shin J, Kim J, Kim I, Choi J, Lee N, Kim B, Lee J (2008) Biomolecular detection with a thin membrane transducer. Lab Chip 8: 932-937.

Chandler EL, Smith AL, Burden LM, Kasianowicz JJ, Burden DL (2004) Membrane surface dynamics of DNA-threaded nanopores revealed by simultaneous single-molecule optical and ensemble electrical recording. Langmuir 20: 898-905.

Chen B, Zhou X, Li C, Wang Q, Liu D, Lin B (2011) Rapid screening of phenylketonuria using a CD microfluidic device. J. Chromatogr. A. 1218:1907-1912.

Chen L, Lee S, Lee M, Lim C, Choo J, Park JY, Lee S, Joo SW, Lee KH, Choi YW (2008a) DNA hybridization detection in a microfluidic channel using two fluorescently labelled nucleic acid probes.Biosens. Bioelectron. 23(12): 1878-1882.

Chen, L, Manz, A, Day PJR (2007) Total nucleic acid analysis integrated on microfluidic devices. Lab Chip 7: 1413-1423.

Chen JF, Wabuyele M, Chen HW, Patterson D, Hupert M, Shadpour H, et al. (2005) Electrokinetically synchronized polymerase chain reaction microchip fabricated in polycarbonate. Anal. Chem. 77(2): 658–66.

Chen JM, Huang P, Lin M (2008b) Analysis and experiment of capillary valves for microfluidics on a rotating disk. Microfluid. Nanofluid. 4: 427-437.

Chen L (2010) DNA hybridization on walls of electrokinetically controlled microfluidic channels. Dissertation, University of Toronto.

Chen S, Yee A, Griffiths M, Larkin C, Yamashiro CT, Behari R, Paszko-Kolva C, Rahn K, Grandis SAD (1997) Evaluation of a fluorogenic polymerase chain reaction assay for the detection of *Salmonella* species in food commodities. Int. J. Food Microbiol. 35: 239-250.

Chen X, Cui DF, Wang L, Wang M, Zhao Q (2002) Development and characterization of DNA hybridization reaction on PDMS Microchip. Int. J. Nonlinear Sci. Numer. Simul. 3: 211-214,

Cheng H, Lei KF, Choy KY, Chow LMC (2009) Single-stranded DNA concentration by electrokinetic forces. J. Micro-Nanolithogr. MEMS MOEMS. 8(2): 21107.

Cheng I, Senapati S, Cheng X, Basuray S, Chang H, Chang H (2010) A rapid field-use assay for mismatch number and location of hybridized DNAs. Lab Chip 10: 828-831.

Cheng SB, Skinner CD, Taylor J, Attiya S, Lee WE, Picelli G, Harrison DJ (2001) Development of a multichannel microfluidic analysis system employing affinity capillary electrophoresis for immunoassay. Anal. Chem. 73: 1472-1479.

Cheow LF, Ko SH, Kim SJ, Kang KH, Han J (2010) Increasing the Sensitivity of Enzyme-Linked Immunosorbent Assay Using Multiplexed Electrokinetic Concentrator. Anal. Chem. 82: 3383-3388.

Chin CD, Linder V, Sia SK (2007) Lab-on-a-chip devices for global health: Past studies and future opportunities. Lab Chip 7: 41-57.

Choi J, Cha M, Lee J (2009) Thin membrane transducer detecting DNA hybridization on chip. In: IEEE Sensors 2009 Conference, Oct.25-28, 2009. IEEE, Christchurch, 815-818.

Chong H. Choi AJ, Beaucage G, Nevin JH, Lee J, Puntambekar A, Lee JY (2004) Disposable Smart Lab on a Chip for Point-of-Care Clinical Diagnostics. Proceedings of The IEEE, 92 (1): 154-173.

Chung Y, Lin Y, Chueh C, Ye C, Lai L, Zhao Q (2008) Microfluidic chip of fast DNA hybridization using denaturing and motion of nucleic acids. Electrophoresis 29: 1859-1865.

Chung Y, Lin Y, Shiu M, Chang WT (2003) Microfluidic chip for fast nucleic acid hybridization. Lab Chip 3: 228-233.

Curey TE, Goodey A, Tsao A, Lavigne J, Sohn Y, McDevitt JT, Anslyn EV, Neikirk D, Shear JB (2001) Characterization of multicomponent monosaccharide solutions using an enzyme-based sensor array. Anal. Biochem. 293: 178-184.

Dexter JP, Parker W (2009) Parallel combinatorial chemical synthesis using single-layer poly(dimethylsiloxane) microfluidic devices. Biomicrofluidics 3: 034106.

Dhopeshwarkar R, Sun L, Crooks RM (2005) Electrokinetic concentration enrichment within a microfluidic device using a hydrogel microplug. Lab Chip 5: 1148-1154.

Eddington DT, Beebe DJ (2004) A valved responsive hydrogel microdispensing device with integrated pressure source. J. Microelectromech. Syst. 13: 586-593.

Edelstein RL, Tamanaha CR, Sheehan PE, Miller MM, Baselt DR, Whitman LJ, Colton RJ (2000) The BARC biosensor applied to the detection of biological warfare agents. Biosens. Bioelectron. 14: 805-813.

Erickson D, Liu X, Krull U, Li D (2004) Electrokinetically controlled DNA hybridization microfluidic chip enabling rapid target analysis. Anal. Chem. 76: 7269-7277.

Esch MB, Locascio LE, Tarley MJ, Durst RA (2001) Detection of viable cryptosporidium parvum using DNA-modified liposomes in a microfluidic chip. Anal. Chem. 73: 2952-2958.

Eyigör A, Goncagül G, Carli KT (2007) A PCR- ELISA for the detection of *Salmonella* from chicken intestine. J. Biol. Environ. Sci. 1(1): 45-49.

Fan ZH., Mangru S, Granzow R, Heaney P, Ho W, Dong Q, Kumar R (1999) Dynamic DNA hybridization on a chip using paramagnetic beads. Anal. Chem. 71: 4851-4859.

Felton MJ (2003) The New Generation of Microvalves. Anal Chem.75 (19):429A-432A.

Feng Y, Zhou,Z, Ye X, Xiong J (2003) Passive valves based on hydrophobic microfluidics. Sens. Actuators A-Phys. 108: 138–143.

Ferguson BS, Buchsbaum SF, Swensen JS, Hsieh K, Lou X, Soh HT (2009) Integrated microfluidic electrochemical DNA sensor. Anal. Chem. 81: 6503-6508.

Flowers RS, Klatt MJ, Mozola MA, Curiale MS, Gabis DA, Silliker JH (1987) DNA hybridization assay for detection of *Salmonella* in foods: collaborative study. J. Assoc. Off. Anal. Chem. 70 (3): 521-529.

Fu AY, Chou HP, Spence C, Arnold FA, Quake SR (2002) An integrated microfabricated cell sorter. Anal. Chem. 74: 2451-2457

Fu C, Rummler Z, Chomburg W (2003) Magnetically driven micro ball valves fabricated by multilayer adhesive film bonding. J. Micromech. Microeng. 13: S96-102.

GeneQuence® kit for Salmonella package insert-Rev. Neogen Corporation, Lansing, MI, 2008

GENE-TRAK® *Salmonella* assay package insert-Rev. Neogen Corporation, Lansing, MI, 2008

Ghosh S, Yang C, Cai T, Hu Z, Neogi A (2009) Oscillating magnetic field-actuated microvalves for micro- and nanofluidics . J. Phys. D: Appl. Phys. 42: 135501 (8pp).

Goettsche T, Kohnle J, Willmann M, Ernst H, Spieth S, Tischler R, Messner S, Zengerle R, Sandmaier H (2005) Novel approaches to particle tolerant valves for use in drug delivery systems. Sensor. Actuat. A-Phys. 118: 70-7.

Goll C, Bacher W, Bustgens B, Maas D, Ruprecht R, Schomburg WK (1997) An electrostatically actuated polymer microvalve equipped with a movable membrane electrode. J. Micromech. Microeng. 7: 224-226.

Gui L, Ren CL (2006) Numerical simulation of heat transfer and electrokinetic flow in an electroosmosis-based continuous-flow PCR chip. Anal. Chem. 78(17): 6215-22.

Hadd AG, Raymond DE, Halliwell JW, Jacobson SC, Ramsey JM (1997) Microchip device for performing enzyme assays. Anal. Chem. 69: 3407-3412.

Haeberle S, Zengerle R (2007) Microfluidic platforms for lab-on-a-chip applications. Lab Chip, 7(9):1094-1110.

Hall BD, Spiegelman S (1961) Sequence complementary of T2-DNA and T2-Specific RNA. Proc Natl Acad Sci U S A. 47: 137-146.

Hasegawa T, Ikuta K, Nakashima K (2003) 10-way micro switching valve chip for multi-directional flow control. Proc. microTAS Workshop 215-218.

Hatakeyama K, Tanaka T, Sawaguchi M, Iwadate A, Mizutani Y, Sasaki K, Tateishi N, Matsunaga T (2009) Microfluidic device using chemiluminescence and a DNA-arrayed thin film transistor photosensor for single nucleotide polymorphism genotyping of PCR amplicons from whole blood. Lab Chip 9: 1052-1058.

Heo J, Hua SZ (2009) An overview of recent strategies in pathogen sensing. Sensors 9: 4483-4502.
Hern ández M, Hansen F, Cook N, Rodr íguez-L ázaro D (2009) Real-time PCR methods for detection of foodborne bacterial pathogens in meat and meat products. Food Microbiol. Food Saf. 4: 426-427.

Herv ás M, L ópez MA., Escarpa A (2011) Integrated electrokinetic magnetic bead-based electrochemical immunoassay on microfluidic chips for reliable control of permitted levels of zearalenone in infant foods. Analyst, 136: 2131-2138.

Heule M, Manz A (2004) Sequential DNA hybridisation assays by fast micromixing. Lab Chip 4: 506-511.

Henry OYF, O'Sullivan CK (2012) Rapid DNA hybridization in microfluidics. TrAC-Trend Anal. Chem. 33: 9-22.

Hu G, Gao Y, Sherman PM, Li D (2005) A microfluidic chip for heterogeneous immunoassay using electrokinetical control. Microfluid. Nanofluid. 1: 346-355.

Hu GQ, Xiang Q, Fu R, Xu B, Venditti R, Li DQ (2006) Electrokinetically controlled real-time polymerase chain reaction in microchannel using Joule heating effect. Anal. Chim. Acta. 557: 146-51.

Huang SQ, Li CY, Lin BC, Qin JH (2010) Microvalve and micropump controlled shuttle flow microfluidic device for rapid DNA hybridization. Lab Chip 10: 2925-2931.

Hunter RJ (1989). Fundations of Colloid Science, Oxford University Press, Oxford.

Javanmard M., Davis RW (2011) A microfluidic platform for electrical detection of DNA hybridization. Sens. Actuators B-Chem. 154: 22-27.

Jin SQ, Yin BC, Ye BC (2009) Multiplexed bead-based mesofluidic system for detection of foodborne pathogenic bacteria. Appl. Environ. Microbiol. 75 (21): 6647-6654.

Jobs M, Fredriksson S, Brookes AJ, Landegren U (2002) Effect of oligonucleotide truncation on single-nucleotide distinction by solid-phase hybridization. Anal. Chem. 74: 199-202.

Joo S, Kim KH, Kim HC, Chung TD (2010) A portable microfluidic flow cytometer based on simultaneous detection of impedance and fluorescence. Biosens. Bioelectron. 25(6): 1509-1515.

Kang T J, Lim D, Nam J, Kim YH (2010) Multifunctional nanocomposite membrane for chemomechanical transducer. Sens. Actuators B-Chem. 147: 691-696.

Kang Y, D Li (2009) Electrokinetic motion of particles and cells in microchannels. Microfluid. Nanofluid. 6: 431-460.

Kawabata T, Wada HG, Watanabe M, Satomura S (2008) Electrokinetic Analyte Transport Assay for 121-fetoprotein immunoassay integrates mixing, reaction and separation on-chip. Electrophoresis 29: 1399-1406.

Kim D, Hwang YW, Park S-J (2009) Passive microfluidic gas valves using capillary pressure. Microsyst. Technol. 15: 919-923.

Kim JH, Marafie A, Jia X, Zoval JV, Madou MJ (2006a) Characterization of DNA hybridization kinetics in a microfluidic flow channel. Sensor. Actuat. B-Chem. 113: 281-289.

Kim J, Heo J, Crooks RM (2006b) Hybridization of DNA to bead-immobilized probes confined within a microfluidic channel. Langmuir 22: 10130-10134.

Kim S, Chen L, Lee S, Seong GH, Choo J, Lee EK, Oh C, Lee S (2007) Rapid DNA hybridization analysis using a PDMS microfluidic sensor and a molecular beacon. Anal. Sci. 23: 401-405.

Kumar S, Balakrishna K, Singh GP, Batra HV (2005) Rapid detection of *Salmonella* typhi in foods by combination of immunomagnetic separation and polymerase chain reaction. World J. Microbiol. Biotechnol. 21: 625-628.

Kwakye S, Baeumner A (2003) A microfluidic biosensor based on nucleic acid sequence recognition. Anal. Bioanal. Chem. 376: 1062-1068.

Kwang WO, Chong HA (2006) A review of microvalves. J. Micromech. Microeng. 16: R13-R39.

Lagally ET, Scherer JR, Blazej RG, Toriello NM, Diep BA, Ramchandani M, Sensabaugh GF, Riley LW, Mathies RA (2004) Integrated portable genetic analysis microsystem for pathogen/infectious disease detection. Anal. Chem. 76: 3162-3170.

Lange SA, Benes V, Kern DP, Hörber JK, Bernard A (2004) Microcontact printing of DNA molecules. Anal. Chem. 76: 1641-1647.

Lee CY, Lee GB, Lin JL, Huang FC, Liao CS (2005) Integrated microfluidic systems for cell lysis, mixing/pumping and DNA amplification. J. Micromech. Microengin.15:1215-23.

Lee DE, Soper S, Wang W (2008) Design and fabrication of an electrochemically actuated microvalve. Microsyst. Technol. 14: 1751-1756.

Lee HJ, Goodrich TT, Corn RM (2001) SPR imaging measurements of 1-D and 2-D DNA microarrays created from microfluidic channels on gold thin films. Anal. Chem. 73: 5525-5531.

Lee JS, Lucyszyn S (2007) Design and pressure analysis for bulk-micromachined electrothermal hydraulic microactuators using a PCM. Sensor. Actuat. A-Phys. 133: 294-300.

Lee JSH, Li D (2006) Electroosmotic flow at a liquid–air interface. Microfluid. Nanofluid. 2: 361-365.

Lei KF, Cheng H, Choy KY, Chow LMC (2009) Electrokinetic DNA concentration in microsystems. Sensor. Actuat. A-Phys. 156: 381-387.

Lewis CL, Choi C, Lin Y, Lee C, Yi H (2010) Fabrication of uniform DNA-conjugated hydrogel microparticles via rReplica molding for facile nucleic acid hybridization assays. Anal. Chem. 82: 5851-5858.

Li B, Chen Q, Lee D, Woolman J, Carman GP (2005) Development of large flow rate, robust, passive micro check valves for compact piezoelectrically actuated pumps. Sensor. Actuat. A-Phys. 117: 325-330.

Li C, Dong X, Qin J, Lin B (2009) Rapid nanoliter DNA hybridization based on reciprocating flow on a compact disk microfluidic device. Anal. Chim. Acta. 640 (1-2): 93-99.

Li H, He Z (2009) Magnetic bead-based DNA hybridization assay with chemiluminescence and chemiluminescent imaging detection. Analyst 134: 800-804.

Li Z, He Q, Ma D, Chen H (2010) On-chip integrated multi-thermo-actuated microvalves of poly(N-isopropylacrylamide) for microflow injection analysis. Anal. Chim. Acta. 665: 107-112.

Liao JC, Mastali M, Gau V, Suchard MA, Moller AK, Bruckner DA, Babbitt JT, Li Y, Gornbein J, Landaw EM, McCabe ERB, Churchill BM, Haake DA (2006) Use of electrochemical DNA biosensor for rapid molecular identification of uropathogens in clinical urine specimens. J. Clin. Microbiol. 44: 561-570.

Lien KY, Lee GB (2010) Miniaturization of molecular biological techniques for gene assay. Analyst 135: 1499-1518.

Lingerfelt L, Karlinsey J, Landers J, Guiseppi-Elie A (2007) Impedimetric detection for DNA hybridization within microfluidic biochips. Methods Mol. Biol. 385: 103-120.

Liu DJ, Perdue RK, Sun L, Crooks RM (2004) Immobilization of DNA onto poly(dimethylsiloxane) surfaces and application to a microelectrochemical enzyme-amplified DNA hybridization assay. Langmuir 20: 5905-5910.

Liu GL, Kim J, Lu Y, Lee LP (2006) Optofluidic control using photothermal nanoparticles. Nat. Mater. 5: 27–32.

Löfström C, Axelsson CE, Rådström P (2008) Validation of a diagnostic PCR method for routine analysis of *Salmonella* spp. in animal feed samples. Food Anal. Methods 1 (1): 23-27.

Lyklema J (1995) Fundamentals of Interface and Colloid Science, Vol. 2, Solid –liquid Interfaces, Academic Press, London.

Lynch MJB, Leon-Velarde CG, McEwen S, Odumeru JA (2004) Evaluation of an automated immunomagnetic separation method for the rapid detection of *Salmonella* species in poultry environmental samples. J. Microbiol. Methods 58: 285-288.

Maciorowski KG, Herrera P, Jones FT, Pillai SD, Ricke SC (2006) Cultural and immunological detection methods for *Salmonella* spp. in animal feeds-a review. Vet. Res. Commun. 30: 127-137.

Madou MJ, Lee LJ, Daunert S, Lai S, Shih C (2001) Design and fabrication of CD-like

microfluidic platforms for diagnostics: Microfluidic functions. Biomed. Microdevices 3: 245-254.

Mai JDH, Gaster RS, Wu A, Gu W, Mach KE, Liao JC (2007) A microfluidic system for rapid bacterial pathogen detection. Proceedings of the 7th IEEE, International Conference on Nanotechnology, Hong Kong.

Mairhofer J, Roppert K, Retl P (2009) Microfluidic Systems for Pathogen Sensing: A Review. Sensors 9: 4804-4823.

Malic L, Veres T, Tabrizian M (2009) Biochip functionalization using electrowetting-on-dielectric digital microfluidics for surface plasmon resonance imaging detection of DNA hybridization. Biosens. Bioelectron. 24: 2218-2224.

Malorny B, Paccassoni E, Fach P, Bunge C, Martin A, Helmuth R (2004) Diagnostic real-time PCR for detection of *Salmonella* in food. Appl. Environ. Microbiol.70 (12): 7046-7052.

McGuinness S, McCabe E, O'Regan E, Dolan A, Duffy G, Burgess C, Fanning S, Barry T, O'Grady J (2009) Development and validation of a rapid real-time PCR based method for the specific detection of *Salmonella* on fresh meat. Meat Sci. 83: 555-562.

MicroSEQ® Salmonella spp. Detection Kit package insert-REV, Life Technologies™ ,Carlsbad, CA, USA, 2013

Mir M, Martínez-Rodríguez S, Castillo-Fernández O, Homs-Corbera, Samitier J. Electrokinetic techniques applied to electrochemical DNA biosensors. Electrophoresis 2011, 32: 811–821.

Misiakos K, Mayrogiannopoulou E, Petrou P, Kakabakos S (2009) Monolithic silicon optical microdevices for biomolecular sensing. In: IEEE Sensors 2009 Conference, Oct.25-28, 2009. IEEE, Christchurch, 17-20.

Mitterer G, Schmidt WM (2006) Microarray-based detection of bacteria by on-Chip PCR. Methods Mol. Biol. 345: 37-51.

Mogensen KB, Klank H, Kutter JP (2002) Recent developments in detection for microfluidic systems. Electrophoresis 25: 3498-3512.

Muldoon MT, Teaney G, Li J, Onisk DV, Stave JW (2007) Bacteriophage-based enrichment coupled to immunochromatographic strip-based detection for the determination of *Salmonella* in meat and poultry. J. Food Prot. 70 (10): 2235-2242.

Mulvaney SP, Cole CL, Kniller MD, Malito M, Tamanaha CR, Rife JC, Stanton MW, Whitman LJ (2007) Biosens. Bioelectron. 23(2): 191-200.

Naravaneni R, Jamil K (2005) Rapid detection of foodborne pathogens by using molecular techniques. J. Med. Microbiol. 54: 51-54.

Niu X, Wen W, Lee Y (2005) Electrorheological-fluid-based microvalves. Appl. Phys. Lett. 87: 243501.

Noerholm M, Bruus H, Jakobsen MH, Tellemanb P, Ramsing NB (2004) Polymer microfluidic chip for online monitoring of microarray hybridizations. Lab Chip 4: 28-37.

Nugen SR, Baeumner AJ (2008) Trends and opportunities in food pathogen detection. Anal. Bioanal. Chem. 391:451-454.

Nygaard AP, Hall BD (1963) A method for the detection of RNA-DNA complexes. Biochem. Biophys. Res. Commun. 12: 98-104.

Oh KW, Park C, Namkoong K, Kim J, Ock K-C, Kim S, Kim Y-A, Cho Y-K, Ko C (2005) World-to-chip microfluidic interface with built-in valves for multichamber chip-based PCR assays. Lab Chip 5: 845-850.

Olsen KG, Ross DJ, Tarlov MJ (2002) Immobilization of DNA hydrogel plugs in microfluidic channels. Anal. Chem. 74: 1436-1441.

Pal R, Yang M, Johnson BN, Burke DT, Burns MA (2004) Phase change microvalve for integrated devices. Anal. Chem. 76(13): 3740-3748.

Pal R, Yang M, Lin R, Johnson BN, Srivastava N, Razzacki SZ (2005) An integrated microfluidic device for influenza and other genetic analyses. Lab Chip 5: 1024-1032.

Park S, Taton TA, Mirkin CA (2002) Array-based electrical detection of DNA with nanoparticle probes. Science 22: 1503-1506.

Pan T, Baldi A, Ziaie B (2007) Remotely adjustable check-valves with an electrochemical release mechanism for implantable biomedical microsystems. Biomed. Microdevices 9: 385-394.

Pan T, McDonald SJ, Kai EM, Ziaie B (2005) A magnetically driven PDMS micropump with ball check-valves. J. Micromech. Microeng. 15: 1021-1026.

Penchovsky R (2013) Programmable and automated bead-based microfluidics for versatile DNA microarrays under isothermal conditions. Lab Chip 13: 2370-2380.

Pui CF, Wong WC, Chai LC, Tunung R, Jeyaletchumi P, Noor Hidayay MS, Ubong A, Farinazleen MG, Cheah YK, Son R (2011) Salmonella: A foodborne pathogen. Int. Food Res. J. 18(2): 465-473.

Quintavalla S, Bolmini L, Dellapina G, Pancini E, Barbuti S (1996) Rapid methods for *Salmonella* detection in meat products: II - Evaluation of two immunochromatographic systems. Ind. Conserve, 71(3): 306-314.

Radisic M, Iyer RK, Murthy SK (2006) Micro- and nano-technology in cell separation. Int. J. Nanomedcine 1: 3-14.

Ramsay G (1998) DNA chips: State-of-the art. Nat. Biotech. 16: 40-44.

Rich CA, Wise KD (2003) A High-Flow Thermopneumatic Microvalve with Improved Efficiency and Integrated State Sensing. J. Microelectromech. Syst. 12(2): 201-208.

Richter A, Howitz S, Paschew G, Klatt S, Lienig J, Arndt K, Adler HP (2008) Review on Hydrogel-based pH Sensors and Microsensors. Sensors 8: 561-581.

Rodriguez-Lazaro D, Hernandez M, Esteve T, Hoorfar J, Pla M (2003) A rapid and direct real time PCR-based method for identification of *Salmonella* spp. J. Microbiol. Methods 54: 381-390.

Rogge T, Rummler Z, Schomburg WK (2004) Polymer micro valve with a hydraulic piezo-drive fabricated by the AMANDA process. Sensor. Actuat.A-Phys. 110: 206-212.

Roman GT, Chen Y, Viberg P, Culbertson AH, Cullbertson CT (2007) Single-cell manipulation and analysis using microfluidic device. Anal. Bioanal. Chem. 387:9-12.

Russom A (2005) Microfluidic bead-based methods for DNA analysis. Dissertation, Royal Institute of Technology, Stockholm, Sweden.

Salimi-Moosavi H, Tang T, Harrison DJ (1997) Electro-osmotic pumping of organic solvents and reagents in microfabricated reactor chips. J. Am. Chem. Soc. 119: 8716-8717.

Satyanarayana S, McCormick DT, Majumdar A (2006) Parylene micro membrane capacitive sensor array for chemical and biological sensing. Sensor. Actuat. B-Chem. 115: 494-502.

Sawada K, Oda C, Takao H, Ishida M (2007) Smart microfluidic electrochemical DNA sensors with signal processing circuits. Jpn. J. App. Phys. 46(5A): 3135-3138.

Scallan E, Hoekstra RM, Angulo FJ, Tauxe RV, Widdowson M, Roy SL, Jones JL, Griffin PM (2011) Foodborne Illness Acquired in the United States—Major Pathogens. Emerg. Infect. Dis. 17(1): 7-15.

Schaechter M, Lederberg J (2004) The desk encyclopedia of microbiology. San Diego, CA, USA.

Schüler T, Asmus T, Fritzsche W, Möller R (2009a) Screen printing as cost-efficient fabrication method for DNA-chips with electrical readout for detection of viral DNA. Biosens. Bioelectron. 24 (7): 2077-2084.

Schüler T, Kretschmer R, Jessing S, Urban M, Fritzsche W, Möller R, Popp J (2009b) A disposable and cost efficient microfluidic device for the rapid chip-based electrical detection of DNA. Biosens. Bioelectron. 25: 15-21.

Senapati S, Mahon AR, Gordon J, Nowak C, Sengupta S, Powell THQ, Feder J, Lodge DM, Chang H (2009) Rapid on-chip genetic detection microfluidic platform for real world applications. Biomicrofluidics 3: 022407.

Seong GH, Zhan W, Crooks RM (2002) Fabrication of microchambers defined by photopolymerized hydrogels and weirs within microfluidic systems: application to DNA hybridization. Anal. Chem. 74: 3372-3377.

Shamansky LM, Davis CB, Stuart JK, Kuhr WG (2001) Immobilization and detection of DNA on microfluidic chips. Talanta 55: 909-918.

Sia SK, Kricka LJ (2008) Microfluidics and point-of-care testing. Lab Chip 8:1982-1983.

Sibley CG, Ahlquist JE (1984) The Phylogeny of the Hominoid Primates, as Indicated by DNA-DNA Hybridization. J. Mol. Evol. 20 (1): 2-15.

Sim WY, Yoon HJ, Jeong OC, Yang SS (2003) A phase-change type microp- ump with aluminum flap valves. J. Micromech. Microeng. 13: 286-294.

Song WH, Kwan J, Kaigala GV, Hoang VN, Backhouse CJ (2008) Readily integrated, electrically controlled Microvalves. J. Micromech. Microeng. 18: 045009.

Sonntag F, Schmieder S, Danz N, Mertig M, Schilling N, Klotzbach U, Beyer E (2009) Novel lab-on-a-chip system for label-free detection of DNA hybridization and protein-protein interaction by surface plasmon resonance (SPR). Bioengineered and Bioinspired Systems IV. Edited by Rodr ́guez-V ́zquez, Ángel B.. Proceedings of the SPIE, 7365: 73650Q-73650Q-9

Strachan T, Read AP. Human Molecular Genetics. 2nd editionNew York: Wiley-Liss, 1999.

Studer V, Jameson R, Pellereau E, Pepin A, Chen Y (2004) A microfluidic mammalian cell sorter based on fluorescence detection. Microelectron. Eng. 73–74: 852-857.

Sugiura S, Sumaru K, Ohi K, Hiroki K, Takagi T, Kanamori T (2007) Photoresponsive polymer gel microvalves controlled by local light irradiation. Sensor. Actuat. A-Phys. 140: 176-184.

Sun Y, Kwok YC (2006) Polymeric microfluidic system for DNA analysis. Anal. Chim. Acta. 556 (1): 80-96.

Sung W, Chen H, Makamba H, Chen S (2009) Functionalized 3D-hydrogel plugs covalently patterned inside hydrophilic poly (dimethylsiloxane) microchannels for flow-through immunoassays. Anal. Chem. 81: 7967-7973.

Swaminathan B, Feng P (1994) Rapid detection of foodborne pathogenic bacteria. Annu. Rev. Microbiol. 48: 401-426.

Taban BM, Ben U, Aytac SA (2009) Rapid detection of *Salmonella* in milk by combined immunomagnetic separation-polymerase chain reaction assay. J. Dairy Sci. 92 (6): 2382-2388.

Tabeling P. Introduction to Microfluidics. Oxford University Press, 2005

Takao H, Miyamura K, Ebi H, Ashiki M, Sawada K, Ishida K (2005) A MEMS microvalve with PDMS diaphragm and two-chamber configuration of thermo-pneumatic actuator for integrated blood test system on silicon. Sensor. Actuat. A-Phys. 119: 468-475.

Taton TA, Mirkin CA, Letsinger RL (2000) Scanometric DNA array detection with nanoparticle probes. Science 8: 1757-1760.

Tavares AJ, Petryayeva E, Algar WR, Chen L, Krull UJ (2010) Toward a hybridization assay using fluorescence resonance energy transfer and quantum dots immobilized in microfluidic channels. Proc. SPIE 7750: 775003.

Teymoori MM, Abbaspour-Sani E (2004) Design and simulation of a novel electrostatic peristaltic micromachined pump for drug delivery applications, Sensor. Actuat. A-Phys. 117(2): 222-229.

Thorns JJ (2000) Bacterial foodborne zoonoses. Rev. Sci. Tech. 19 (1): 226-239.

Thomas G, El-Giar EM, Locascio LE, Tarlov MJ (2006) Methods in Molecular Biology 321: In: Minteer SD (ed) Microfluidic Techniques: Reviews and Protocols, Humana Press Inc., Totowa, NJ, pp 1-247.

Urata M, Iwata R, Noda K, Murakami Y, Kuroda A (2009) Detection of living *Salmonella* cells using bioluminescence. Biotechnol. Lett. 31: 737-741.

Van der Wijngaart W, Ask H, Enoksson P, Stemme G (2002) A high-stroke, high-pressure electrostatic actuator for valve applications. Sensor. Actuat. A-Phys. 100: 264-271.

Velusamy V, Arshak K, Korostynska O, Oliwa K, Adley C (2010) An overview of foodborne pathogen detection: in the perspective of biosensors. Biotechnol. Adv. 28: 232-254.

Vojtíšek M, Iles A, Pamme N (2010) Rapid, multistep on-chip DNA hybridisation in continuous flow on magnetic particles. Biosens. Bioelectron. 25: 2172-2176.

Wang C, Chang P, Huang C (2008) Optimization of diffuser valves. J. Mar. Sci. Technol. 16 (2): 134-138.

Wang J, Chen Z, Mauk M, Hong K, Li M, Yang S, Bau HH (2005) Self-actuated, thermo-responsive hydrogel valves for Lab on a Chip. Biomed. Microdevices 7 (4): 313-322.

Wang J, Chen ZY, Corstjens PLAM, Mauk MG, Bau HH (2006) A Disposable Microfluidic Cassette for DNA Amplification and Detection. Lab Chip 6: 46-53.

Wang L, Li PCH (2011) Microfluidic DNA microarray analysis: a review. Anal. Chim. Acta 687: 12-27.

Wang X, Chen X, Ma X, Kong X, Xu Z, Wang J (2011) Fast DNA hybridization on a microfluidic mixing device based on pneumatic driving. Talanta 84: 565-571.

Wang Y, Vaidya B, Farquar HD, Stryjewski W, Hammer RP, McCarley RL, Soper SA (2003) Microarrays assembled in microfluidic chips fabricated from poly (methyl methacrylate) for the detection of low-abundant DNA mutations. Anal. Chem. 75: 1130-1140.

Wen J, Yanga X, Wang K, Tana W, Zhou L, Zuo X, Zhang H, Chen Y (2007) One-dimensional microfluidic beads array for multiple mRNAs expression detection. Biosens. Bioelectron. 22 (11): 2759-2762.

Weng X, Jiang H, Chon CH, Chen S, Cao H, Li D (2011) An RNA-DNA hybridization assay chip with electrokinetically controlled oil droplet valves for sequential microfluidic operations. J. Biotechnol. 155 (3): 330-337.

West J, Becker M, Tombrink S, Manz A (2008) Micro total analysis systems: Latest achievements. Anal. Chem. 80: 4403-4419.

Whitesides GM (2006) The origins and the future of microfluidics. Nature, 442 (27): 368-373.

Wong PK, Chen C-Y, Wang T-H, Ho C-M (2004) Electrokinetic Bioprocessor for Concentrating Cells and Molecules. Anal. Chem. 76: 6908-6914.

Wyatt GM, Dionysou S, Lee HA, Morgan MRA, Stokely D, Richards J, Al-Hajji A H, Sillis A, Parker S, Jones P (1995) Application of an ELISA for the routine detection of *Salmonella* in chicken. Food Agric. Immunol. 7(4): 345-350.

Xu H, Ewing AG (2005) High-throughput enzyme assay on a multichannel microchip using optically gated sample introduction. Electrophoresis 26: 4711-4717. Yamahata C, Lacharme F, Burri Y, Gijs MAM (2005) A ball valve micropump in glass fabricated by powder blasting. Sensor. Actuat. B-Chem. 110: 1-7.

Yamashita K, Yamaguchi Y, Miyazaki M, Nakamura H, Shimizu H, Maeda H (2004) Sequence-selective DNA detection using multiple laminar streams: a novel microfluidic analysis method. Lab Chip 4: 1-3.

Yang B, Lin Q (2009) A latchable phase-change microvalve with integrated heaters. J Microelectromech. Syst. 18(4): 860-867.

Yang TL, Jung SY, Mao HB, Cremer PS (2001) Fabrication of phospholipid bilayer-coated microchannels for on-chip immunoassays. Anal. Chem. 73: 165-169.

Yang X, Zhao X, Zuo X, Wang K, Wen J, Zhang H (2009) Nucleic acids detection using cationic fluorescent polymer based on one-dimensional microfluidic beads array. Talanta 77: 1027-1031.

Yasuda T, Ishizuka K, Ezoe M (2008) A superhydrophobic microvalve for manipulating microliquids containing biological molecules. IEEJ T Electr. Electr. 3: 290-296.

Yi C, Li C, Ji S, Yang M (2006) Microfluidics technology for manipulation and analysis of biological cells. Anal. Chim. Acta 560: 1-23.

Yuen PK, Li GS, Bao YJ, Muller UR (2003) Microfluidic devices for fluidic circulation and mixing improve hybridization signal intensity on DNA arrays. Lab Chip 3: 46-50.

Zangmeister RA, Tarlov MJ (2004) DNA displacement assay integrated into microfluidic channels. Anal. Chem. 76: 3655-3659.

Zangmeister RA, Tarlov MJ (2003) UV graft polymerization of polyacrylamide hydrogel plugs in microfluidic channels. Langmuir 19: 6901-6904.

Zangmeister RA, Tarlov MJ (2009) Selective DNA screening in microfluidic channels by electrophoresis through hydrogel matrices. The National Institute of Standards and Technology (NIST) Web. http://www.nt.ntnu.no/users/skoge/prost/proceedings/aiche 2004/ pdffiles/ papers/ 137c.pdf. Accessed 18 August 2009.

Zaytseva NV, Goral VN, Montagna RA, Baeumner AJ (2005) Development of a microfluidic biosensor module for pathogen detection. Lab Chip 5: 805-811.

Zhang C, Xing D, Li Y (2007) Micropumps, microvalves, and micromixers within PCR microfluidic chips: Advances and trends. Biotechnol. Adv. 25: 483-514.

Zhang H, Yang X, Wang K, Tan W, Li H, Zuo X, Wen J (2008) On-chip oligonucleotide ligation assay using one-dimensional microfluidic beads array for the detection of low-abundant DNA point mutations. Biosens. Bioelectron. 23: 945-951.

Zhang Y, Yu H, Dong X, Qin J, Lin B (2009) Immobilization of DNA hydrogel plugs in glass microfluidic channels and its applications. Chem. J. Chinese U. 30(6): 1128-1130.